

NASA CONTRACTOR REPORT



NASA CR-1036

NASA CR-1036

GPO PRICE \$ _____

CFSTI PRICE(S) \$ _____

Hard copy (HC) _____

Microfiche (MF) _____

ff 653 July 65

FACILITY FORM 602

(ACCESSION NUMBER)	(THRU)
(PAGES)	(CODE)
NASA CR OR TAX OR AD NUMBER	CATEGORY

TIME-OPTIMAL RENDEZVOUS FOR ELLIPTIC ORBITS

by Y. Kasbiwagi and K. T. Alfriend

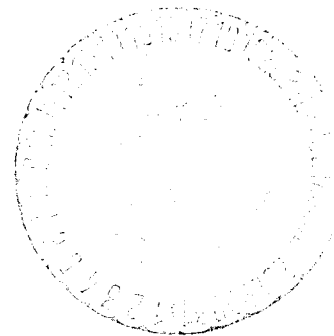
Prepared by

VIRGINIA POLYTECHNIC INSTITUTE

Blacksburg, Va.

for

NATIONAL AERONAUTICS AND SPACE ADMINISTRATION • WASHINGTON, D. C. • MAY 1968



TIME-OPTIMAL RENDEZVOUS FOR ELLIPTIC ORBITS

By Y. Kashiwagi and K. T. Alfriend

Distribution of this report is provided in the interest of information exchange. Responsibility for the contents resides in the author or organization that prepared it.

Prepared under Grant No. NGR 47-004-006 by
VIRGINIA POLYTECHNIC INSTITUTE
Blacksburg, Va.

for

NATIONAL AERONAUTICS AND SPACE ADMINISTRATION

For sale by the Clearinghouse for Federal Scientific and Technical Information
Springfield, Virginia 22151 - CFSTI price \$3.00

ABSTRACT

Time-optimal rendezvous maneuvers are studied. The system considered in this report consists of two space vehicles namely, a target vehicle (non-maneuvering vehicle) and an interceptor vehicle (maneuvering vehicle) under the influence of the earth gravity. An interceptor vehicle has propulsive jet systems which can produce a variable thrust (positive or negative) independently in three perpendicular directions. The case where the target vehicle is in the elliptic orbit is mainly considered and some analytical difficulties involved in the circular orbit case are discussed. Several time-optimal trajectories for different configurations are shown.

PRECEDING PAGE BLANK NOT FILMED.

TABLE OF CONTENTS

	<u>Page</u>
ABSTRACT	iii
TABLE OF CONTENTS	v
LIST OF ILLUSTRATIONS	vii
LIST OF SYMBOLS	xiii
SUMMARY	1
I. INTRODUCTION	2
II. FORMULATION OF THE PROBLEM	8
A. Derivation of Equations of Motion	8
B. Solution of Equations of Motion	16
III. THE OPTIMAL CONTROL PROBLEM	21
A. Statement of the Problem	21
B. Pontryagin's Maximum Principle	23
C. Neustadt's Method	28
IV. CIRCULAR ORBIT	36
V. DISCUSSION OF RESULTS	41
A. In-plane Motion	41
B. Out-of-plane Motion	48
VI. CONCLUSIONS	50
VII. BIBLIOGRAPHY	53

PRECEDING PAGE BLANK NOT FILMED.

	<u>Page</u>
APPENDIX A	99
APPENDIX B	105
APPENDIX C	108
APPENDIX D	112

LIST OF ILLUSTRATIONS

<u>Figure</u>	<u>Page</u>
1. Coordinate system	58
2. Optimal isochrones	59
3. Geometrical properties of Neustadt's method	60
4. Stopping time and error vector magnitude vs. number of iterations for Fletcher-Powell method	61
5. Comparison of convergence rate of Fletcher-Powell method and method of steepest ascent with optimum steps	62
6. Optimal isochrones for a singular control problem	63
7. Optimum rendezvous trajectories in x - y plane for various initial conditions with $A_{\max} = 0.25 \text{ ft/sec}^2$ and $\theta_0 = 0$ degrees	64
8. Optimum rendezvous trajectories in x - y plane for various initial conditions with $A_{\max} = 0.25 \text{ ft/sec}^2$ and $\theta_0 = 0$ degrees	65
9. Optimum rendezvous trajectories in x - y plane for various initial conditions with $A_{\max} = 0.25 \text{ ft/sec}^2$ and $\theta_0 = 0$ degrees	66

<u>Figure</u>	<u>Page</u>
10. Optimum rendezvous trajectories in x - y plane for various initial conditions with $A_{\max} = 0.5 \text{ ft/sec}^2$ and $\theta_0 = 0$ degrees	67
11. Optimum rendezvous trajectories in x - y plane for various initial conditions with $A_{\max} = 0.5 \text{ ft/sec}^2$ and $\theta_0 = 0$ degrees	68
12. Optimum rendezvous trajectories in x - y plane for various initial conditions with $A_{\max} = 0.75 \text{ ft/sec}^2$ and $\theta_0 = 0$ degrees	69
13. Optimum rendezvous trajectories in x - y plane for various initial conditions with $A_{\max} = 0.75 \text{ ft/sec}^2$ and $\theta_0 = 0$ degrees	70
14. Optimum rendezvous trajectories in x - y plane for various initial conditions with $A_{\max} = 1.0 \text{ ft/sec}^2$ and $\theta_0 = 0$ degrees	71
15. Optimum rendezvous trajectories in x - y plane for various initial conditions with $A_{\max} = 1.0 \text{ ft/sec}^2$ and $\theta_0 = 0$ degrees	72
16. Optimum rendezvous trajectories in x - y plane for various initial conditions with $A_{\max} = 0.25 \text{ ft/sec}^2$ and $\theta_0 = 90$ degrees	73

<u>Figure</u>	<u>Page</u>
17. Optimum rendezvous trajectories in x - y plane for various initial conditions with $A_{\max} = 0.25 \text{ ft/sec}^2$ and $\theta_o = 90$ degrees	74
18. Optimum rendezvous trajectories in x - y plane for various initial conditions with $A_{\max} = 0.25 \text{ ft/sec}^2$ and $\theta_o = 90$ degrees	75
19. Optimum rendezvous trajectories in x - y plane for various initial conditions with $A_{\max} = 0.25 \text{ ft/sec}^2$ and $\theta_o = 180$ degrees	76
20. Optimum rendezvous trajectories in x - y plane for various initial conditions with $A_{\max} = 0.25 \text{ ft/sec}^2$ and $\theta_o = 180$ degrees	77
21. Optimum rendezvous trajectories in x - y plane for various initial conditions with $A_{\max} = 0.25 \text{ ft/sec}^2$ and $\theta_o = 180$ degrees	78
22. Optimum rendezvous trajectories in x - y plane for various initial conditions with $A_{\max} = 0.5 \text{ ft/sec}^2$ and $\theta_o = 180$ degrees	79
23. Optimum rendezvous trajectories in x - y plane for various initial conditions with $A_{\max} = 0.5 \text{ ft/sec}^2$ and $\theta_o = 180$ degrees	80

<u>Figure</u>	<u>Page</u>
24. Optimum rendezvous trajectories in x - y plane for various initial conditions with $A_{\max} = 0.25 \text{ ft/sec}^2$ and $\theta_o = 270$ degrees	81
25. Optimum rendezvous trajectories in x - y plane for various initial conditions with $A_{\max} = 0.25 \text{ ft/sec}^2$ and $\theta_o = 270$ degrees	82
26. Optimum rendezvous trajectories in x - y plane for various initial conditions with $A_{\max} = 0.25 \text{ ft/sec}^2$ and $\theta_o = 270$ degrees	83
27. Optimum rendezvous trajectories in x - y plane for different maximum allowable accelerations	84
28. Optimum rendezvous trajectories in x - y plane for different maximum allowable accelerations	85
29. Optimum rendezvous trajectories in x - y plane for different maximum allowable accelerations	86
30. Optimum rendezvous trajectories in x - y plane for different maximum allowable accelerations	87
31. Optimum time vs. maximum allowable acceleration	88
32. Optimum rendezvous trajectories in x - y plane for various initial values of the true anomaly with $A_{\max} = 0.25 \text{ ft/sec}^2$	89

<u>Figure</u>	<u>Page</u>
33. Optimum rendezvous trajectories in x - y plane for various initial values of the true anomaly with $A_{\max} = 0.25 \text{ ft/sec}^2$	90
34. Optimum rendezvous trajectories in x - y plane for various initial values of the true anomaly with $A_{\max} = 0.25 \text{ ft/sec}^2$	91
35. Optimum rendezvous trajectories in x - y plane for various values of the eccentricity with $A_{\max} = 0.5 \text{ ft/sec}^2$	92
36. Optimum rendezvous trajectories in x - y plane for various values of the eccentricity with $A_{\max} = 0.5 \text{ ft/sec}^2$	93
37. Comparison of single engine control and multiple engine control	94
38. Comparison of single engine control and multiple engine control	95
39. Optimum rendezvous trajectories in x - y plane for various initial conditions with a circular target vehicle orbit	96
40. z - \dot{z} plots with $U_{\max} = 0.25 \text{ ft/sec}^2$	97
41. Switching surface for Bushaw's problem	98

LIST OF SYMBOLS

A_{\max}	maximum allowable thrust, ft/sec ²
e	eccentricity of target vehicle orbit
H	Hamiltonian
L	characteristic length
m	mass of interceptor vehicle
$\vec{n}_1, \vec{n}_2, \vec{n}_3$	unit vectors in the x, y, z directions
\underline{p}	adjoint vector
R_p	perigee distance of target vehicle orbit
\vec{r}_i	radius vector from earth center to interceptor vehicle
\vec{r}_t	radius vector from earth center to rendezvous vehicle
\vec{T}	thrust vector of interceptor vehicle with components T_x, T_y, T_z
t	real time
t_0	initial time
\underline{u}	control vector
U_{\max}	maximum allowable thrust in the x, y, z directions, ft/sec ²
x, y, z	cartesian coordinates
\underline{x}	state vector
$X(\theta, \theta_0)$	state transition matrix

PRECEDING PAGE BLANK NOT FILMED.

\vec{p}	radius vector from target vehicle to interceptor vehicle
θ	true anomaly of target vehicle orbit
θ_0	initial value of θ
ξ, η, ζ	dimensionless coordinates, $(x/r_t), (y/r_t), (z/r_t)$
μ	gravitational constant
$(\dot{\quad})$	differentiation with respect to time t
$(\quad)'$	differentiation with respect to θ
$(\underline{\quad})$	n dimensional vector or column matrix
$(\quad)^T$	transpose of a matrix

Plus miscellaneous symbols defined in the text.

SUMMARY

Time-optimal trajectories have been generated for the elliptic orbit rendezvous problem. A multiple engine control system which can apply a variable thrust (positive or negative) independently in three perpendicular directions is used. The optimal control law is found using Pontryagin's maximum principle. Neustadt's method is then used to find the initial values of the adjoint variables which arise in the use of the maximum principle. Neustadt's method transforms the two-point boundary value problem into one of maximizing a function where the location of the maximum is the optimum adjoint initial condition, and the value of the function at the maximum is the optimum (minimum) time. The Fletcher-Powell modification of Davidon's method is used to find the maximum of the function.

A comparison is made of the multiple engine control system used in this investigation and the single engine control system for which the magnitude and direction of the thrust vector are found as a function of time.

A computer program has been developed which will solve the time-optimal control problem for an n-dimensional time-varying linear system with r control variables, $r \leq n$, with the control constraint $|u_i| \leq 1, i = 1, 2, \dots, r$, or $\sum_{i=1}^r u_i^2 \leq 1$.

I. INTRODUCTION

A vital part of space missions today is the rendezvous maneuver. In the United States manned lunar mission, the Apollo program, the LEM vehicle, after leaving the moon, must rendezvous with the Apollo vehicle before returning to Earth. In many space missions, minimizing the fuel consumption during the rendezvous maneuver will be desirable. However, in a rescue mission, minimizing the time duration of the rendezvous maneuver will be of utmost importance.

The rendezvous maneuver is usually separated into three phases as follows:

1. The ascent or launch phase in which the maneuvering vehicle, hereafter called the interceptor vehicle, is launched into some parking orbit.
2. The terminal phase in which the interceptor is maneuvered from the parking orbit to the immediate neighborhood (possibly a few hundred feet) of the non-maneuvering or target vehicle, which is moving in a known Keplerian orbit, so that the docking maneuver can take place.

3. The docking phase in which the two vehicles are brought together.

In the last several years many papers have appeared in the literature on all phases of the rendezvous maneuver. The early investigations of the terminal phase were terminal control problems, in other words, they were concerned with guidance schemes which were not optimal but would complete the rendezvous maneuver. These guidance schemes were of two types:

1. Impulsive guidance schemes based on orbital mechanics.
2. Continuously burning rockets usually based on proportional navigation.

In the impulsive guidance schemes one or more impulses are imparted to the interceptor so that it will meet the target vehicle at a prescribed point in space. Another impulse is then applied to reduce the relative velocity between the two vehicles to zero. However, there is one drawback to this scheme; instantaneous velocity changes are not possible. The rockets must burn for a finite period of time, and large errors can occur if these burning times are not short enough to validate the assumption of an instantaneous velocity change. This has been shown by Stapleford (1962). Impulsive guidance schemes have been studied by Clohessy and Wiltshire (1960), Hornby (1962), Eggleston (1962), and Bender (1963).

In proportional navigation the thrust function is determined so that the angular velocity of the relative velocity vector is proportional to the angular velocity of the line of sight vector. By controlling the angular velocities of these two vectors in this manner the two vehicles will be brought together at some later time. A study utilizing proportional navigation was performed by Cicolani (1961). Harrison (1963) investigated the rendezvous maneuver using collision course and pursuit course guidance, which are forms of proportional navigation.

With the basic rendezvous maneuver well established, the next step is to develop guidance schemes which will achieve rendezvous, but will also be optimal with respect to some criteria, i.e., fuel, energy, time. This changes the problem from one of terminal control to one of optimal control. The object of most rendezvous optimization studies has been minimization of fuel consumption. Studies of this type have been performed by Goldstein et al. (1963), Tschauner and Hempel (1964), Tschauner (1965), Meditch and Neustadt (1963), and Kaminski (1966). Kaminski's study was also minimum time because of the constraint of a continuous, constant thrust.

Although minimizing fuel consumption during rendezvous is important, another area of importance is minimizing the time required to complete the rendezvous maneuver. This would be of prime

importance in a rescue mission. An investigation of time-optimal rendezvous was performed by Kelley and Dunn (1963), but no synthesis procedure was developed. Paiewonsky and Woodrow (1965) investigated time-optimal rendezvous with limited fuel when the target vehicle is in a circular orbit. However, no studies of time-optimal rendezvous have been performed when the target vehicle is moving in an elliptic orbit. The maneuvering vehicle in the studies by Paiewonsky and Woodrow (1965) and Kelley and Dunn (1963) is one with a single engine, and the attitude of the thrust vector with respect to some reference is found as a function of time so that rendezvous is completed in the minimum possible time. However, rather than having a single engine, the propulsion system may be one which can apply small thrusts independently in the longitudinal and the two transverse directions. The Gemini vehicle is an example of this type. A study of the rendezvous maneuver with this type of space vehicle was performed by Stapleford (1963), but the maneuver was not an optimal one.

The object of this investigation is to find the control or guidance law, subject to certain constraints, which will bring the interceptor into coincidence with the target vehicle with zero relative velocity when the target vehicle is moving in a known elliptic orbit, and will perform this maneuver in the minimum possible time. The interceptor vehicle considered will be one which

can impart a variable thrust independently in three perpendicular directions. Thus, the problem is to find the magnitude and direction (positive or negative) of the three thrust values so that the rendezvous maneuver is completed in the minimum possible time.

The equations of motion are written with respect to a moving coordinate system whose origin is located at the target vehicle and which rotates with the angular velocity of the radius vector from the earth's center to the target vehicle. Using the true anomaly of the target vehicle orbit as the independent variable and the ratio of the difference-coordinates to the length of the radius vector from the earth's center to the target vehicle as the dependent variables, a system of linear differential equations with periodic coefficients is obtained. The linearization of the equations is valid if the distance between the two vehicles is small compared to the length of the radius vector from the earth's center to the target vehicle. This linearization allows the equations of motion describing motion in the plane of the target vehicle orbit and those describing motion normal to the orbit plane to be decoupled. Thus, the two problems can be handled separately. The out-of-plane motion is that of a simple oscillator where the coefficient of the forcing function is periodic.

The optimal control law is found by application of Pontryagin's maximum principle. However, use of the maximum principle introduces

the adjoint variables for which the initial conditions are unknown. An iterative procedure developed by Neustadt (1960) is then used to find the initial conditions of the adjoint variables. Neustadt's procedure transforms the two-point boundary value problem into one of maximizing a function where the location of the maximum is the desired adjoint initial condition, and the value of the function at the maximum is the optimum (minimum) time. A convergence technique developed by Fletcher and Powell (1963) is used to find the maximum of the function.

Optimum rendezvous trajectories for various initial conditions, maximum allowable accelerations, and values of the target vehicle orbit eccentricity are presented. A comparison of the single engine control and multiple engine control is also given.

II. FORMULATION OF THE PROBLEM

In this section the derivation and the solution of the equations of motion for the terminal phase of the rendezvous maneuver are presented.

Several assumptions are made in the analysis, however, these are standard assumptions in rendezvous studies. The assumptions are:

1. The earth is spherical. Any perturbing forces due to a non-spherical earth are not considered.
2. The distance between the two vehicles is small relative to the distance of the target vehicle from the earth's center.
3. The interceptor is a point mass. The attitude stability of the vehicle is not considered.
4. The orientation of the interceptor is such that the directions of the three independent components of thrust coincide with the x, y, z directions shown in Figure 1.

A. Derivation of Equations of Motion.

The problem is to describe the relative motion between a reference body (target vehicle) moving in a known elliptic orbit of

eccentricity e and another body (interceptor) which is in the neighborhood of the reference body. A moving coordinate system centered at the target vehicle and rotating with the orbital angular velocity of the target vehicle is employed as shown in Figure 1. The x-axis is directed outward along the radius vector from the earth's center to the target vehicle; the y axis is perpendicular to the x axis, lies in the target vehicle orbit plane, and is directed in the direction of motion of the target vehicle; the z axis is normal to the target vehicle orbit plane, and its direction is such that a right-handed coordinate system is formed.

The equation of motion of the target vehicle is

$$\ddot{\vec{r}}_t \equiv \frac{I_d^2 \vec{r}_t}{dt^2} = - \frac{\mu \vec{r}_t}{r_t^3} \quad (2.1)$$

where $\frac{I_d(\)}{dt} = (\dot{\ })$ denotes differentiation with respect to time in an inertial reference frame, \vec{r}_t is the vector from the earth's center to the target vehicle, and μ is the gravitational constant.

The equation of motion of the interceptor is given by

$$\ddot{\vec{r}}_i \equiv \frac{I_d^2 \vec{r}_i}{dt^2} = - \frac{\mu \vec{r}_i}{r_i^3} + \frac{\vec{T}}{m} \quad (2.2)$$

where \vec{r}_i is the vector from the earth's center to the interceptor, \vec{T} is the thrust vector, and m is the mass.

The position of the interceptor relative to the target vehicle is

$$\vec{\rho} = \vec{r}_i - \vec{r}_t = x \vec{n}_1 + y \vec{n}_2 + z \vec{n}_3, \quad (2.3)$$

and

$$\ddot{\vec{\rho}} = \ddot{\vec{r}}_i - \ddot{\vec{r}}_t = -\mu \left(\frac{\vec{r}_i}{r_i^3} - \frac{\vec{r}_t}{r_t^3} \right) + \frac{\vec{T}}{m}. \quad (2.4)$$

From equation (2.3) we have

$$\vec{r}_i = (r_t + x) \vec{n}_1 + y \vec{n}_2 + z \vec{n}_3. \quad (2.5)$$

Now consider the term $\frac{1}{r_i^3}$.

$$\frac{1}{r_i^3} = \frac{1}{|\vec{r}_t + \vec{\rho}|^3} = \frac{1}{r_t^3} \left[1 + \frac{2x}{r_t} + \frac{(x^2 + y^2 + z^2)}{r_t^2} \right]^{-3/2} \quad (2.6)$$

Equation (2.6) is now expanded in a Taylor series, and the assumption that the distance ρ between the two vehicles is small relative to the distance r_t of the target vehicle from the earth's center allows higher order terms to be neglected. Equation (2.6) becomes

$$\frac{1}{r_i^3} = \frac{1}{r_t^3} \left[1 - \frac{3x}{r_t} + 0 \left(\left(\frac{\rho}{r_t} \right)^2 \right) \right]. \quad (2.7)$$

Substitution of equations (2.5) and (2.7) into equation (2.4) gives

$$\ddot{\vec{p}} = -\frac{\mu}{r_t^3} [-2x \vec{n}_1 + y \vec{n}_2 + z \vec{n}_3] + \frac{\vec{T}}{m} . \quad (2.8)$$

Now consider the differentiation of \vec{p} with respect to time in an inertial reference frame.

$$\dot{\vec{p}} \equiv \frac{I_{d\vec{p}}}{dt} = \frac{R_{d\vec{p}}}{dt} + \vec{\omega} \times \vec{p} \quad (2.9)$$

where $\frac{R_{d\vec{p}}}{dt}$ denotes differentiation with respect to time in the rotating reference frame and is given by

$$\frac{R_{d\vec{p}}}{dt} = \dot{x} \vec{n}_1 + \dot{y} \vec{n}_2 + \dot{z} \vec{n}_3 . \quad (2.10)$$

$\vec{\omega}$, which is given by

$$\vec{\omega} = \dot{\theta} \vec{n}_3 , \quad (2.11)$$

is the orbital angular velocity of the target vehicle. Differentiating equation (2.9) once more gives

$$\ddot{\vec{p}} = \frac{R_{d^2\vec{p}}}{dt^2} + 2 \vec{\omega} \times \frac{R_{d\vec{p}}}{dt} + \frac{R_{d\vec{\omega}}}{dt} \times \vec{p} + \vec{\omega} \times (\vec{\omega} \times \vec{p}) . \quad (2.12)$$

After substituting equations (2.10) and (2.11) into (2.12) and equating (2.8) and (2.12), the scalar equations of motion are obtained:

$$\ddot{x} - 2\dot{\theta}\dot{y} - \ddot{\theta}y - \left(\dot{\theta}^2 + \frac{2\mu}{r_t^3}\right) x = \frac{T_x}{m} \quad (2.13a)$$

$$\ddot{y} + 2\dot{\theta}\dot{x} + \ddot{\theta}x - \left(\dot{\theta}^2 - \frac{\mu}{r_t^3}\right) y = \frac{T_y}{m} \quad (2.13b)$$

$$\ddot{z} + \frac{\mu z}{r_t^3} = \frac{T_z}{m} \quad (2.13c)$$

This is a set of linear differential equations with periodic coefficients since r_t , $\dot{\theta}$, $\ddot{\theta}$ are periodic with a period equal to the orbital period of the target vehicle. However, one obtains a much simpler form of the equations if the true anomaly θ is used as the independent variable, and if one makes the transformation

$$\xi = \frac{x}{r_t}, \quad \eta = \frac{y}{r_t}, \quad \zeta = \frac{z}{r_t} \quad (2.14)$$

The following identities are obtained by differentiation:

$$\dot{\theta} r_t \xi' = \dot{x} - \frac{e \dot{\theta} \sin \theta}{1+e \cos \theta} x, \quad (2.15)$$

$$\dot{\theta}^2 r_t \xi'' = \ddot{x} + \left(\frac{\mu}{r_t^3} - \dot{\theta}^2\right) x, \quad (2.16)$$

$$\ddot{\theta} = -\frac{2 \dot{\theta}^2 e \sin \theta}{1+e \cos \theta} \quad (2.17)$$

where ()' denotes differentiation with respect to the true anomaly θ .

The scalar equations of motion become:

$$\xi'' - \frac{3\xi}{1+e \cos \theta} - 2\eta' = \frac{1}{m r_t \dot{\theta}^2} T_x \quad (2.18a)$$

$$\eta'' + 2 \xi' = \frac{1}{m r_t \dot{\theta}^2} T_y \quad (2.18b)$$

$$\zeta'' + \zeta = \frac{1}{m r_t \dot{\theta}^2} T_z \quad (2.18c)$$

Also,

$$\frac{1}{r_t \dot{\theta}^2} = \frac{R_p^2 (1+e)^2}{\mu (1+e \cos \theta)^3} \quad (2.19)$$

where R_p is the perigee distance of the target vehicle orbit.

For computational purposes it is advantageous to make the following transformations:

$$\begin{aligned} x_1 &= \frac{R_p}{L} \xi, & x_2 &= \frac{R_p}{L} \xi', \\ x_3 &= \frac{R_p}{L} \eta, & x_4 &= \frac{R_p}{L} \eta', \\ x_5 &= \frac{R_p}{L} \zeta, & x_6 &= \frac{R_p}{L} \zeta', \end{aligned} \quad (2.20)$$

and

$$\frac{T_x}{m} = \frac{U_{\max}}{\beta(\theta)} u_x ,$$

$$\frac{T_y}{m} = \frac{U_{\max}}{\beta(\theta)} u_y , \quad (2.21)$$

$$\frac{T_z}{m} = \frac{U_{\max}}{\beta(\theta)} u_z$$

where L is an arbitrary length whose magnitude is chosen so that

$x_i = O(1)$, $i = 1, 2, \dots, 6$. A reasonable value of L is

$$L^2 = x^2(t_0) + y^2(t_0) + z^2(t_0) . \quad (2.22)$$

U_{\max} is the maximum allowable thrust per unit mass, and $\beta(\theta)$ is the ratio of the mass of the interceptor to the initial mass. The control functions u_x, u_y, u_z , are restricted to

$$|u_\alpha| \leq 1 , \quad \alpha = x, y, z . \quad (2.23)$$

Using matrix notation, the equation of motion becomes

$$\underline{x}'(\theta) = A(\theta) \underline{x}(\theta) + B(\theta) \underline{u}(\theta) \quad (2.24)$$

where $\underline{x}(\theta)$ is the state vector defined by

$$\underline{x} = \begin{pmatrix} x_1 \\ x_2 \\ x_3 \\ x_4 \\ x_5 \\ x_6 \end{pmatrix} , \quad (2.25)$$

$\underline{u}(\theta)$ is the control vector defined by

$$\underline{u}(\theta) = \begin{bmatrix} u_x \\ u_y \\ u_z \end{bmatrix}, \quad (2.26)$$

and

$$A = \begin{bmatrix} 0 & 1 & 0 & 0 & 0 & 0 \\ \frac{3}{1+e \cos \theta} & 0 & 0 & 2 & 0 & 0 \\ 0 & 0 & 0 & 1 & 0 & 0 \\ 0 & -2 & 0 & 0 & 0 & 0 \\ 0 & 0 & 0 & 0 & 0 & 1 \\ 0 & 0 & 0 & 0 & -1 & 0 \end{bmatrix}, \quad (2.27)$$

$$B = \frac{U_{\max} LR_p (1+e)^2}{\mu(1+e \cos \theta)^3} \begin{bmatrix} 0 & 0 & 0 \\ 1 & 0 & 0 \\ 0 & 0 & 0 \\ 0 & 1 & 0 \\ 0 & 0 & 0 \\ 0 & 0 & 1 \end{bmatrix}. \quad (2.28)$$

From equations (2.13) or (2.18) one sees that the equations governing motion in the orbit plane of the target vehicle are decoupled from the equations governing motion normal to the orbit plane, thus the one problem can be broken up into two completely independent problems.

B. Solution of Equations of Motion.

The problem under consideration is the solution of the set of n first order linear differential equations

$$\underline{x}'(\theta) = A(\theta) \underline{x}(\theta) + B(\theta) \underline{u}(\theta) \quad (2.29)$$

where $A(\theta + 2\pi) = A(\theta)$. From linear system theory (see Appendix A) it is known that the homogeneous part of (2.29) is reducible, that is, by a linear transformation

$$\underline{x}(\theta) = Q(\theta) \underline{y}(\theta) \quad (2.30)$$

where $Q(\theta)$ is a $n \times n$ nonsingular matrix, the system (2.29) can be reduced to the form

$$\underline{y}'(\theta) = D \underline{y}(\theta) \quad (2.31)$$

where D is a $n \times n$ constant matrix. It is sometimes said that (2.29) and (2.31) are kinematically equivalent. The system (2.31) possesses the state transition matrix

$$Y(\theta, \theta_0) = \exp [(\theta - \theta_0) D] . \quad (2.32)$$

Substitution of (2.30) into the homogeneous portion of (2.29) gives

$$Q' \underline{y} + Q \underline{y}' = A Q \underline{y} , \quad (2.33)$$

and since $Q(\theta)$ is nonsingular

$$\underline{y}' = Q^{-1} (A Q - Q') \underline{y} . \quad (2.34)$$

Hence,

$$D = Q^{-1} (A Q - Q') . \quad (2.35)$$

The matrix $Q(\theta)$ is called a Lyapunov transformation. By another linear transformation

$$\underline{y} = R \underline{z} \quad (2.36)$$

the system (2.31) can be transformed into its Jordan canonical form:

$$\underline{z}' = \Lambda \underline{z} \quad (2.37)$$

where

$$\Lambda = R^{-1} DR \quad (2.38)$$

The state transition matrix of the system (2.29) is then given by

$$X(\theta, \theta_0) = P(\theta) \exp [(\theta - \theta_0) \Lambda] P^{-1}(\theta_0) \quad (2.39)$$

where

$$\underline{x}(\theta) = P(\theta) \underline{z}(\theta) \quad (2.40)$$

The matrix $P^{-1}(\theta)$ has been obtained by Tschauner and Hempel (1965) and the following specific form is obtained from Lange and Smith (1965).

$$P^{-1}(\theta) = \begin{bmatrix} c & p & 1/3 & -q_2 & 0 & 0 \\ -2q_1 + e\mu' & -e\mu & 0 & -q_1 & 0 & 0 \\ -\frac{e \sin\theta}{2} & -\frac{1+e \cos\theta}{2} & \frac{e \cos\theta}{2} & 0 & 0 & 0 \\ -\frac{3+e \cos\theta}{2} & 0 & -\frac{e \sin\theta}{2} & -\frac{2+e \cos\theta}{2} & 0 & 0 \\ 0 & 0 & 0 & 0 & 1 & 0 \\ 0 & 0 & 0 & 0 & 0 & 1 \end{bmatrix} \quad (2.41)$$

where:

$$c = \frac{1}{e} \left[1 - (1+2e^2)\sqrt{1-e^2} \right] \sin \theta - (2+3e \cos \theta + e^2) \sin^{-1} \lambda \quad (2.42)$$

$$p = -\frac{1}{6} (1 + 3\sqrt{1-e^2}) - \frac{1}{3e} \left[1 - (1-e^2)^{3/2} \right] \cos \theta$$

$$+ \frac{1}{6} \left[(1+2e^2)\sqrt{1-e^2} - 1 \right] \cos 2\theta - e \mu \sin^{-1} \lambda \quad (2.43)$$

$$q_1 = (1 + e \cos \theta)^2 \quad (2.44)$$

$$q_2 = \frac{1}{3e} \left[(2+e^2)\sqrt{1-e^2} - 2 \right] \sin \theta + \frac{1}{6} \left[(1+2e^2)\sqrt{1-e^2} - 1 \right] \sin 2\theta$$

$$+ (1+e \cos \theta)^2 \sin^{-1} \lambda \quad (2.45)$$

$$\mu = \sin \theta (1+e \cos \theta) \quad (2.46)$$

$$\lambda = \sin \theta \frac{e + (1 - \sqrt{1-e^2}) \cos \theta}{1+e \cos \theta} \quad (2.47)$$

The Jordan canonical form of D is

$$\Lambda = \begin{bmatrix} 0 & 1 & 0 & 0 & 0 & 0 \\ 0 & 0 & 0 & 0 & 0 & 0 \\ 0 & 0 & 0 & 1 & 0 & 0 \\ 0 & 0 & -1 & 0 & 0 & 0 \\ 0 & 0 & 0 & 0 & 0 & 1 \\ 0 & 0 & 0 & 0 & -1 & 0 \end{bmatrix}, \quad (2.48)$$

and the state transition matrix $\exp [(\theta - \theta_0) \Lambda]$ is given by

$$\begin{bmatrix} 1 & (\theta - \theta_0) & 0 & 0 & 0 & 0 \\ 0 & 1 & 0 & 0 & 0 & 0 \\ 0 & 0 & \cos(\theta - \theta_0) & \sin(\theta - \theta_0) & 0 & 0 \\ 0 & 0 & -\sin(\theta - \theta_0) & \cos(\theta - \theta_0) & 0 & 0 \\ 0 & 0 & 0 & 0 & \cos(\theta - \theta_0) & \sin(\theta - \theta_0) \\ 0 & 0 & 0 & 0 & -\sin(\theta - \theta_0) & \cos(\theta - \theta_0) \end{bmatrix} \quad (2.49)$$

The canonical form (2.48) corresponds to three decoupled second-order systems: a pure inertia or $1/s^2$ plant and two harmonic oscillators with a natural period equal to that of the orbit period. The $1/s^2$ plant may be interpreted physically as motion in a similar coplanar coaxial ellipse with higher or lower total energy. One harmonic oscillator corresponds to motion in a coplanar ellipse with the same period, but with different eccentricity and/or orientation.¹

The other harmonic oscillator corresponds to the out-of-plane motion and can be interpreted physically as motion in an ellipse with the same period but with different inclination.

¹

This interpretation was obtained from Lange and Smith (1965).

The solution of (2.24) or (2.29) is given by

$$\underline{x}(\theta) = X(\theta, \theta_0) \left[\underline{x}_0 + \int_{\theta_0}^{\theta} X^{-1}(\tau, \theta_0) B(\tau) \underline{u}(\tau) d\tau \right] \quad (2.50)$$

where \underline{x}_0 is the initial value of the state vector, and

$$X(\theta, \theta_0) = P(\theta) \exp \left[(\theta - \theta_0) \Lambda \right] P^{-1}(\theta_0) \quad (2.51)$$

Also, $X^{-1}(\theta, \theta_0)$ is given by the relation

$$X^{-1}(\theta, \theta_0) = X(\theta_0, \theta) \quad (2.52)$$

Summarizing, the problem is: given the system governed by (2.24) with the solution given by (2.50), find the control $\underline{u}(\theta)$ among all admissible controls, i.e., $|u_\alpha| \leq 1$, $\alpha = x, y, z$, which brings the system from its initial state $\underline{x}(\theta_0)$ to the origin, i.e., $\underline{x}(\theta_f) = \underline{0}$, in the minimum possible time.

III. THE OPTIMAL CONTROL PROBLEM

In this section the basic optimal control problem is stated. This is followed by a synopsis of Pontryagin's maximum principle which is then applied to the rendezvous problem. Finally, Neustadt's method, an iterative procedure for computing the initial value of the adjoint vector which arises in the use of the maximum principle, is presented.

A. Statement of the Problem.

The motion of the system to be controlled is assumed to be described by the set of n first order differential equations.¹

$$\dot{\underline{x}}(t) = \underline{f}(\underline{x}, \underline{u}, t) \quad (3.1)$$

where:

- (i) $\underline{x}(t)$ is an n -dimensional vector called the state vector which at any instant describes the state of the system;
- (ii) $\underline{u}(t)$ is an r -dimensional, $r \leq n$, vector called the control input to the system. The magnitudes of the components $u_1(t), u_2(t), \dots, u_r(t)$, of the

¹ In the discussion of the general problem t is used as the independent variable but when the rendezvous problem is discussed, θ is the independent variable.

control vector $\underline{u}(t)$ are limited by the physical bounds of the system. This is stated mathematically as

$$\underline{u} \in U \quad (3.2)$$

where U is a closed set in the r -dimensional space and is called the control constraint set. The control functions $u_i(t)$, $i = 1, 2, \dots, r$, are assumed to be piecewise continuous. Any control which is piecewise continuous and satisfies (3.2) is called an admissible control.

(iii) $\underline{f}(\underline{x}, \underline{u}, t)$ is an n -dimensional vector function.

The optimal control problem is to find the control function $\underline{u}(t)$ which

- (i) is admissible,
- (ii) brings the system from its initial state $\underline{x}(t_0)$ to some prescribed final state $\underline{x}(t_f)$, and
- (iii) minimizes the performance index or cost function J of the system where

$$J = \int_{t_0}^{t_f} g(\underline{x}, \underline{u}, t) dt \quad (3.3)$$

A control $\underline{u}(t)$ which satisfies these three requirements is called an optimal control.

The total transition time ($t_f - t_o$) may be either an unknown quantity or a prescribed constant, depending on the problem. For the minimum-time problem the total time is to be minimized, hence $g(\underline{x}, \underline{u}, t) = 1$. When the performance index is fuel consumption the final time t_f is specified, and $g(\underline{x}, \underline{u}, t) = h(\underline{u})$, where $h(\underline{u})$ is the relation between the rate of flow of fuel and the control $\underline{u}(t)$.

B. Pontryagin's Maximum Principle.

Pontryagin's maximum principle furnishes a necessary condition for a control to be optimal. However, the existence and uniqueness of an optimal control must be determined by other means. To be presented here is the statement of the maximum principle and its application to the rendezvous problem. The original proof of the maximum principle can be found in Pontryagin et al. (1962). A geometric proof has been provided by Halkin (1963).

Consider the function¹

$$H = \underline{p}^T \dot{\underline{x}} - g(\underline{x}, \underline{u}, t) \quad (3.4)$$

where H is called the Hamiltonian due to its similarity to the Hamiltonian in classical mechanics. The components of the vectors

¹ Note that $\min(J) = -\max(-J)$. Hence, if one wanted to maximize the performance index J , equation (3.3), $+g(\underline{x}, \underline{u}, t)$ would appear in the Hamiltonian rather than $-g(\underline{x}, \underline{u}, t)$.

$\underline{p}(t)$ and $\underline{x}(t)$ satisfy the differential equations

$$\frac{dp_i}{dt} = - \frac{\partial H}{\partial x_i}, \quad i = 1, 2, \dots, n, \quad (3.5)$$

and

$$\frac{dx_i}{dt} = \frac{\partial H}{\partial p_i}, \quad i = 1, 2, \dots, n. \quad (3.6)$$

Note that no boundary conditions are given for $\underline{p}(t)$, hence equation (3.5) does not define a unique vector function. The vector $\underline{p}(t)$ is called the adjoint or costate vector.

Pontryagin's maximum principle states:

Let $\underline{u}^*(t)$ be some admissible control and let $\underline{x}^*(t)$ be the corresponding trajectory. If $\underline{u}^*(t)$ is an optimal control then there exists a vector $\underline{p}^*(t)$ satisfying (3.5) such that at every instant t , $t_0 \leq t \leq t_f$,

$$H(\underline{x}^*, \underline{u}^*, \underline{p}^*, t) \geq H(\underline{x}, \underline{u}, \underline{p}, t) \quad (3.7)$$

with respect to all admissible controls.

That is, the optimal control function $\underline{u}^*(t)$ is that control function which maximizes the Hamiltonian for any given state.

$$\underline{u}^*(t) = \underset{\underline{u} \in U}{\operatorname{argmax}} H(\underline{x}, \underline{p}, \underline{u}, t) \quad (3.8)$$

The maximum principle is now applied to the minimum-time rendezvous problem. The governing differential equation with θ as the independent variable is

$$\underline{x}'(\theta) = A(\theta) \underline{x}(\theta) + B(\theta) \underline{u}(\theta) \quad (3.9)$$

where A and B are defined by equations (2.27) and (2.28). The final state of the system is the origin, i.e., $\underline{x}(\theta_f) = \underline{0}$. The control constraint set is the unit hypercube, i.e., $|u_\alpha| \leq 1$, $\alpha = x, y, z$.

The cost function J is

$$J = \int_{\theta_0}^{\theta_f} d\theta = \theta_f - \theta_0 . \quad (3.10)$$

The Hamiltonian becomes

$$H = \underline{p}^T A \underline{x} + \underline{p}^T B \underline{u} - 1 . \quad (3.11)$$

The optimal control $\underline{u}^*(\theta)$ is given by

$$\underline{u}^*(\theta) = \text{sgn} (B^T \underline{p}) , \quad (3.12)$$

or

$$u_\alpha^*(\theta) = \text{sgn} (B^T \underline{p})_\alpha , \alpha = x, y, z . \quad (3.13)$$

Thus, the system always operates at maximum power, and the components of $\underline{u}^*(\theta)$ have the value +1 or -1. This is the so-called bang-bang control problem. The governing differential equation for the adjoint vector is

$$\underline{p}'(\theta) = -A^T(\theta) \underline{p}(\theta) . \quad (3.14)$$

The solution of (3.14) is

$$\underline{p}(\theta) = X^{-1T}(\theta, \theta_0) \underline{p}(\theta_0) . \quad (3.15)$$

The optimal control $\underline{u}^*(\theta)$ becomes

$$\underline{u}^*(\theta) = \text{sgn} \left[B^T X^{-1T} (\theta, \theta_0) \underline{p}(\theta_0) \right]. \quad (3.16)$$

The components of the optimal control function $\underline{u}^*(\theta)$ are¹

$$\begin{aligned} u_x^* = \text{sgn} \left\{ p_1(\theta_0) \left[-\frac{1}{6} (1 + 3\sqrt{1-e^2}) - \frac{1}{3e} (1 - (1-e^2)^{3/2}) \right] \cos \theta \right. \\ \left. + \frac{1}{6} ((1 + 2e^2) \sqrt{1-e^2} - 1) \cos 2\theta - e \sin \theta (1+e \cos \theta) \sin^{-1} \lambda \right. \\ \left. + e \Delta\theta \sin \theta (1+e \cos \theta) \right] + p_2(\theta_0) \left[-e \sin \theta (1+e \cos \theta) \right] \\ - \frac{1}{2} p_3(\theta_0) \cos \Delta\theta (1+e \cos \theta) \\ \left. - \frac{1}{2} p_4(\theta_0) \sin \Delta\theta (1+e \cos \theta) \right\}, \quad (3.17) \end{aligned}$$

$$\begin{aligned} u_y^* = \text{sgn} \left\{ p_1(\theta_0) \left[-\frac{1}{3e} ((2+e^2) \sqrt{1-e^2} - 2) \sin \theta \right. \right. \\ \left. - \frac{1}{6} ((1+2e^2) \sqrt{1-e^2} - 1) \sin 2\theta - (1+e \cos \theta)^2 \sin^{-1} \lambda \right. \\ \left. + (1+e \cos \theta)^2 \Delta\theta \right] - p_2(\theta_0) (1+e \cos \theta)^2 \\ \left. + \frac{1}{2} p_3(\theta_0) \sin \Delta\theta (2+e \cos \theta) - \right. \\ \left. - \frac{1}{2} p_4(\theta_0) \cos \Delta\theta (2+e \cos \theta) \right\}, \quad (3.18) \end{aligned}$$

$$u_z^* = \text{sgn} \left[-p_5(\theta_0) \sin \Delta\theta + p_6(\theta_0) \cos \Delta\theta \right] \quad (3.19)$$

¹ The canonical form of the equations of motion has been used for this calculation.

where

$$\lambda = \frac{\sin \theta [e + (1 - \sqrt{1-e^2}) \cos \theta]}{1 + e \cos \theta}, \quad (3.20)$$

$$\Delta\theta = \theta - \theta_0. \quad (3.21)$$

When the vehicle is controlled by a single engine for which the direction of the thrust is to be found the control constraint set is the unit hypersphere. The optimal control then takes the form

$$\underline{u}^*(\theta) = \frac{B^T X^{-1T}(\theta, \theta_0) \underline{p}(\theta_0)}{\|B^T X^{-1T}(\theta, \theta_0) \underline{p}(\theta_0)\|}. \quad (3.22)$$

Thus, the engine operates at maximum power, and the direction cosines of the thrust vector are given by equation (3.22).

The optimal control, equation (3.16), is not specified uniquely since the initial value of the adjoint vector $\underline{p}(\theta_0)$ is not known. Thus, the calculation of the optimal control requires the determination of $\underline{p}(\theta_0)$. In linear two-dimensional systems and some simple three-dimensional systems, this problem can be solved by running the system backwards, that is, replace t with $-t$, start at the origin and investigate the solution. This procedure gives surfaces, commonly called switching surfaces, on which the components of the control vector change sign. Thus, the optimal control function is known as a function of the state of the system, i.e., a feedback control system. Since

this can only be done in the simpler cases some other procedure must be used for the more complicated problems. One such procedure has been developed by Neustadt (1960).

C. Neustadt's Method.

1. Theory

Under consideration is the determination of the control which will bring a given system from its initial state $\underline{x}(t_0)$ to the origin in the minimum possible time. The motion of the system is assumed to be described by the set of n first order linear differential equations

$$\dot{\underline{x}}(t) = A(t) \underline{x}(t) + B(t) \underline{u}(t) \quad (3.23)$$

where $\underline{u}(t)$ is an r -dimensional piecewise continuous function of time and is constrained to a compact, convex set U which contains the origin; in this particular case the unit hypercube, i.e., $|u_i| \leq 1, i = 1, 2, \dots, r$. The solution of (3.23) is given by

$$\underline{x}(t) = X(t, t_0) \left[\underline{x}_0 + \int_{t_0}^t X^{-1}(\tau, t_0) B(\tau) \underline{u}(\tau) d\tau \right] \quad (3.24)$$

where $\underline{x}_0 = \underline{x}(t_0)$.

Define

$$C(t) = \left\{ - \int_{t_0}^t X^{-1}(\tau, t_0) B(\tau) \underline{u}(\tau) d\tau : \underline{u}(\tau) \text{ admissible} \right\} \quad (3.25)$$

$C(t)$ is called the set of reachable events and consists of those

points which can be transferred to the origin in time $(t - t_0)$, using an admissible control. The boundary of $C(t)$ is a surface of constant optimal time. Each point \underline{x} is a point on the boundary of $C(t)$ for some time t . At the point \underline{x} , the normal to the surface directed toward $C(t)$ is the optimal initial value of the adjoint vector. This has been shown by many authors, in particular, Halkin (1963). These surfaces are continuous but they are not necessarily smooth; corners may exist as shown in Figure 2.

Since U is a compact, convex set, $C(t')$ is contained in $C(t)$, i.e., $C(t') \subset C(t)$, for $t' < t$. Thus, there is a smallest t , t^* , for which $\underline{x}_0 \in C(t^*)$, i.e., there is a control which transfers \underline{x}_0 to the origin in the minimum possible time. Also, \underline{x}_0 is a boundary point of $C(t^*)$.

Use of Neustadt's method requires that the control system be a normal control system. This requirement is satisfied for our problem and discussed in Appendix B.

Define

$$\underline{\psi} \equiv - \underline{p}(t_0) \quad , \quad (3.26)$$

and

$$\underline{z}(t, \underline{\psi}) = - \int_{t_0}^t X^{-1}(\tau, t_0) B(\tau) \underline{u}(\tau, \underline{\psi}) \, d\tau \quad (3.27)$$

where $\underline{u}(\tau, \underline{\psi})$ is given by

$$\underline{u}(\tau, \underline{\psi}) = - \left[\text{sgn} \quad B^T(\tau) X^{-1T}(\tau, t_0) \underline{\psi} \right] . \quad (3.28)$$

The problem now is to find a vector $\underline{\psi}$ which will map the vector $\underline{z}(t, \underline{\psi})$ into \underline{x}_0 . Neustadt's method is an iterative procedure which performs this mapping.

Consider the function

$$f(t, \underline{\psi}; \underline{x}_0) = \underline{\psi} \cdot [\underline{z}(t, \underline{\psi}) - \underline{x}_0] . \quad (3.29)$$

Let the domain of $\underline{\psi}$ be restricted to those $\underline{\psi}$ for which $\underline{\psi} \cdot \underline{x}_0 > 0$. This makes no restrictions on the problem since $C(t)$ is convex and the optimal $\underline{\psi}, \underline{\psi}^*$, is the vector normal to $C(t^*)$ at \underline{x}_0 and directed away from $C(t^*)$. Hence,

$$\underline{\psi}^* \cdot \underline{x}_0 > 0 .$$

For $\underline{\psi} \neq 0$ it can be shown that $f(t, \underline{\psi}; \underline{x}_0)$ is a continuous, strictly monotonically increasing function of t . Since $C(t)$ is convex

$$\underline{\psi} \cdot \underline{z}(t, \underline{\psi}) > \underline{\psi} \cdot \underline{y} \quad \text{for all } \underline{y} \in C(t), \underline{y} \neq \underline{z}(t, \underline{\psi}) \quad (3.30)$$

as shown in Figure 3b. Therefore, if $\underline{z}(t^*, \underline{\psi}) \neq \underline{x}_0$

$$\underline{\psi} \cdot \underline{z}(t^*, \underline{\psi}) \geq \underline{\psi} \cdot \underline{x}_0 ,$$

hence

$$f(t^*, \underline{\psi}; \underline{x}_0) = \underline{\psi} \cdot [\underline{z}(t^*, \underline{\psi}) - \underline{x}_0] > 0 .$$

Since $f(t_0, \underline{\psi}; \underline{x}_0)$ is negative and $f(t^*, \underline{\psi}; \underline{x}_0)$ is positive,

at some time $\bar{t} < t^*$, $f(\bar{t}, \underline{\psi}; \underline{x}_0) = 0$. This is the time for which the \underline{z} trajectory passes through the hyperplane which passes through \underline{x} with normal $\underline{\psi}$ as shown in Figure 3a. This $\underline{\psi}$ is the optimal $\underline{\psi}$ for the point $\underline{z}(\bar{t}, \underline{\psi})$, hence it is normal to the boundary of $C(\bar{t})$.

Define $F(\underline{\psi}; \underline{x}_0)$ as

$$f(F(\underline{\psi}; \underline{x}_0), \underline{\psi}; \underline{x}_0) = 0 \quad (3.31)$$

Therefore, $t_0 < F(\underline{\psi}; \underline{x}_0) \leq t^*$. Also, $F(\underline{\psi}; \underline{x}_0) = t^*$, the optimum time, if, and only if $\underline{z}(t^*, \underline{\psi}) = \underline{x}_0$, in which case $\underline{u}(t, \underline{\psi})$ is the optimal control which transfers \underline{x}_0 to the origin in the time $(t^* - t_0)$. The validity of these statements can be seen from the convexity of $C(t)$. It was shown that

$$\underline{\psi} \cdot \underline{z}(F(\underline{\psi}; \underline{x}_0), \underline{\psi}) \geq \underline{\psi} \cdot \underline{y}$$

for all $\underline{y} \in C(F(\underline{\psi}; \underline{x}_0))$. But, by definition of $F(\underline{\psi}; \underline{x}_0)$

$$\underline{\psi} \cdot \underline{z}(F(\underline{\psi}; \underline{x}_0), \underline{\psi}) = \underline{\psi} \cdot \underline{x}_0$$

Therefore, if $\underline{z}(F(\underline{\psi}; \underline{x}_0), \underline{\psi}) \neq \underline{x}_0$, \underline{x}_0 cannot lie inside $C(F(\underline{\psi}; \underline{x}_0))$ and must lie outside of $C(F(\underline{\psi}; \underline{x}_0))$. Since $C(t^*)$ is convex and \underline{x}_0 is a boundary point of $C(t^*)$, $F(\underline{\psi}; \underline{x}_0) < t^*$, unless $\underline{z}(F(\underline{\psi}; \underline{x}_0), \underline{\psi}) = \underline{x}_0$, in which case $F(\underline{\psi}; \underline{x}_0) = t^*$. Thus, the maximum value of $F(\underline{\psi}; \underline{x}_0)$ occurs when $\underline{z}(F(\underline{\psi}; \underline{x}_0), \underline{\psi}) = \underline{x}_0$.

Therefore, the goal is to find a value of $\underline{\psi}$ which will maximize the function $F(\underline{\psi}; \underline{x}_0)$, where the maximum value of $F(\underline{\psi}; \underline{x}_0)$ is the optimum (minimum) time, and the location of the maximum determines the optimal control.

One aspect of Neustadt's method which makes it extremely useful is that the gradient of $F(\underline{\psi}; \underline{x}_0)$ with respect to $\underline{\psi}$ is proportional to the "error vector" $[\underline{z}(F(\underline{\psi}; \underline{x}_0), \underline{\psi}) - \underline{x}_0]$.

2. Computation

The iterative procedure for finding the maximum of the function $F(\underline{\psi}; \underline{x}_0)$ will now be presented.

The iterative procedure is started by making an initial guess for $\underline{\psi}$, designated by $\underline{\psi}_0$. A reasonable guess is the unit vector parallel to the initial state vector, i.e.,

$$\underline{\psi}_0 = \frac{\underline{x}_0}{\|\underline{x}_0\|} \quad (3.33)$$

Let $\underline{\psi}_i$ be the i -th guess. The function $\underline{z}(t, \underline{\psi}_i)$ is then generated as a function of time until

$$f(t, \underline{\psi}_i; \underline{x}_0) = \underline{\psi}_i \cdot [\underline{z}(t, \underline{\psi}_i) - \underline{x}_0] = 0$$

This time is $F(\underline{\psi}_i; \underline{x}_0)$, and the gradient is given by

$$\nabla F(\underline{\psi}_i; \underline{x}_0) = - \left(\frac{\partial f}{\partial t} \right)^{-1} \left[\underline{z}(F(\underline{\psi}_i; \underline{x}_0), \underline{\psi}_i) - \underline{x}_0 \right] \quad (3.34)$$

where $\left(\frac{\partial f}{\partial t} \right)$ is a non-negative function. A correction is now made to $\underline{\psi}_i$ and the procedure repeated with

$$\underline{\psi}_{-i+1} = \underline{\psi}_{-i} + \delta \underline{\psi}_{-i} \quad (3.35)$$

Computation is stopped when the magnitude of the error vector is less than some small value ϵ :

$$\| \underline{z}(F(\underline{\psi}_i; \underline{x}_0), \underline{\psi}_i) - \underline{x}_0 \| < \epsilon \quad (3.36)$$

Since the gradient is known the method of steepest ascent can be used for the correction, i.e., the correction is made in the direction of the gradient of F :

$$\delta \underline{\psi}_i = K_1 \nabla F(\underline{\psi}_i; \underline{x}_0) = - K_2 \left[\underline{z}(F(\underline{\psi}_i; \underline{x}_0), \underline{\psi}_i) - \underline{x}_0 \right] \quad (3.37)$$

It can then be shown (if K_2 is sufficiently small) that

$$F(\underline{\psi}_{-i+1}; \underline{x}_0) > F(\underline{\psi}_i; \underline{x}_0) \quad (3.38)$$

Hence, the iteration method will converge to a value of $\underline{\psi}$ which will define the time-optimal control $\underline{u}(t, \underline{\psi})$, and will maximize the function $F(\underline{\psi}; \underline{x}_0)$. However, Neustadt and Paiewonsky (1963) have shown that finding the optimum $\underline{\psi}$ may be difficult. In many

cases the function $F(\underline{\psi}; \underline{x}_0)$ is a very flat function of $\underline{\psi}$, in which case a small change in $\underline{\psi}$ from the optimum creates a very small change in $F(\underline{\psi}; \underline{x}_0)$ but a large displacement in the trajectory

$$[\underline{z}(F(\underline{\psi}; \underline{x}_0), \underline{\psi}) - \underline{x}_0] .$$

Because the function $F(\underline{\psi}; \underline{x}_0)$ is so flat the method of steepest ascent converges slowly. A search was made to find a more rapid convergent method. The convergence method used in this study was developed by Fletcher and Powell (1963). It converges rapidly and is also easy to program. This method is a modification of the variable metric method developed by Davidon (1959). The Fletcher-Powell method has second order convergence, i.e., the procedure converges in n iterations when the function is a quadratic of n variables. The correction $\delta\underline{\psi}_i$ is not made in the direction of the gradient (method of steepest ascent), but in a modified direction defined by

$$\delta\underline{\psi}_i = H_i \nabla F(\underline{\psi}_i; \underline{x}_0) \quad (3.39)$$

where H_i is a positive definite, symmetric, $n \times n$ matrix. A description of the Fletcher-Powell method is given in Appendix C.

The convergence rate of the Fletcher-Powell method for a rendezvous problem is shown in Figure 4. In this example the

criteria for terminating the computation was

$\|\underline{z}(F(\underline{\psi}; \underline{x}_0), \underline{\psi}) - \underline{x}_0\| < 10^{-3}$. Fifteen optimum steps¹ requiring 70 iterations were required for convergence. Although the stopping time (time at which $f(t, \underline{\psi}; \underline{x}_0) = 0$) increases each step, the magnitude of the error vector $[\underline{z}(F(\underline{\psi}; \underline{x}_0), \underline{\psi}) - \underline{x}_0]$ does not necessarily decrease each step. In fact, it generally does not decrease much until the optimum time is established, at which time it starts to decrease rapidly each step. In the example shown in Figure 4, the magnitude of the error vector is larger after 57 iterations than after the first iteration, but it then decreases three orders of magnitude in the next 13 iterations. This same example was worked using the method of steepest ascent with optimum steps. A comparison of the two methods is given in Figure 5. Using the method of steepest ascent with optimum steps the optimum time was not obtained after 300 iterations as compared to the 70 iterations required to obtain the optimum time using the Fletcher-Powell method.

¹ See Appendix C for a description of an optimum step.

IV. CIRCULAR ORBIT

If the control system is normal (see Appendix B) the optimal control, if it exists, is unique. However, when the control system is not normal there may be more than one optimal control. There will be an optimal control which is bang-bang, but there may be others which are not bang-bang. When the target vehicle orbit is elliptic the normality condition is satisfied, but when it is circular the control system is not normal. Neustadt's method is restricted to normal control systems, therefore the circular orbit problem must be given further consideration.

The optimal control equations (equations (3.17) and (3.18)) for a circular target vehicle orbit are

$$u_x^* = - \operatorname{sgn} \left[\frac{4}{3} p_1(\theta_0) + p_3(\theta_0) \cos \Delta\theta + p_4(\theta_0) \sin \Delta\theta \right], \quad (4.1)$$

and

$$u_y^* = -\operatorname{sgn} \left[-p_1(\theta_0) \Delta\theta + p_2(\theta_0) - p_3(\theta_0) \sin \Delta\theta + p_4(\theta_0) \cos \Delta\theta \right]. \quad (4.2)$$

Now let $p_1(\theta_0) = p_3(\theta_0) = p_4(\theta_0) = 0$, $p_2(\theta_0) \neq 0$, and the optimal control becomes

$$u_x^* = \operatorname{sgn} [0], \quad (4.3)$$

and

$$u_y^* = \operatorname{sgn} [p_2(\theta_0)]. \quad (4.4)$$

$\operatorname{Sgn} [0]$ is undefined, hence u_x^* is not uniquely defined; it can

take on any value between +1 and -1. However, if there is more than one optimal control at least one will be bang-bang. Therefore, no generality is lost if u_x^* is restricted to +1 and -1. This type of control is called singular control.

A requirement for the use of Neustadt's method is that the control system be normal. It will now be shown that for non-normal control systems Neustadt's method will not give a wrong solution. It may not give a solution but if it does, the solution is optimal. An example will then be given to illustrate the singular control problem.

La Salle (1960) has shown that the set of reachable events $C(t)$ is convex. Therefore, if an admissible control satisfying (3.16) is found which will bring the system from its initial state \underline{x}_0 to the origin it is an optimal control. At some t \underline{x}_0 is a point on the boundary of $C(t)$. The normal to the boundary of $C(t)$ at \underline{x}_0 , if it exists, directed toward $C(t)$ is the optimum initial adjoint vector. The direction of the normal, if it exists, is unique. Therefore, a unique solution is defined by the normal to $C(t)$ except when the direction of the normal is such that the singular control condition $\text{sgn}(0)$ occurs, in which case the optimal control is not unique. The set of reachable events consists of two subsets: 1) the set of points which can be reached by non-singular control, and 2) the set of points which can be reached only by singular control. If \underline{x}_0 is a point which can be reached by non-singular control Neustadt's

method will give the solution since the direction of the normal to $C(t)$ is unique. When \underline{x}_0 is a point which can be reached only by singular control Neustadt's method will not give the solution. The optimal control is defined by $\text{sgn}(0)$ and this is not defined. If enough iterations are made Neustadt's method will give a value of the optimum time which is less than but a good approximation of the optimum time, and it will give a value of the initial adjoint vector which is close to the optimum initial adjoint vector. The initial values of the adjoint variables which define singular control in this investigation are $p_1(\theta_0) = p_3(\theta_0) = p_4(\theta_0) = 0$, and $p_2(\theta_0) \neq 0$. The portions of the boundary of $C(t)$ which are defined by singular control are hyperplanes since the normal to the boundary at each point has the same direction. However, this is not true in all singular control problems.

Theoretically, this singular control problem could be circumvented by using a very small value of the target vehicle orbit eccentricity e . The control system is then normal, and the optimum control is unique. However, the portions of the boundary which would be defined by singular control for a circular orbit are very flat, and it may be difficult to obtain a solution. Extreme accuracy would be required to obtain a solution, and double precision would probably have to be used in the computer program.

Now consider the example

$$\begin{aligned}\dot{x}_1 &= x_2 + u_1 \\ \dot{x}_2 &= u_2\end{aligned}\tag{4.5}$$

with the constraint

$$|u_1| \leq 1, \quad |u_2| \leq 1 \quad .\tag{4.6}$$

The optimal control functions found by applying Pontryagin's maximum principle are

$$u_1^* = \text{sgn} [p_1(0)]\tag{4.7}$$

$$u_2^* = \text{sgn} [-p_1(0)t + p_2(0)] \quad .\tag{4.8}$$

Therefore, in non-singular control u_1 is constant and u_2 switches at most once. In singular control, $p_1(0) = 0$, u_2 is constant and u_1 can be any value between +1 and -1.

Optimal isochrones (boundary of $C(t)$) and optimum trajectories are shown in Figure 6. The boundary of $C(t)$ for $t = 1.5$ is given by the curve ABCDA. The region defined by non-singular control is that portion of the plane to the right of the curve BOC and the portion to the left of the curve AOD. For any point to the right of the curve BOC, for example point E, the optimal control is initially $u_1 = -1$ and $u_2 = -1$. When the trajectory intersects the curve OC u_2 switches to +1 and the trajectory goes into the origin. The optimum initial values of the adjoint variables for this region

are $p_1(0) < 0$ and $p_2(0) < 0$. Similar conditions exist for the region to the left of AOD. For any point in this region, for example point F, the optimal control is initially $u_1 = 1$ and $u_2 = 1$. When the trajectory intersects the curve OA u_2 switches to -1 . The optimum initial values of the adjoint variable in this region are $p_1(0) > 0$ and $p_2(0) > 0$. The singular control condition is $p_1(0) = 0$ and $p_2(0) \neq 0$. Thus, $u_1 = \text{sgn}(0)$ and $u_2 = \text{sgn}(p_2(0))$. The region defined by singular control is the area bounded by the curve AOB and the area bounded by COD. Now consider a point in the singular control region, point G. There are an infinite number of ways to reach the origin from point G. Three ways will be given:

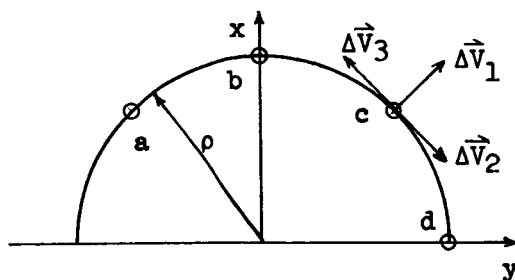
- 1) Initially let $u_1 = -1$ and $u_2 = -1$. The trajectory is the curve GHO as shown. When the trajectory intersects the curve OA switch u_1 from -1 to $+1$.
- 2) Initially let $u_1 = 1$ and $u_2 = -1$. The trajectory is the curve GJO. When the trajectory reaches the curve OB switch u_1 from $+1$ to -1 .
- 3) Let $u_1 = -0.08$ and $u_2 = -1$. The trajectory will go directly to the origin without any switching being required as shown by the curve GO.

Since the singular control condition is $p_1(0) = 0$ and $p_2(0) \neq 0$ the portions of the boundary of $C(t)$ defined by singular control are flat as shown by the curves AB and DC. The curves OA, OB, OC, and OD are called switching curves.

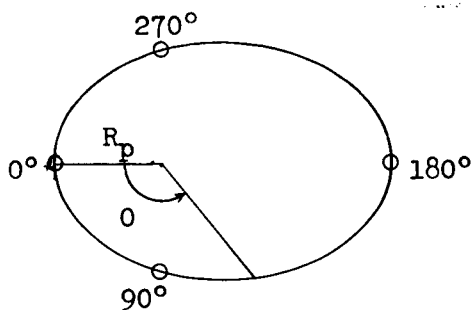
V. DISCUSSION OF RESULTS

A. In-plane Motion.

Because of the large number of parameters involved, thrust level, orbit eccentricity, initial value of the true anomaly, initial conditions, it is impractical to present results of a general nature. However, so that some insight of the time-optimal maneuver can be obtained, the initial conditions are chosen in the following manner: at a separation distance ρ of $150,000\sqrt{2}$ ft. with a relative velocity $\Delta\vec{V}$ of $100\sqrt{2}$ ft./sec. three situations are considered as shown at point c in the figure below. 1) the interceptor moving away from the target vehicle along the line of sight ($\Delta\vec{V}_1$), 2) the interceptor moving perpendicular to the line of sight in the clockwise direction ($\Delta\vec{V}_2$), and 3) the interceptor moving perpendicular to the line of sight in the counterclockwise direction ($\Delta\vec{V}_3$); these three situations are considered at four points in the x - y plane as shown in the following figure;



initial values of the true anomaly considered are 0° (perigee), 90° , 180° (apogee), 270° as shown in the following figure;



an orbital eccentricity of 0.5 and a perigee distance of 4100 miles are used. Only points in the upper half of the $x - y$ plane have been considered since the optimal control function \underline{u}^* for the initial condition $-\underline{x}_0$ is just the negative of the optimal control function for the initial condition \underline{x}_0 . In this investigation the maximum allowable thrust acceleration is assumed to be constant. Inclusion of the effect of a variable mass is not difficult. However, including this effect makes the presentation of any concise results difficult if a range of specific impulse is considered. The total thrust acceleration¹, A_{\max} , considered in the above cases is 0.25 ft/sec^2 . Total thrust accelerations of 0.5, 0.75, 1.0 are then considered for the above conditions only with $\theta_0 = 0^\circ$ (perigee). Optimum rendezvous trajectories for the above conditions are presented in Figures 7 - 26.

¹ This is the total thrust acceleration, hence the value of the components is $U_{\max} = A_{\max} \frac{\sqrt{2}}{2}$.

In Figures 7, 10, 12, 14, 16, 19, 22, 24 optimum rendezvous trajectories are given for the situation when the interceptor is initially moving away from the target vehicle along the line of sight. In all of these examples the interceptor moves in the counterclockwise direction. Optimum rendezvous trajectories for the situation when the interceptor is initially moving perpendicular to the line of sight in the counterclockwise direction are given in Figures 9, 18, 21, 26. In each of these cases the interceptor continues to move in the counterclockwise direction. Optimum rendezvous trajectories are presented in Figures 8, 11, 13, 15, 17, 20, 23, 25 for the situation when the interceptor is initially moving perpendicular to the line of sight in the clockwise direction. Except for the case when $\theta_0 = 180^\circ$ (apogee) the interceptor must reverse direction and move in the counterclockwise direction before rendezvous occurs. Hence, the time duration of the rendezvous maneuver when the interceptor is initially moving in the clockwise direction is greater than the time duration when the interceptor is initially moving in the counterclockwise direction. For instance, consider the example when the interceptor is initially above the target and $A_{\max} = 0.25$, $\theta_0 = 0^\circ$. Slightly more than one orbit is required to complete the rendezvous maneuver when the interceptor is initially moving in the clockwise direction (Figure 8, case b) and 1/2 of an orbit is required when the interceptor is initially

moving in the counterclockwise direction (Figure 9, case b). For the case when the target vehicle is initially at apogee ($\theta_0 = 180^\circ$) the gravity force is much smaller, and the interceptor does not need to reverse direction to complete the rendezvous maneuver in the minimum possible time. The effect of the gravity force on the maneuver can also be seen by comparing the trajectories of the examples when the interceptor is above (below) the target vehicle and forward (behind) the target vehicle. As an example consider the trajectories given in Figure 7. The interceptor is initially $150,000\sqrt{2}$ feet from the target vehicle and is moving away at a velocity of $100\sqrt{2}$ ft/sec. When the interceptor is initially above the target vehicle (case b) the maximum excursion from the target vehicle is 3,500,000 feet as compared to 250,000 feet when it is initially in front of the target vehicle (case d). The time duration of these two maneuvers is $2/3$ of an orbit and $1/3$ of an orbit.

Optimum rendezvous trajectories for different maximum allowable thrust levels are presented in Figures 27 - 30. The relation of the optimum time to the thrust level for the examples presented in Figures 27 and 28 is given in Figure 31. For the example shown in Figure 28 there is a tremendous difference in the trajectories as the thrust level increases from 0.25 to 0.5 ft/sec^2 . The difference in the trajectories shown in Figure 27 is not as great. This effect is also seen by an inspection of the curves given in Figure 31. The

optimum time decreases more rapidly for the example shown in Figure 28 than for the one shown in Figure 27.

Optimum rendezvous trajectories for various initial values of the true anomaly θ are presented in Figures 32 - 34. These trajectories are also given in Figures 1 - 26 but are presented in this manner so that the effect of the starting point on the orbit can be seen better.

The effect of the orbit eccentricity on the optimum rendezvous trajectory is shown in Figures 35 and 36. The initial conditions chosen are a separation distance of 200,000 feet with the interceptor moving away from the target vehicle at a velocity of 150 ft/sec. In Figure 35 the interceptor is initially above the target vehicle and in Figure 36 it is initially in front of the target vehicle. The effect of the orbit eccentricity on the trajectory is greater when the interceptor is initially above the target vehicle. The basic reason for this is that when the interceptor is initially forward of the target vehicle the effect of gravity on the relative motion of the two vehicles is less than when the interceptor is initially above the target vehicle. Hence, a change in the gravity force because of the eccentricity of the orbit does not have as much effect when the interceptor is forward of the target vehicle. Another contributing factor is that the time duration of the rendezvous maneuver when the interceptor is initially

forward of the target vehicle is less than the time duration when the interceptor is initially above the target vehicle. Since the time duration of the maneuver is less, the change in the gravity force due to the eccentricity is less.

In figures 37 and 38 a comparison of the multiple engine control to the single engine control is given. The total thrust acceleration is the same for both cases. The time required for rendezvous using multiple engine control will always be greater than or equal to the time required for rendezvous using single engine control. The reason for this is very simple. In the single engine control the control constraint set U is the hypersphere (in two dimensions a circle), and the optimum control is some point on the surface of this hypersphere. In the multiple engine control the control constraint set is the hypercube (square in two dimensions), and the optimum control is one of the vertices of this hypercube. Hence, the optimum control in the multiple engine case is restricted to one of the four points on the circle as compared to any point on the circle in the single engine control. In the examples considered the minimum time required for rendezvous using single engine control was 5 percent - 20 percent less than the time required using multiple engine control. However, inspection of the optimum thrust angle vs. time curve shows that there is a rapid change of 120° to 180° in the optimum thrust angle. In reality, this rapid change may be very

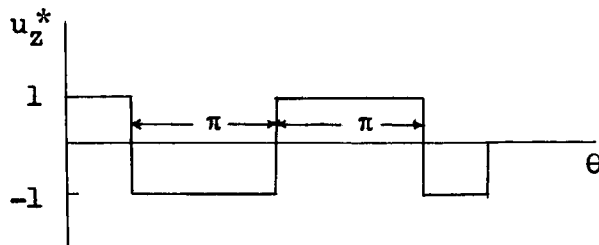
difficult to obtain, and large errors could result. The optimum thrust angle vs. time plots given in Kaminski (1966) and Paiewonsky and Woodrow (1965) show this same characteristic.

As was stated in Chapter IV when the target vehicle is in a circular orbit there are certain initial conditions for which the optimal control is not unique. For these initial conditions Neustadt's method will not yield a solution. The same set of initial conditions that were investigated for the elliptic orbit case were investigated for the circular orbit case. Solutions were obtained and optimum rendezvous trajectories for the case when the interceptor is initially moving away from the target vehicle are given in Figure 39. To investigate the singular region the coordinates of a point in the singular region were found by integrating the equations of motion in backward time from the origin using singular control. The coordinates of this point were then input into the computer program as initial conditions. A solution could not be obtained. The optimum time calculated by Neustadt's method was very close to the actual optimum time, and the initial value of the adjoint vector was approaching the optimum one. The optimum time was 1.57 and the optimum time computed by Neustadt's method after 129 iterations was 1.53. The optimum adjoint initial conditions were $p_1(\theta_0) = p_3(\theta_0) = p_4(\theta_0) = 0$ and $p_2(\theta_0) > 0$. The adjoint initial conditions obtained by Neustadt's method were

$p_1(\theta_0) = -4 \times 10^{-9}$, $p_3(\theta_0) = 3 \times 10^{-9}$, $p_4(\theta_0) = 5 \times 10^{-9}$ and $p_2(\theta_0) = 2$. Thus, one can see that the optimum adjoint initial conditions are being approached, but a solution cannot be obtained for the singular control condition until they are matched identically, and this is impossible using a digital process. An eccentricity of 0.01 was then used, but a solution could not be obtained. A unique solution exists, however, to obtain the accuracy that would be needed to get a solution double precision would have to be used.

B. Out-of-Plane Motion.

The out-of-plane motion is that of a simple oscillator with a period equal to the period of the target vehicle orbit. Equation (3.19) shows that u_z^* is always +1 or -1 and switches between these two values every π units of time, except for the first and last intervals of time which may be less than π as shown in the following figure.



Generally, only one switching will occur since less than 1/2 of an orbit is usually required to nullify the out-of-plane motion. The coefficient of the control function u_z is periodic except when the

target vehicle orbit is circular, in which case it becomes constant. When this coefficient is constant a switching surface can be determined for u_z^* as shown in Figure 41. This problem was first solved by Bushaw (1958).

Typical out-of-plane motions are shown by the $z - \dot{z}$ plots in Figure 40. The initial conditions are $z = 100,000$ feet and $\dot{z} = 100$ ft/sec. The curves for $e = 0$ and $e = 0.5$ are very close together. This suggests that an approximate switching surface could be used by assuming the coefficient of u_z to be constant and using the switching surface from Bushaw's problem.

VI CONCLUSIONS

The rendezvous maneuver will be a very important part of space missions in the future. In a rescue mission, minimizing the time duration of the rendezvous maneuver will be of utmost importance. This investigation is a study of the time-optimal rendezvous maneuver when the target vehicle is moving in a known elliptic orbit. The propulsion system of the maneuverable or interceptor vehicle is a multiple engine system which can impart a variable thrust independently in three perpendicular directions. It is assumed that the orientation of the interceptor is such that the directions of the three independent thrust components are:

- 1) perpendicular to the orbit plane of the target vehicle,
 - 2) along the radius vector from the center of the earth to the target vehicle, and
 - 3) perpendicular to the radius vector from the center of the earth to the target vehicle and in the orbit plane of the target vehicle.
- The attitude stability of the vehicle is not considered in this study.

The equations of motion are written with respect to a moving coordinate system whose origin is located at the target vehicle and which rotates with an angular velocity equal to the angular velocity of the radius vector from the center of the earth to the target vehicle. The true anomaly of the target vehicle orbit is used as the independent

variables, and the ratio of the difference coordinates to the distance of the target vehicle from the center of the earth are the dependent variables. By making the assumption that the distance between the two vehicles is small compared to the distance of the target vehicle from the center of the earth a system of linear equations with periodic coefficients is obtained. This linearization allows the equations of motion describing motion in the orbit plane of the target vehicle to be decoupled from the equations describing motion perpendicular to the orbit plane. Thus, the two problems can be handled separately.

Pontryagin's maximum principle is used to find the optimal control law. Use of the maximum principle introduces the adjoint variables for which the initial conditions are unknown. Neustadt's method is used to find these initial conditions. Neustadt's method transforms the two-point boundary value problem into one of maximizing a function where the location of the maximum is the desired adjoint initial condition, and the value of the function at the maximum is the optimum (minimum) time. The Fletcher-Powell modification of Davidon's variable metric method is used to find the maximum of the function.

Optimum rendezvous trajectories for various initial conditions, maximum allowable thrust accelerations, and values of the target vehicle eccentricity are presented. Maximum allowable thrust accelerations from 0.25 to 1.0 ft/sec² are considered. Orbital eccentricities from 0 to 0.6 are investigated.

A comparison is made of the multiple engine control system used in

this investigation and the single engine control system for which the magnitude and direction of the thrust vector are found as a function of time. This comparison shows that the single engine control system takes less time than the multiple engine control system. However the difference is very small compared to the total optimal time. This comparison also shows the difference between the degrees of complexity for handling the interceptor vehicle (maneuvering vehicle). In the single engine control system, the vehicle needs to be rotated almost 180° in a short period of time. On the other hand, in the multiple engine control system, the attitude of the interceptor needs to be changed in a similar way as the target vehicle whose attitude changes very smoothly and slowly.

VII BIBLIOGRAPHY

1. ATHANS, M. and FALB, P. (1966): Optimal Control, McGraw-Hill, 1966.
2. BENDER, D. F. (1963): "Rendezvous Possibilities with the Impulse of Optimum Two-Impulse Transfer," Adv. in the Astronautical Sciences, Vol. 16, 1963, pp. 271-291.
3. BUSHAW, D. W. (1958): "Optimal Discontinuous Forcing Terms," Contributions to the Theory of Nonlinear Oscillations, Vol. IV, Princeton University Press, 1958, pp. 29-52.
4. CARNEY, T. M. (1963): On Energy-Optimal Trajectories in Three Dimensions for the Terminal Phase of Rendezvous, NASA TR R-175, December 1963.
5. CICOLANI, L. S. (1961): Trajectory Control in Rendezvous Problems Using Proportional Navigation, NASA TN D-772, April 1961.
6. CLOHESSY, W. H. and WILTSHIRE, R. S. (1960): "Terminal Guidance System for Satellite Rendezvous," Jour. of Aero/Space Sciences, Vol. 27, No. 9, September 1960, pp. 653-658.
7. CODDINGTON, E. A. and LEVINSON, N. (1955): Theory of Ordinary Differential Equations, McGraw-Hill, 1955.

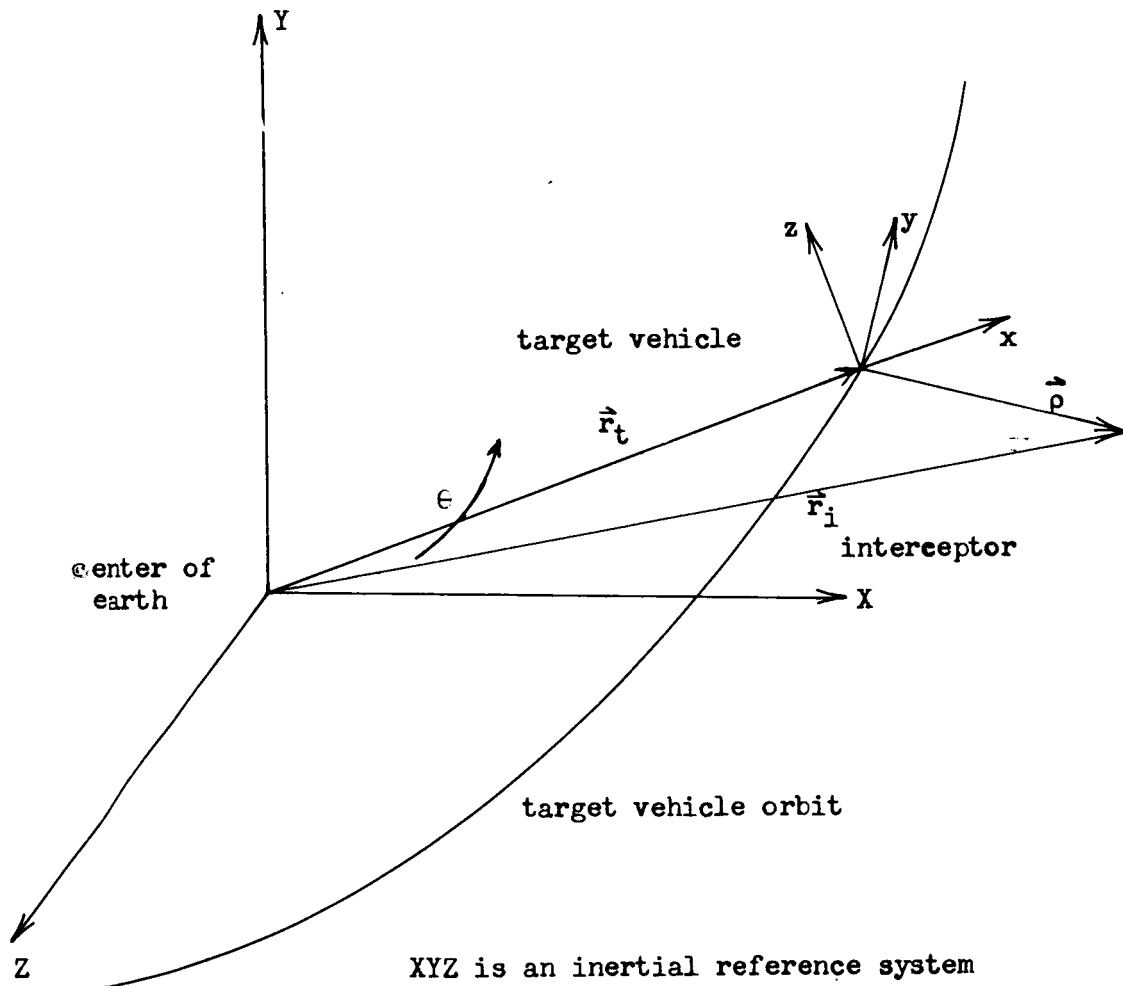
8. DAVIDON, W. C. (1959): Variable Metric Method for Minimization, Argonne Natl. Lab. Report ANL-5990, May 1959.
9. DEUTSCH, R. A. (1963): Orbital Dynamics of Space Vehicles, Prentice-Hall, 1963.
10. EGGLESTON, J. M. (1961): A Study of the Optimum Velocity Change to Intercept and Rendezvous, NASA TN 1029, February 1962.
11. FLETCHER, R. and POWELL, M. J. D. (1963): "A Rapidly Convergent Descent Method for Minimization," The Computer Journal, July 1963, pp. 163-168.
12. GOLDSTEIN, A. A., GREENE, A. H. and JOHNSON, A. T. (1963): "Fuel Optimization in Orbital Rendezvous," Progress in Astronautics and Aeronautics, Vol. 13, pp. 865-885.
13. HALKIN, H. (1963): "The Principle of Optimal Evolution," Nonlinear Differential Equations and Nonlinear Mechanics, J. P. LaSalle and S. Lefschetz (eds.), Academic Press, 1963.
14. HARRISON, E. (1963): "Rendezvous Energy Required for Collision and Pursuit Course Guidance," Adv. in the Astronautical Sciences, Vol. 16, 1963, pp. 271-291.
15. HORNBY, H. (1962): An Analytical Study of Orbital Rendezvous for Least Fuel and Least Energy, NASA TN D-1207, March 1962.
16. KAMINSKI, P. G. (1966): Optimal Co-Altitude Rendezvous with Constant Thrust Acceleration, M. S. Thesis, Departments of

Aeronautics and Astronautics and Electrical Engineering,
Mass. Inst. of Technology, 1966.

17. KELLEY, H. J. and DUNN, J. C. (1963): "An Optimal Guidance Approximation for Quasi-Circular Orbital Rendezvous," Proc. 2nd Int. Congress on Automatic Control, Basle, Sept. 1963, pp. 274-282.
18. LANGE, B. O. and SMITH, R. G. (1965): The Application of Floquet Theory to the Computation of Small Orbital Perturbations Over Long Time Intervals Using the Tschauner-Hempel Equations, Dept. of Aeronautics and Astronautics, Stanford University, SUDAER No. 241, 1965.
19. LASALLE, J. P. (1960): "The Time Optimal Control Problem," Contributions to the Theory of Nonlinear Oscillations, Vol. V, Princeton Univ. Press, 1960, pp. 1-24.
20. MEDITCH, J. S. and NEUSTADT, L. W. (1963): "An Application of Optimal Control to Midcourse Guidance," Proc. 2nd Congress on Automatic Control, Basle, September 1963, pp. 292-299.
21. NELSON, W. C. and LOFT, E. E. (1962): Space Mechanics, Prentice-Hall, 1962.
22. NEUSTADT, L. W. (1960): "Synthesizing Time Optimal Control Systems," Journal of Mathematical Analysis and Applications, Vol. 1, No. 4, 1960, pp. 484-492.

23. NEUSTADT, L. W. and PAIEWONSKY, B. H. (1963): "On Synthesizing Optimal Controls," Proc. 2nd Congress on Automatic Control, Basle, September 1963, pp. 283-291.
24. PAIEWONSKY, B. H. and WOODROW, P. J. (1965): A Study of Time-Optimal Rendezvous in Three Dimensions, AFFDL-TR-65-20, January 1965.
25. PONTRYAGIN, L. S., BOLTYANSKII, V. G., GAMKRELIDZE, R. V. and MISHCHENKO, E. F. (1962): The Mathematical Theory of Optimal Processes, Interscience Publishers, 1962.
26. STAPLEFORD, R. I. (1962): A Study of the Two Basic Approximations in the Impulsive Guidance Techniques for Orbital Rendezvous. ASD-TDR-62-83, July 1962.
27. STAPLEFORD, R. (1963): "An Automatic Flight Path Control System for the Terminal Phase of Rendezvous," Adv. in The Astronautical Sciences, Vol. 11, 1963, pp. 193-218.
28. TSCHAUNER, J. and HEMPEL, P. (1964): "Optimale Bescheunigungsprogramme fur das Rendezvous-Manover," Astronautica Acta, Vol. 10, No. 2, 1964, pp. 296-307.
29. TSCHAUNER, J. and HEMPEL, P. (1965): "Rendezvous zu einem in Elliptischer Bahn um laufenden Ziel," Astronautica Acta, Vol. 11, No. 2, 1965, pp. 104-109.
30. TSCHAUNER, J. (1965): "Neue Darstellung des Rendezvous bei elliptischer Zielbahn," Astronautica Acta, Vol. 11, No. 5, pp. 312-321.

31. WOODROW, P. J. (1963): Methods for Locating Extrema of Multi-variate Functions, Princeton Univ., Dept. of Elec. Eng. Control System Lab. TR No. 4, November 1963.
32. ZADEH, L. A. and DESOER, C. A. (1963): Linear System Theory, McGraw-Hill, 1963.



XYZ is an inertial reference system

x-axis is directed along radius vector from center of the earth

y-axis is perpendicular to x-axis in orbit plane and directed in increasing θ direction

z-axis is perpendicular to orbit plane such that a right-handed coordinate system is formed

Figure 1. Coordinate system

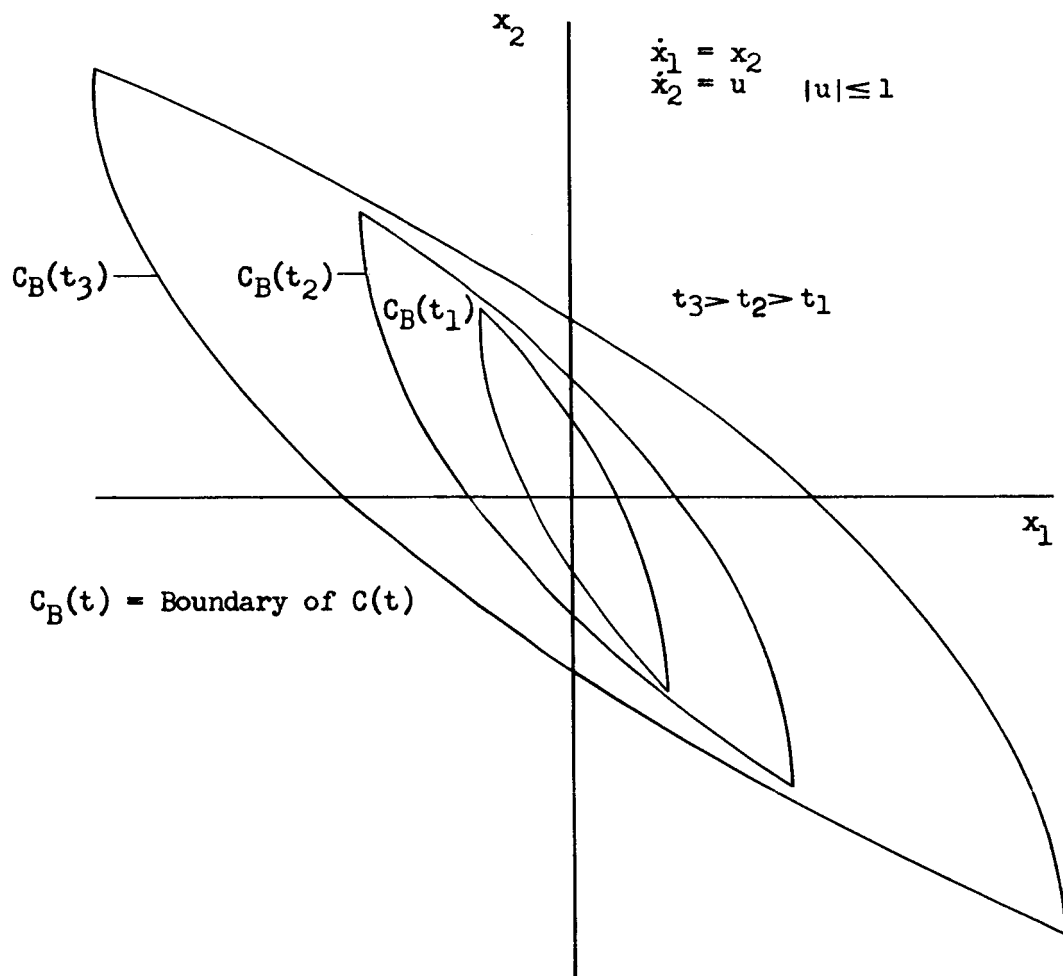
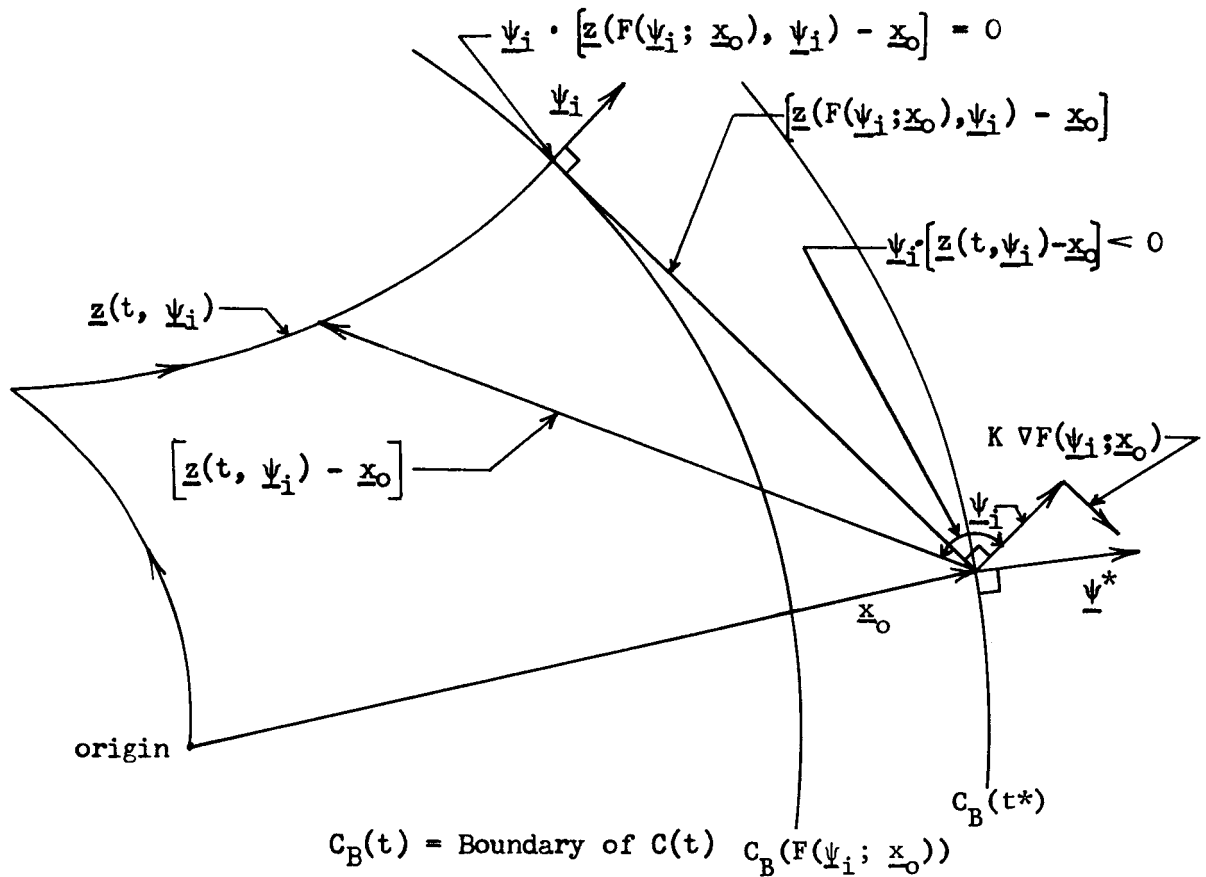
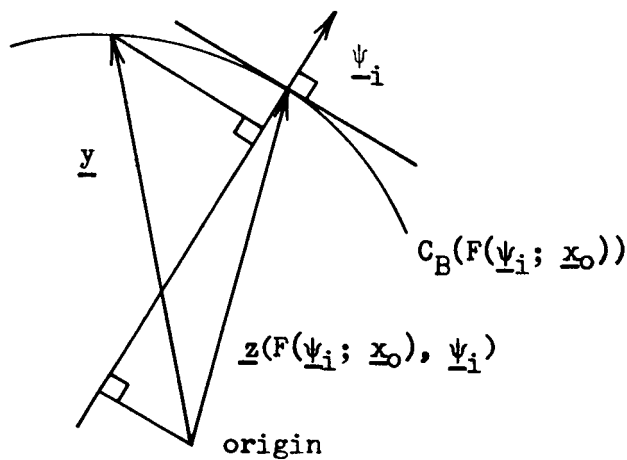


Figure 2. Optimal isochrones



a)



b)

Figure 3. Geometrical properties of Neustadt's Method

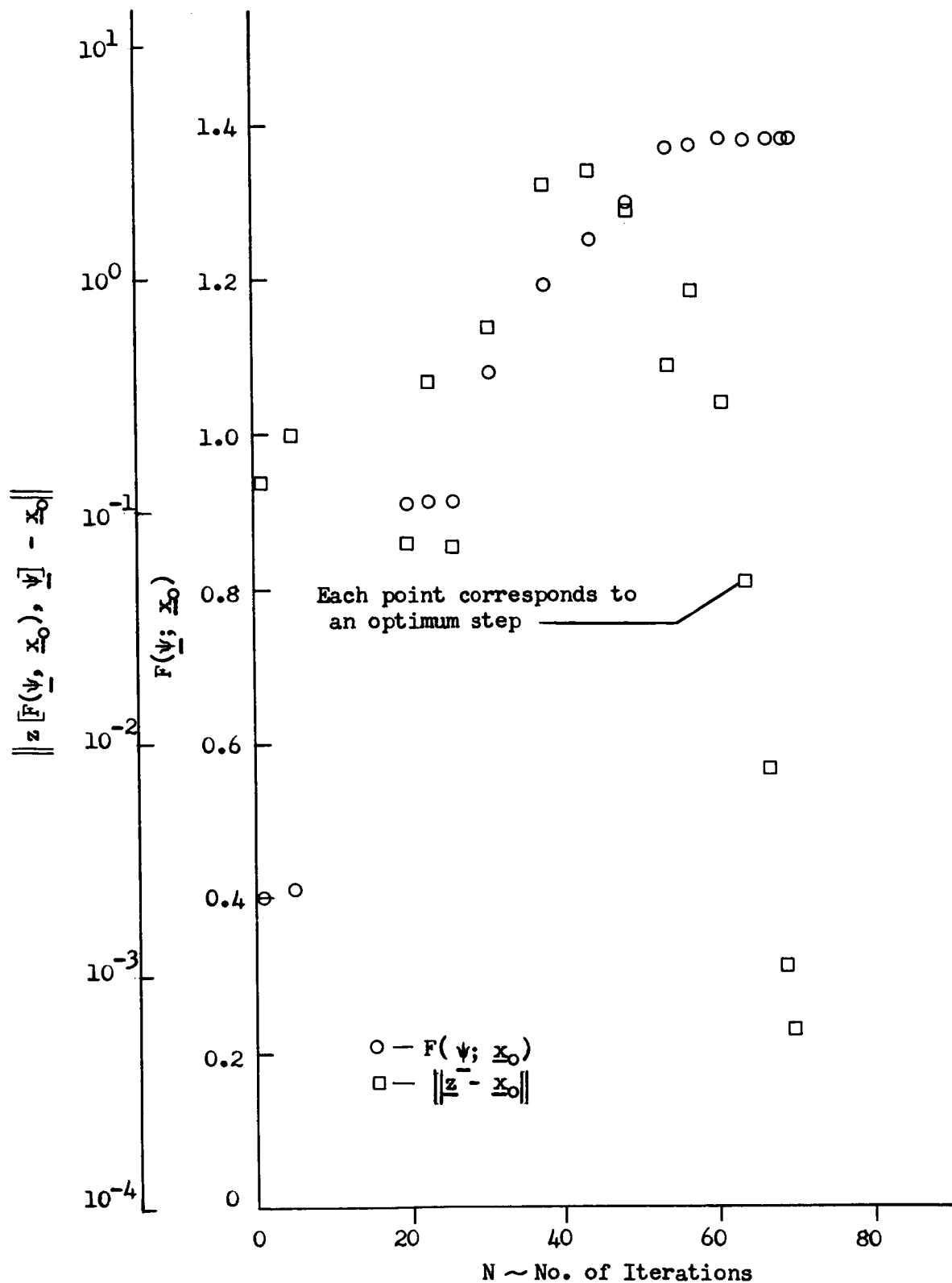


Figure 4. Stopping time and error vector magnitude vs. number of iterations for Fletcher-Powell Method

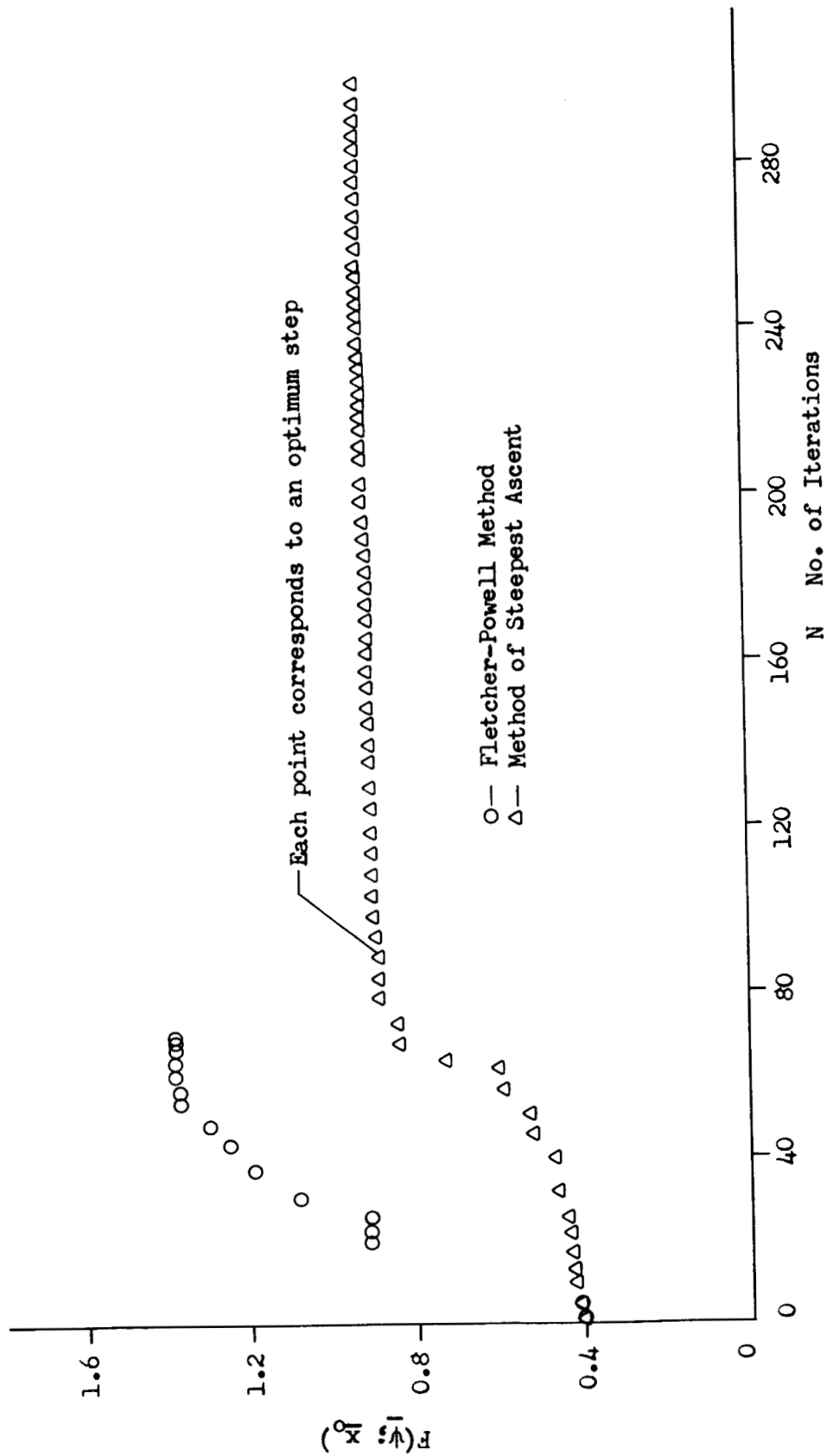


Figure 5. Convergence rate comparison of Fletcher-Powell method and method of steepest ascent with optimum steps

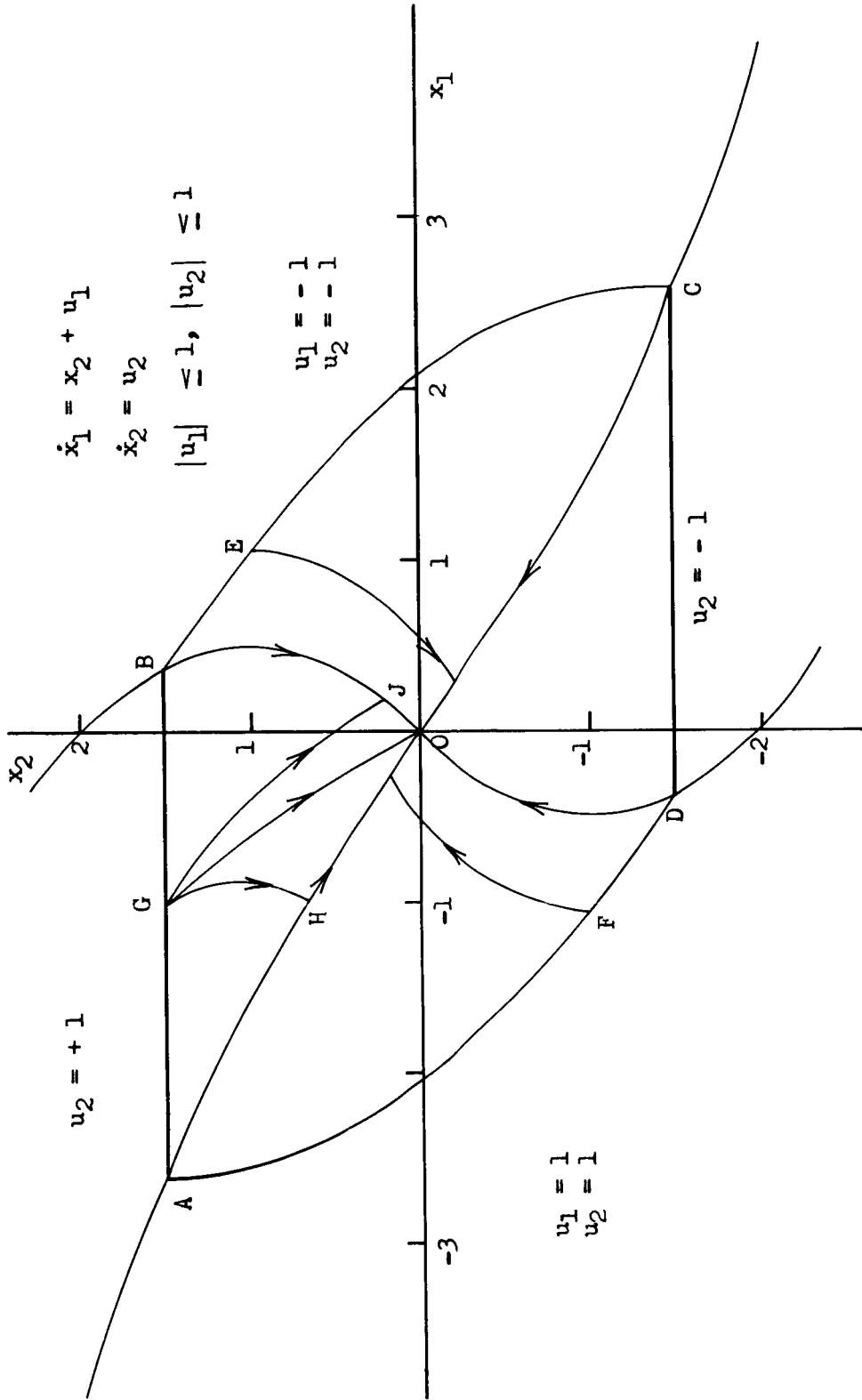


Figure 6. Optimal isochrones for a singular control problem

	$x(0)$ (ft)	$\dot{x}(0)$ (ft/sec)	$y(0)$ (ft)	$\dot{y}(0)$ (ft/sec)	θ_f (deg)
(a)	150,000	100	-150,000	-100	172.7
(b)	150,000 $\sqrt{2}$	100 $\sqrt{2}$	0	0	244.0
(c)	150,000	100	150,000 $\sqrt{2}$	100	209.9
(d)	0	0	150,000 $\sqrt{2}$	100 $\sqrt{2}$	120.7

$\theta_0 = 0$ deg

$e = 0.5$

$A_{max} = 0.25$ ft/sec²

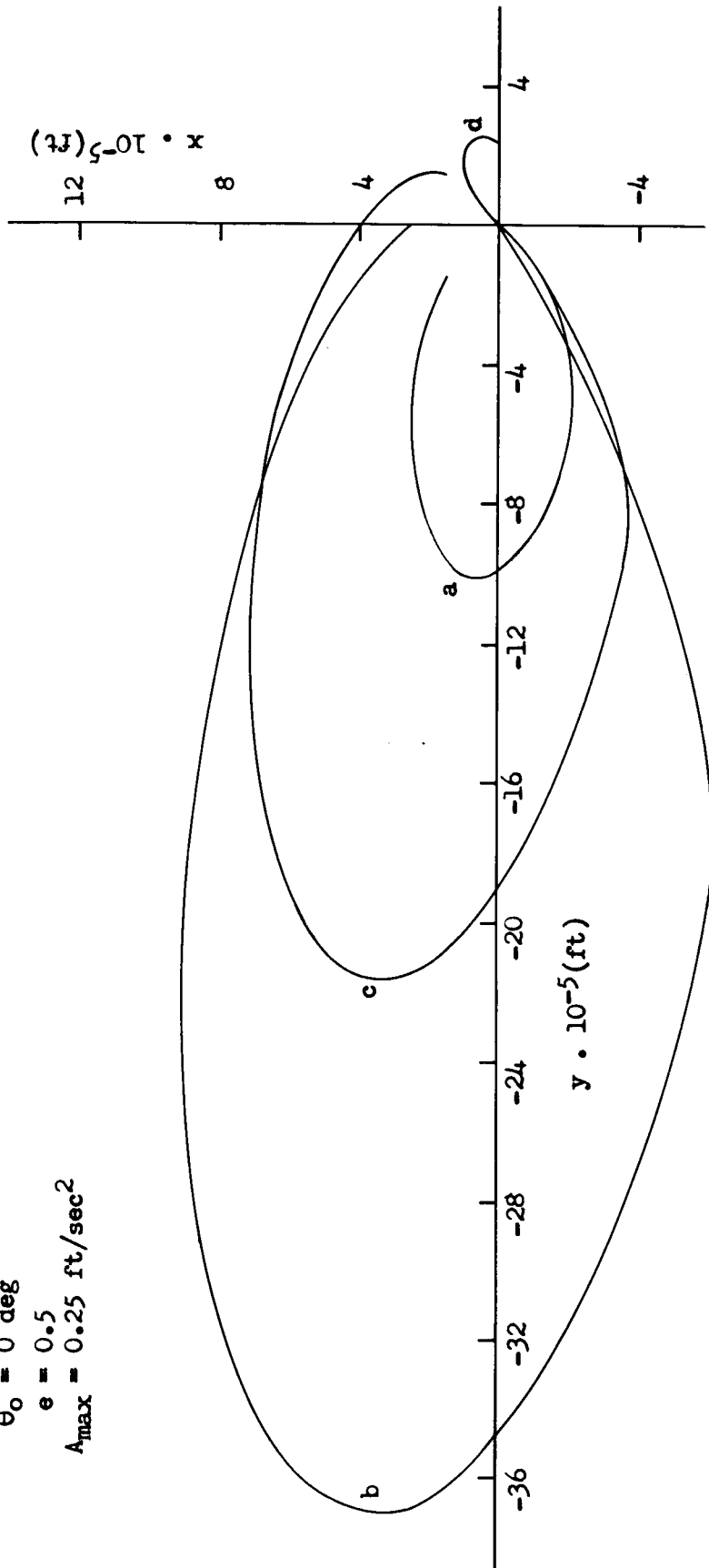


Figure 7. Optimum rendezvous trajectories in x-y plane for various initial conditions with $A_{max} = 0.25$ ft/sec² and $\theta_0 = 0$ degrees

	$x(0)$ (ft)	$\dot{x}(0)$ (ft/sec)	$y(0)$ (ft)	$\dot{y}(0)$ (ft/sec)	θ_f (deg)
(a)	150,000	100	-150,000	100	223.7
(b)	150,000 $\sqrt{2}$	0	0	100 $\sqrt{2}$	392.8
(c)	150,000	-100	150,000	100	192.5
(d)	0	-100 $\sqrt{2}$	150,000 $\sqrt{2}$	0	136.3

$\theta_0 = 0$ deg

$e = 0.5$

$A_{max} = 0.25$ ft/sec²

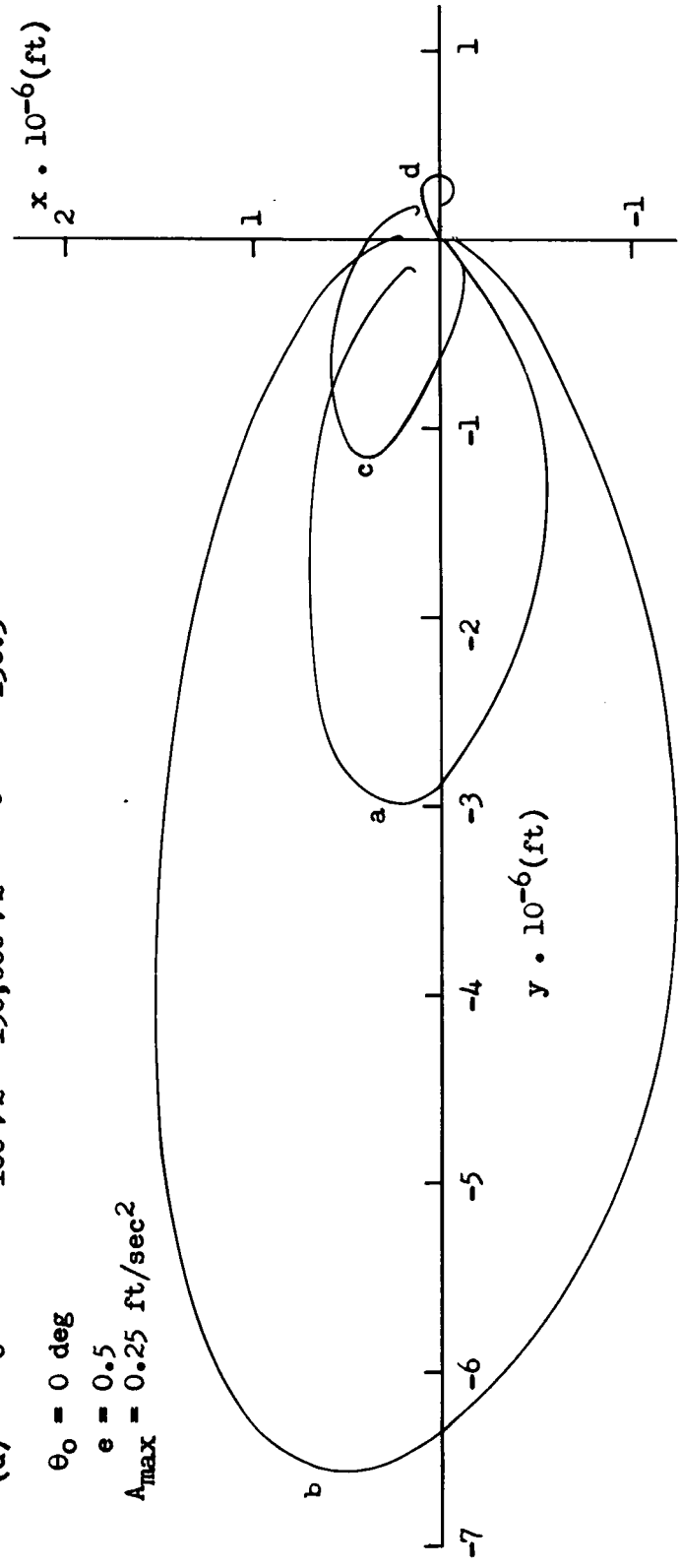


Figure 8. Optimum rendezvous trajectories in x-y plane for various initial conditions with $A_{max} = 0.25$ ft/sec² and $\theta_0 = 0$ degrees

	$x(0)$ (ft)	$\dot{x}(0)$ (ft/sec)	$y(0)$ (ft)	$\dot{y}(0)$ (ft/sec)	θ_f (deg)
(a)	150,000	-100	-150,000	-100	150.1
(b)	150,000 $\sqrt{2}$	0	0	-100 $\sqrt{2}$	181.6
(c)	150,000	100	150,000	-100	154.7
(d)	0	100 $\sqrt{2}$	150,000 $\sqrt{2}$	0	100.8

$\theta_0 = 0$ deg
 $e = 0.5$
 $A_{max} = 0.25$ ft/sec²

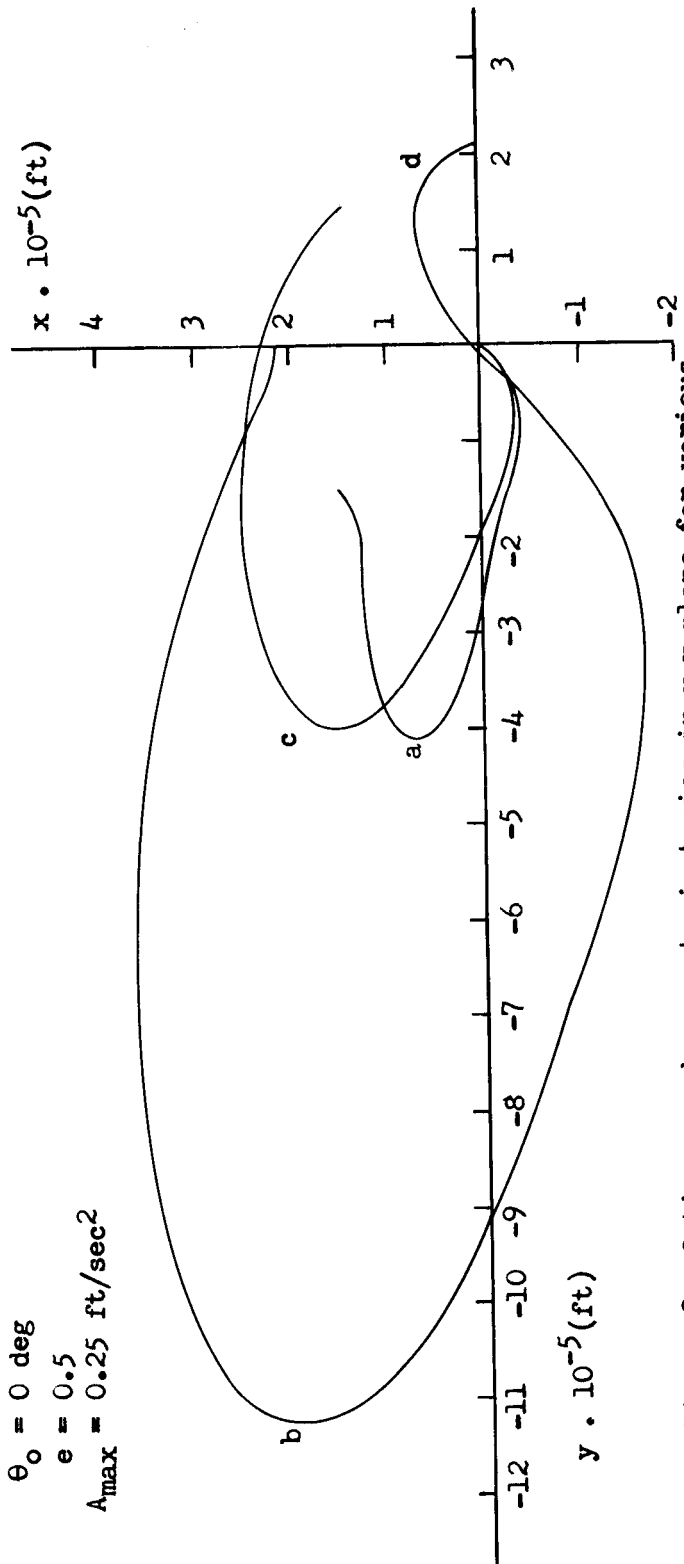


Figure 9. Optimum rendezvous trajectories in x-y plane for various initial conditions with $A_{max} = 0.25$ ft/sec² and $\theta_0 = 0$ degrees

	$x(0)$ (ft)	$\dot{x}(0)$ (ft/sec)	$y(0)$ (ft)	$\dot{y}(0)$ (ft/sec)	θ_f (deg)
(a)	150,000	100	-150,000	-100	132.4
(b)	150,000 $\sqrt{2}$	100 $\sqrt{2}$	0	0	158.4
(c)	150,000	100	150,000	100	138.9
(d)	0	0	150,000 $\sqrt{2}$	100 $\sqrt{2}$	98.9

$\theta_0 = 0$ deg

$e = 0.5$

$A_{\max} = 0.5$ ft/sec²

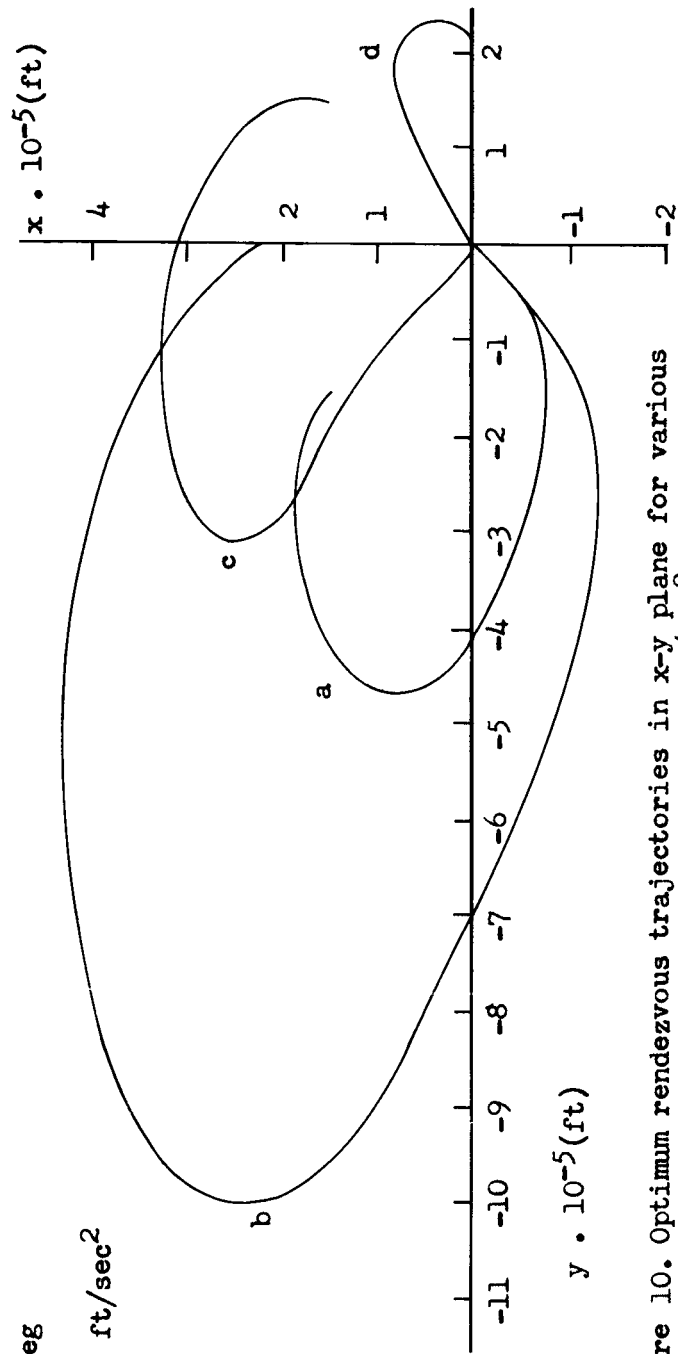


Figure 10. Optimum rendezvous trajectories in x - y plane for various initial conditions with $A_{\max} = 0.5$ ft/sec² and $\theta_0 = 0$ degrees

	$x(0)$ (ft)	$\dot{x}(0)$ (ft/sec)	$y(0)$ (ft)	$\dot{y}(0)$ (ft/sec)	θ_f (deg.)
(a)	150,000	100	-150,000	100	153.9
(b)	$150,000\sqrt{2}$	0	0	$100\sqrt{2}$	168.1
(c)	150,000	-100	150,000	100	115.9
(d)	0	$-100\sqrt{2}$	$150,000\sqrt{2}$	0	109.0

$\theta_0 = 0$ deg
 $e = 0.5$
 $A_{max} = 0.5$ ft/sec²

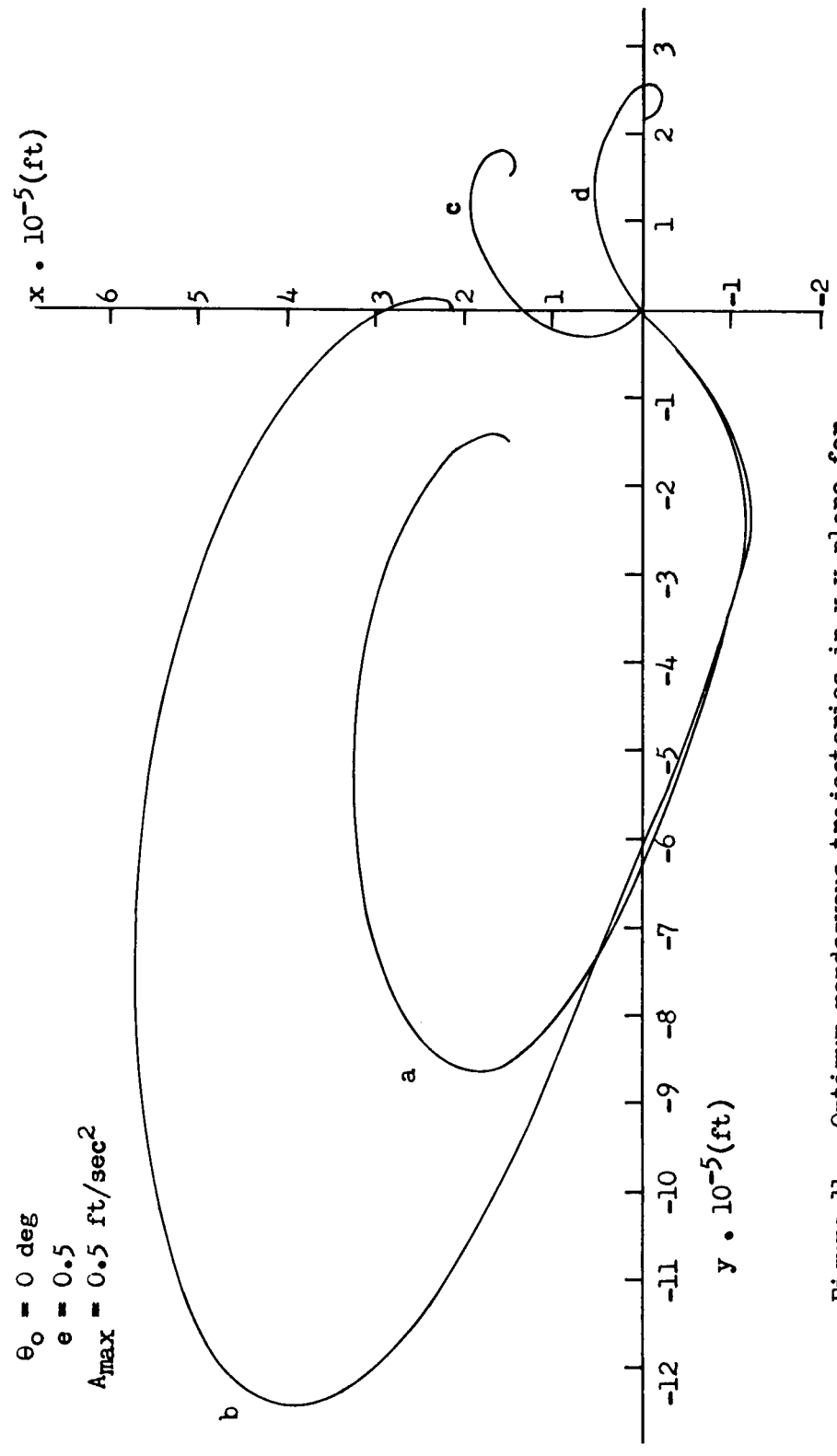


Figure 11. Optimum rendezvous trajectories in x-y plane for various initial conditions with $A_{max} = 0.5$ ft/sec² and $\theta_0 = 0$ degrees

	$x(0)$ (ft)	$\dot{x}(0)$ (ft/sec)	$y(0)$ (ft)	$\dot{y}(0)$ (ft/sec)	θ_f (deg)
(a)	150,000	100	-150,000	-100	111.8
(b)	150,000 $\sqrt{2}$	100 $\sqrt{2}$	0	0	129.8
(c)	150,000	100	150,000 $\sqrt{2}$	100	104.4
(d)	0	0	150,000 $\sqrt{2}$	100 $\sqrt{2}$	86.0

$\theta_0 = 0 \text{ deg}$

$e = 0.5$

$A_{\max} = 0.75 \text{ ft/sec}^2$

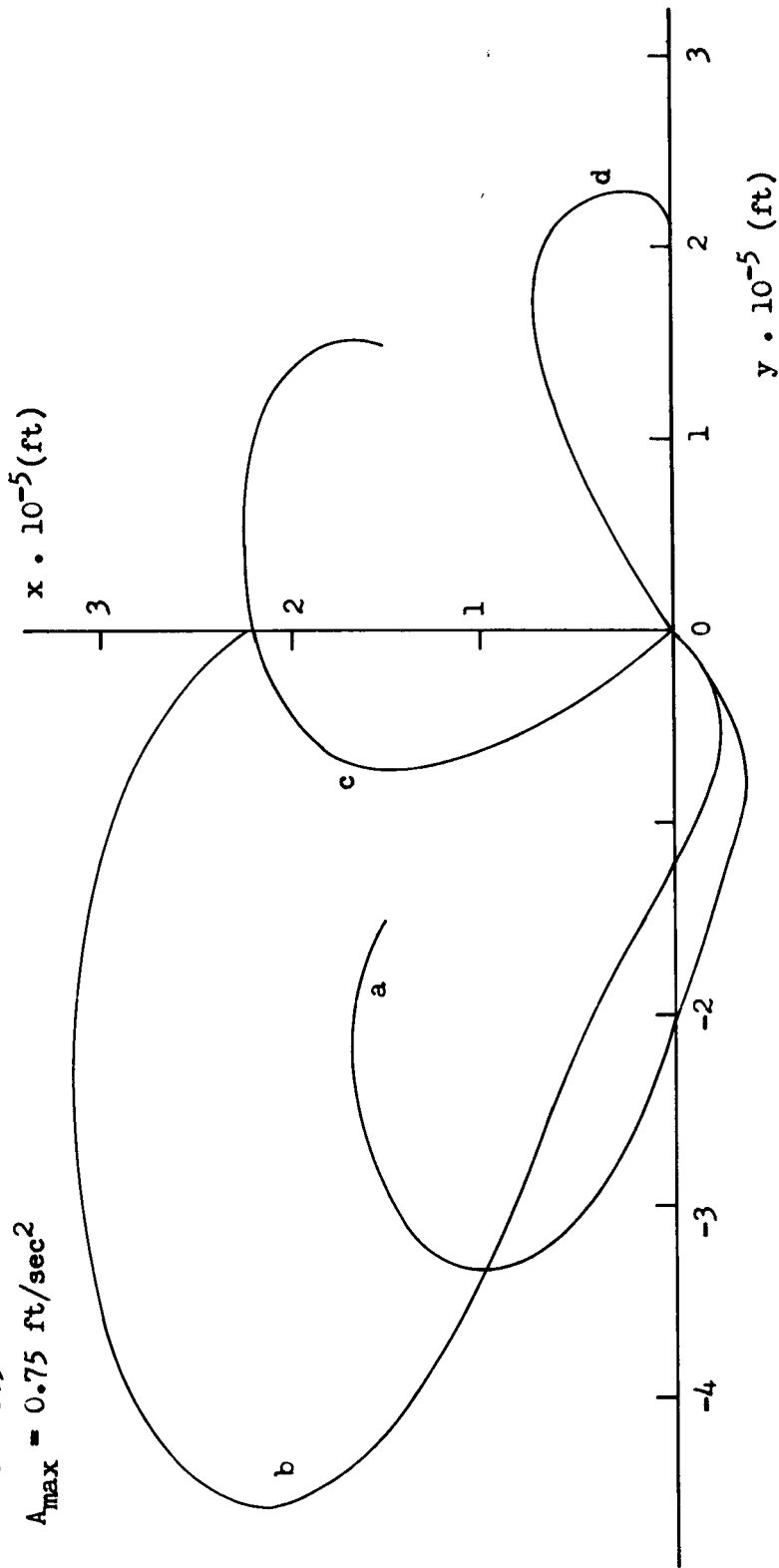


Figure 12. Optimum rendezvous trajectories in x-y plane for various initial conditions with $A_{\max} = 0.75 \text{ ft/sec}^2$ and $\theta_0 = 0 \text{ degrees}$

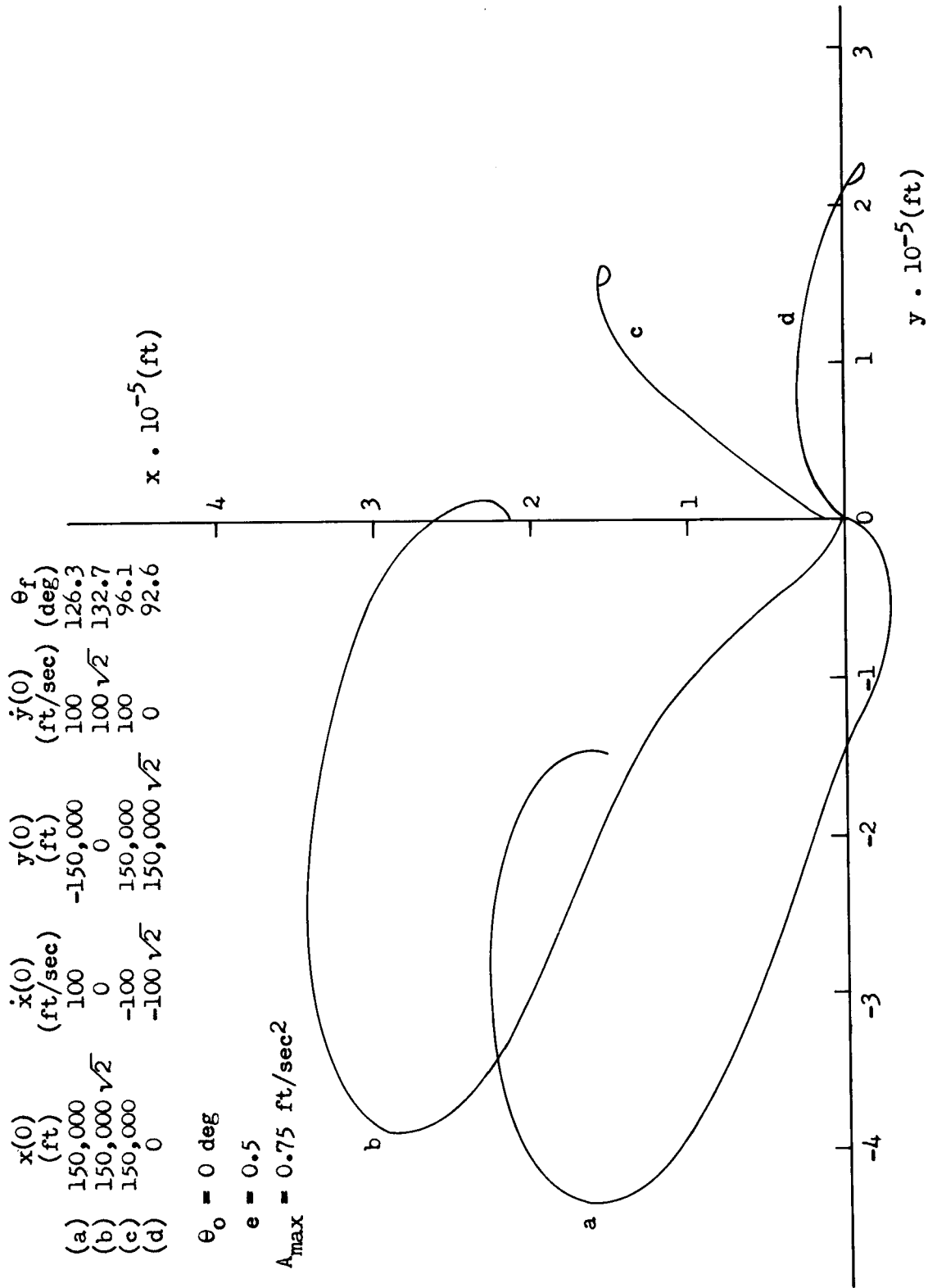


Fig. 13. Optimum rendezvous trajectories in x-y plane for various initial conditions with $A_{max} = 0.75$ ft/sec² and $\theta_0 = 0$ degrees

	$x(0)$ (ft)	$\dot{x}(0)$ (ft/sec)	$y(0)$ (ft)	$\dot{y}(0)$ (ft/sec)	θ_f (deg)
(a)	150,000	100	-150,000	-100	98.1
(b)	150,000 $\sqrt{2}$	100 $\sqrt{2}$	0	0	110.4
(c)	150,000	100	150,000	100	86.8
(d)	0	0	150,000 $\sqrt{2}$	100 $\sqrt{2}$	77.2

$\theta_0 = 0 \text{ deg}$
 $e = 0.5$
 $A_{\max} = 1.0 \text{ ft/sec}^2$

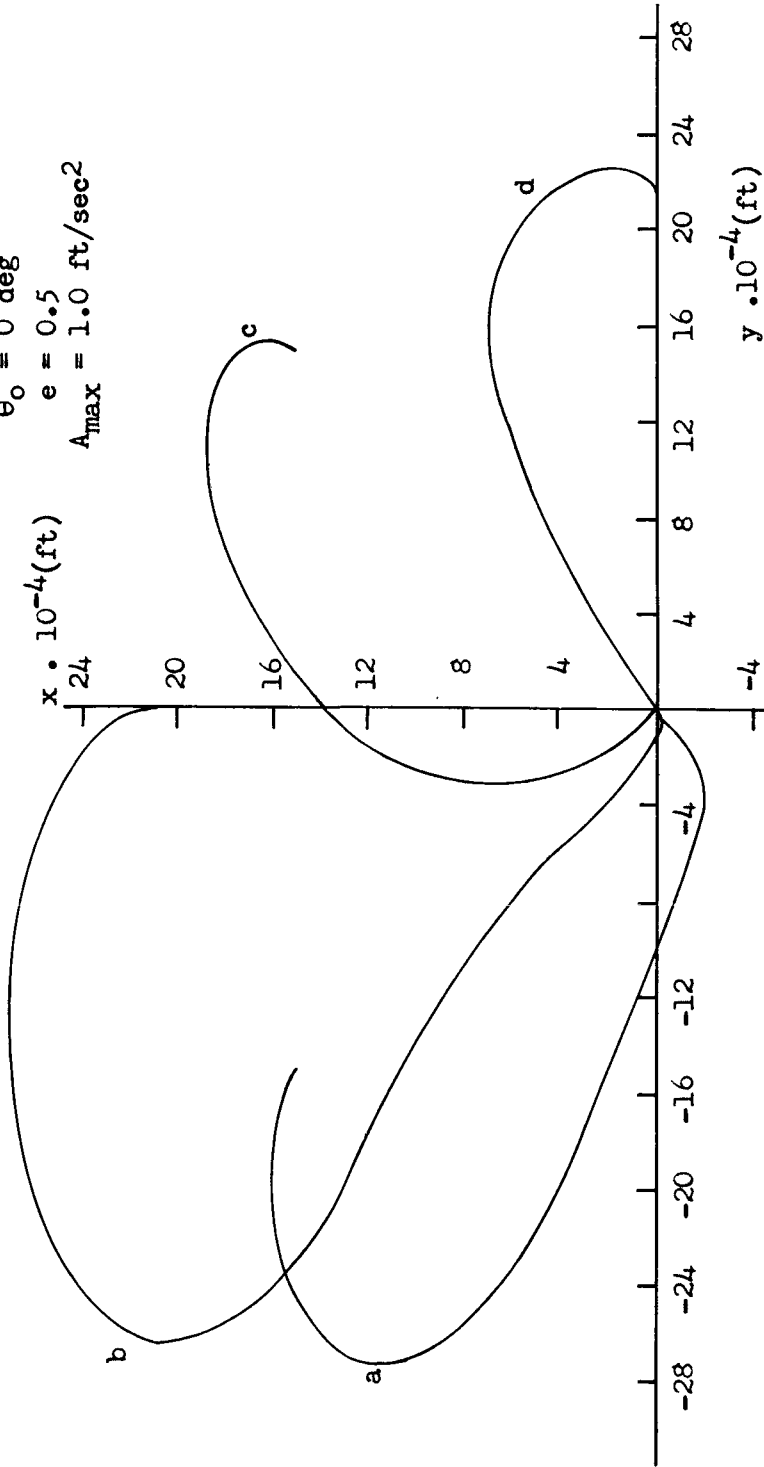


Figure 14. Optimum rendezvous trajectories in x-y plane for various initial conditions with $A_{\max} = 1.0 \text{ ft/sec}^2$ and $\theta_0 = 0 \text{ degrees}$

	$x(0)$ (ft)	$\dot{x}(0)$ (ft/sec)	$y(0)$ (ft)	$\dot{y}(0)$ (ft/sec)	θ_f (deg)
(a)	150,000	100	-150,000	100	107.8
(b)	150,000 $\sqrt{2}$	0	0	100 $\sqrt{2}$	108.3
(c)	150,000	-100	150,000	100	84.5
(d)	0	-100 $\sqrt{2}$	150,000 $\sqrt{2}$	0	81.0

$$\theta_0 = 0 \text{ deg}$$

$$e = 0.5$$

$$A_{\max} = 1.0 \text{ ft/sec}^2$$

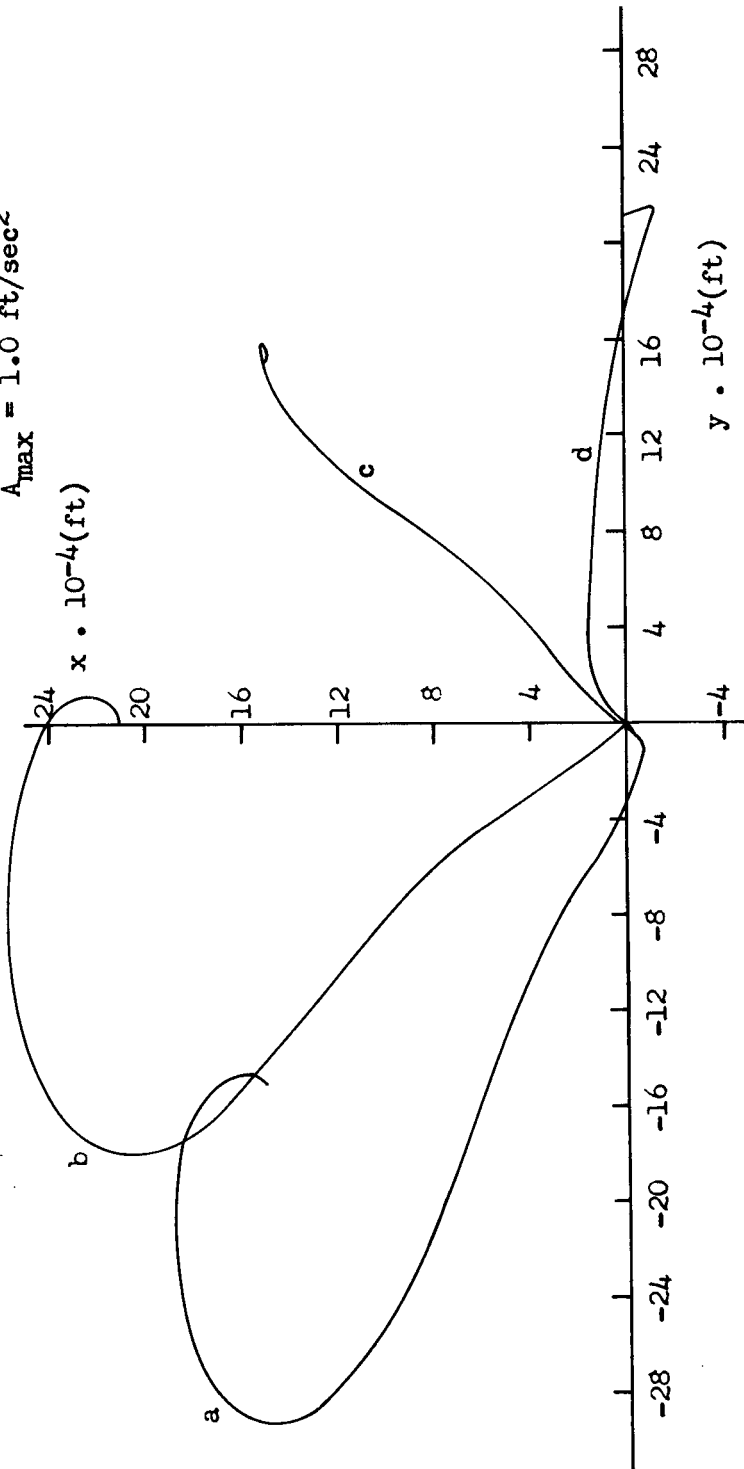


Figure 15. Optimum rendezvous trajectories in x-y plane for various initial conditions with $A_{\max} = 1.0 \text{ ft/sec}^2$ and $\theta_0 = 0 \text{ degrees}$

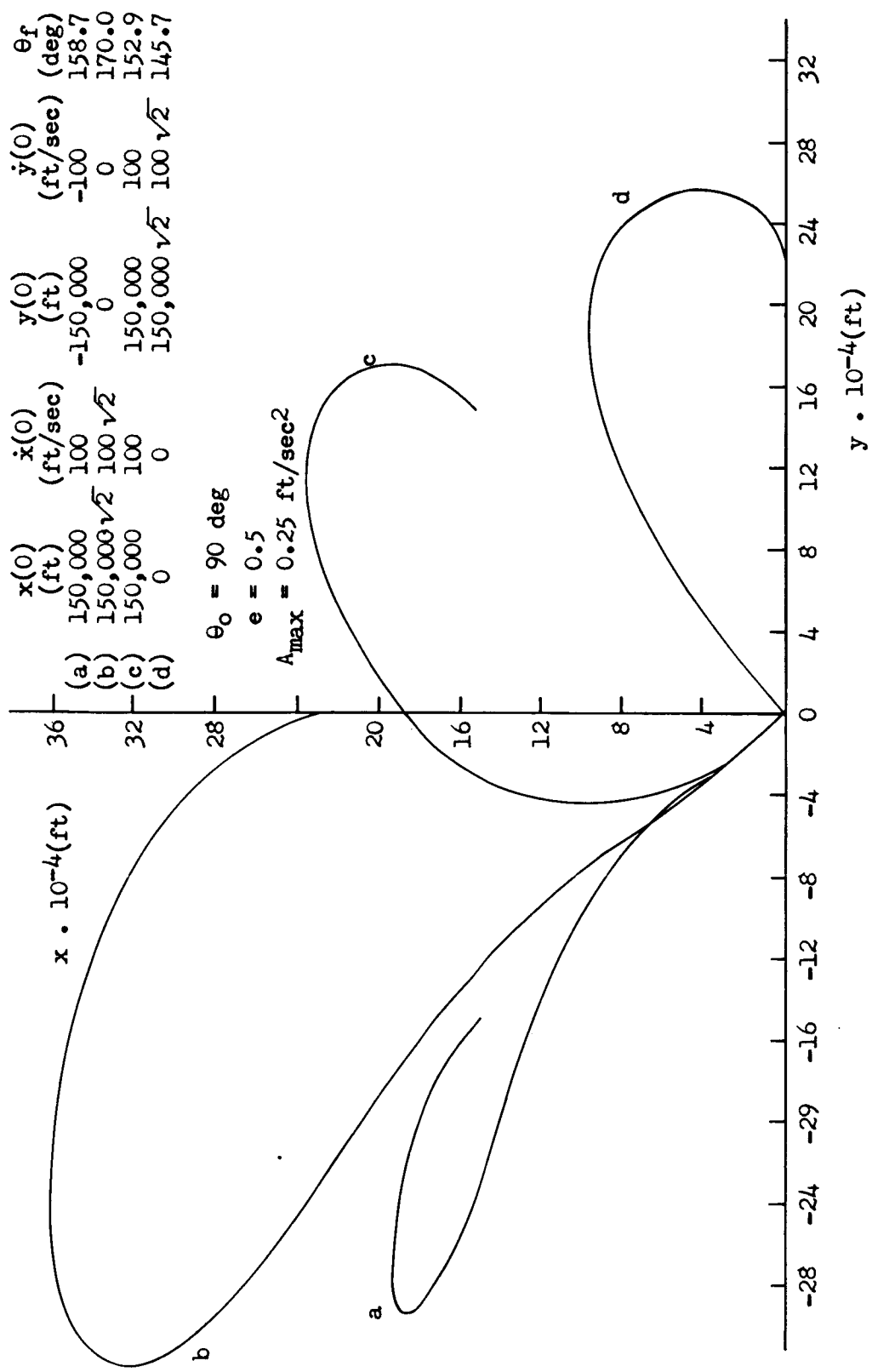
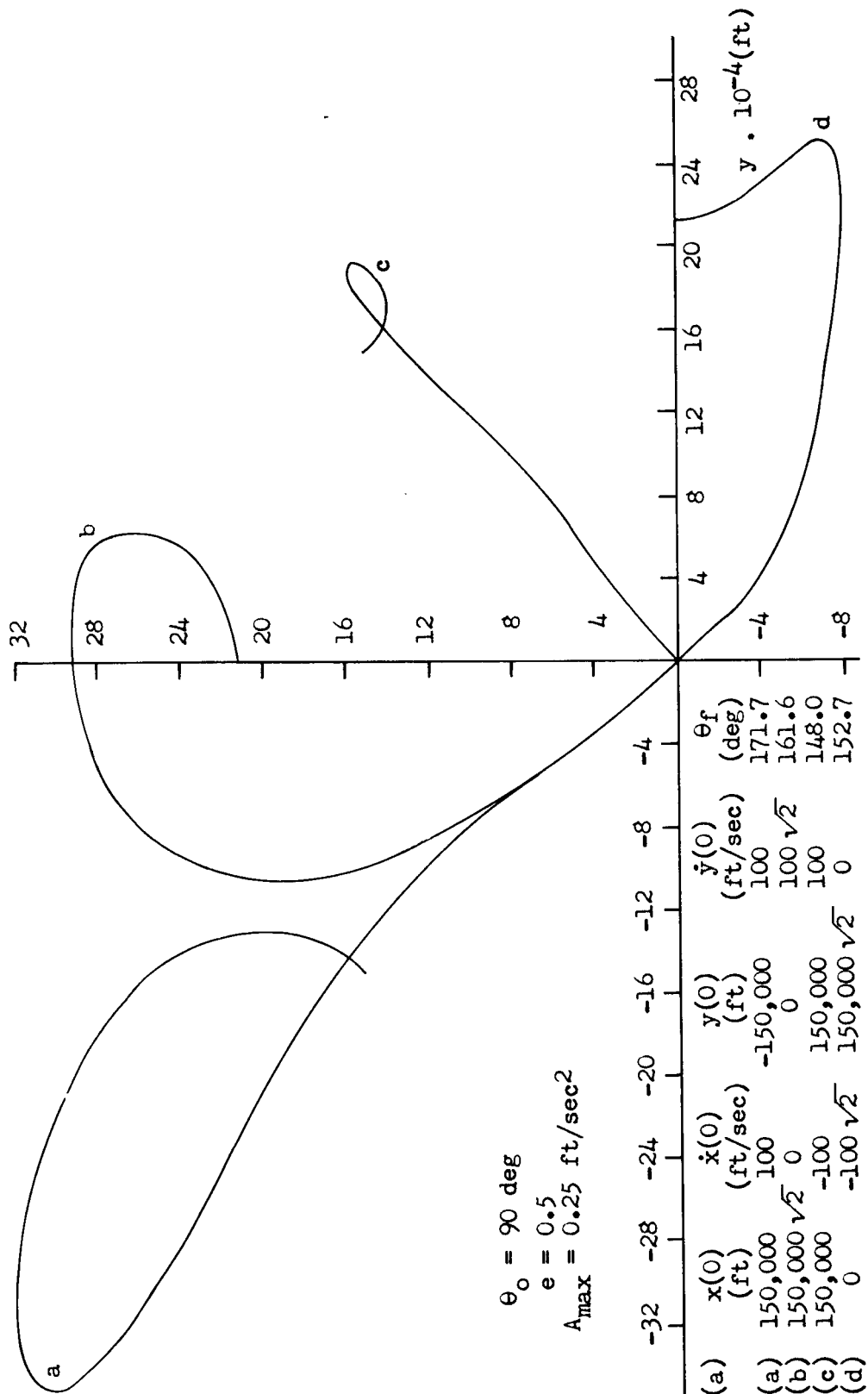


Figure 16. Optimum rendezvous trajectories in x-y plane for various initial conditions with $A_{max} = 0.25$ ft/sec² and $\theta_0 = 90$ degrees

$x \cdot 10^{-4}(\text{ft})$



$\theta_0 = 90 \text{ deg}$
 $e = 0.5$
 $A_{\text{max}} = 0.25 \text{ ft/sec}^2$

Figure 17. Optimum rendezvous trajectories in x-y plane for various initial conditions with $A_{\text{max}} = 0.25 \text{ ft/sec}^2$ and $\theta_0 = 90 \text{ degrees}$

	$x(0)$ (ft)	$\dot{x}(0)$ (ft/sec)	$y(0)$ (ft)	$\dot{y}(0)$ (ft/sec)	θ_f (deg)
(a)	150,000	-100	-150,000	-100	136.4
(b)	150,000 $\sqrt{2}$	0	0	-100 $\sqrt{2}$	142.1
(c)	150,000	100	150,000	-100	139.6
(d)	0	100 $\sqrt{2}$	150,000 $\sqrt{2}$	0	133.5

$\theta_0 = 90$
 $e = 0.5$
 $A_{max} = 0.25 \text{ ft/sec}^2$

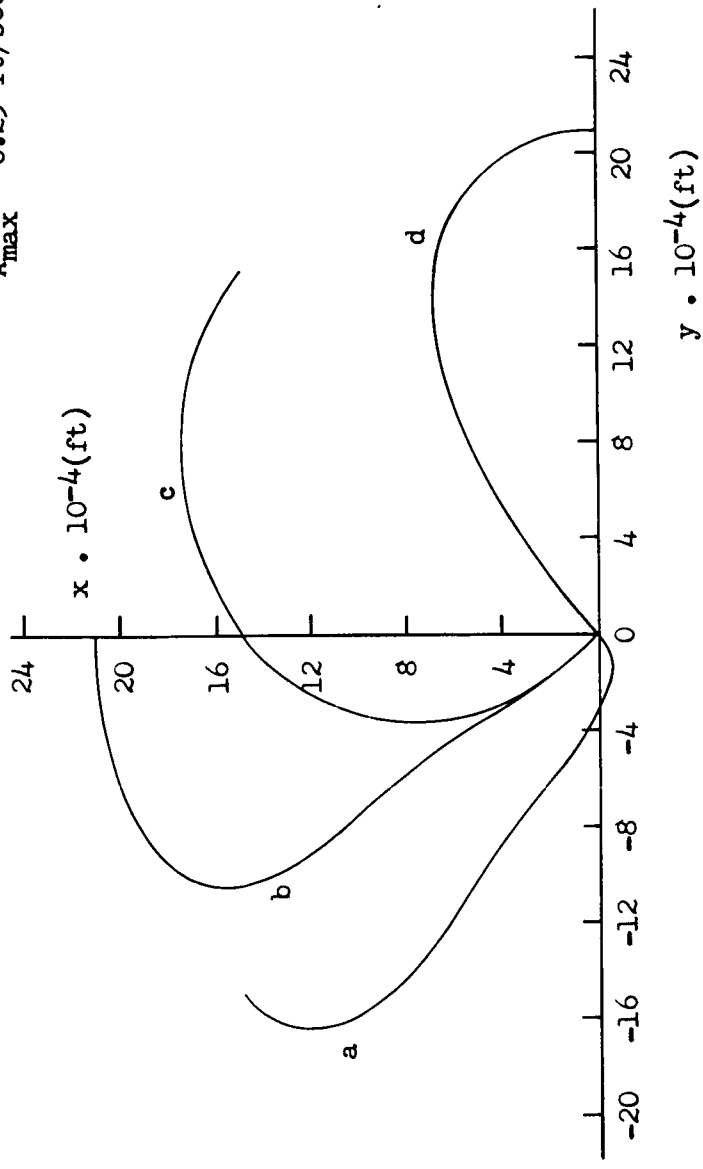


Figure 18. Optimum rendezvous trajectories in x-y plane for various initial conditions with $A_{max} = 0.25 \text{ ft/sec}^2$ and $\theta_0 = 90$ degrees

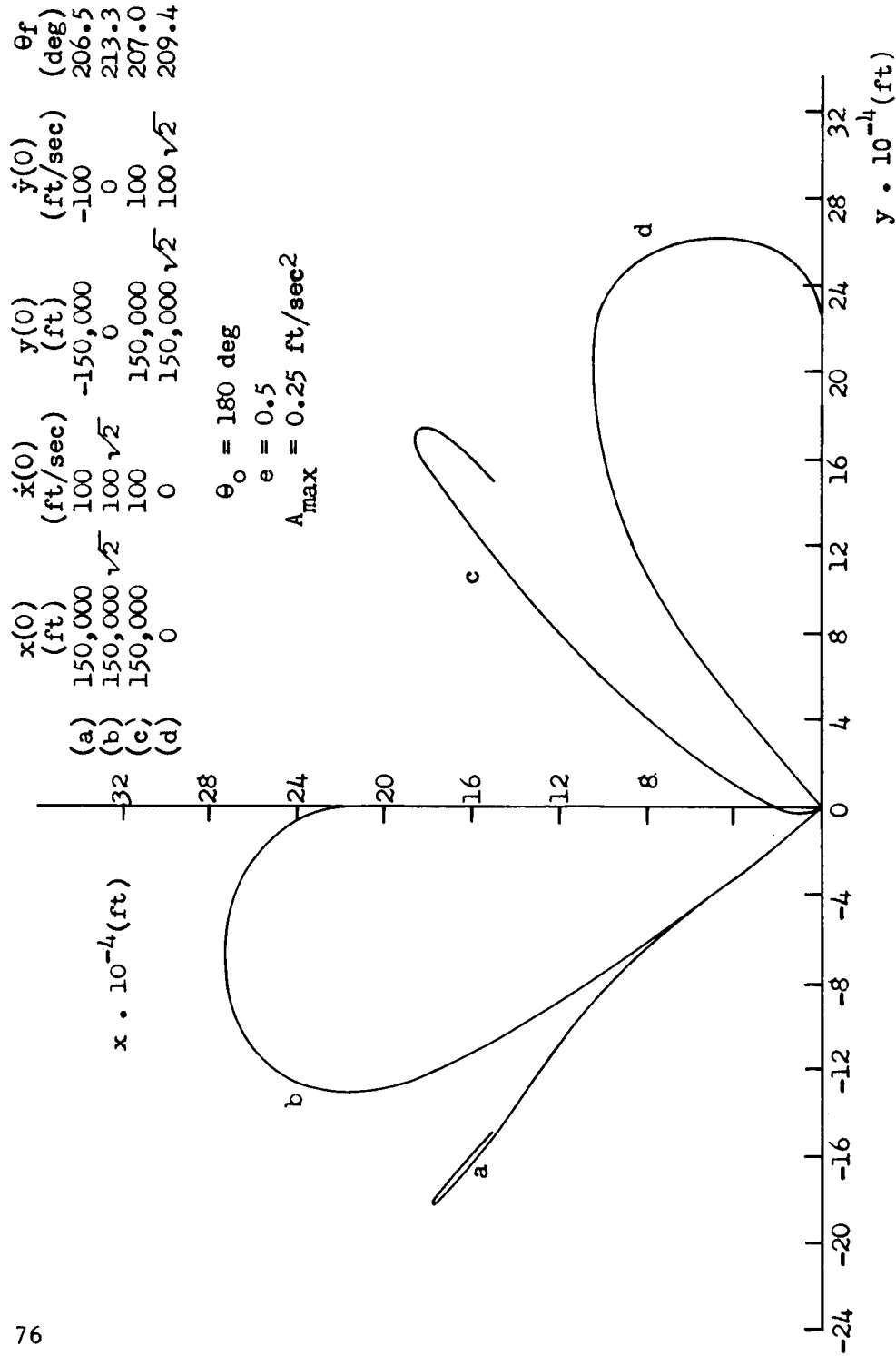


Figure 19. Optimum rendezvous trajectories in x-y plane for various initial conditions with $A_{max} = 0.25$ ft/sec² and $\theta_0 = 180$ degrees

	$x(0)$ (ft)	$\dot{x}(0)$ (ft/sec)	$y(0)$ (ft)	$\dot{y}(0)$ (ft/sec)	θ_f (deg)
(a)	150,000	100	-150,000	100	207.5
(b)	150,000 $\sqrt{2}$	0	0	100 $\sqrt{2}$	203.2
(c)	150,000	-100	150,000	100	205.1
(d)	0	-100 $\sqrt{2}$	150,000 $\sqrt{2}$	0	202.4

$\theta_0 = 180 \text{ deg}$
 $e = 0.5$
 $A_{\text{max}} = 0.25 \text{ ft/sec}^2$

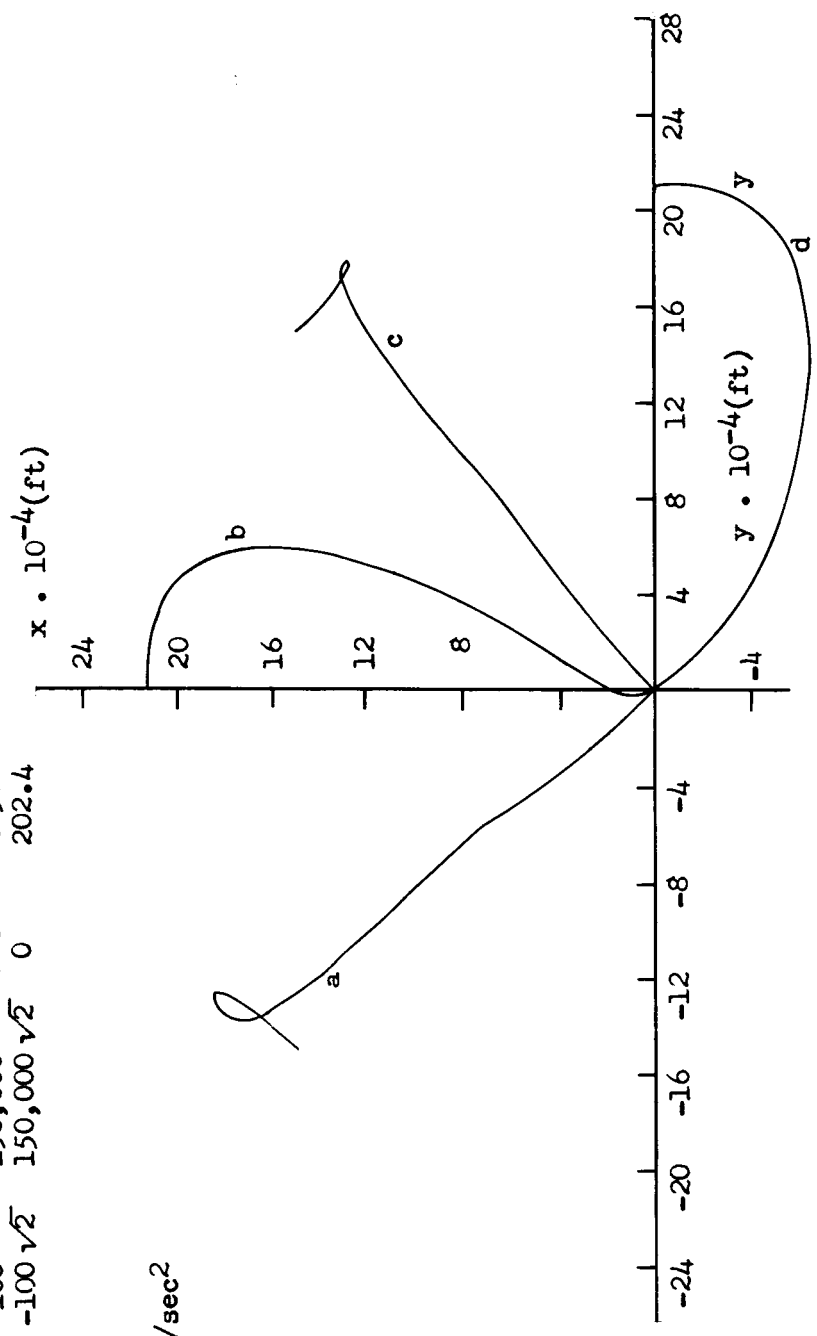


Figure 20. Optimum rendezvous trajectories in x-y plane for various initial conditions with $A_{\text{max}} = 0.25 \text{ ft/sec}^2$ and $\theta_0 = 180 \text{ degrees}$

	$x(0)$ (ft)	$\dot{x}(0)$ (ft/sec)	$y(0)$ (ft)	$\dot{y}(0)$ (ft/sec)	θ_f (deg)
(a)	150,000	-100	-150,000	-100	201.8
(b)	150,000 $\sqrt{2}$	0	0	-100 $\sqrt{2}$	200.2
(c)	150,000	100	150,000	-100	202.9
(d)	0	100 $\sqrt{2}$	150,000 $\sqrt{2}$	0	199.5

$\theta_0 = 180 \text{ deg}$
 $e = 0.5$
 $A_{\text{max}} = 0.25 \text{ ft/sec}^2$

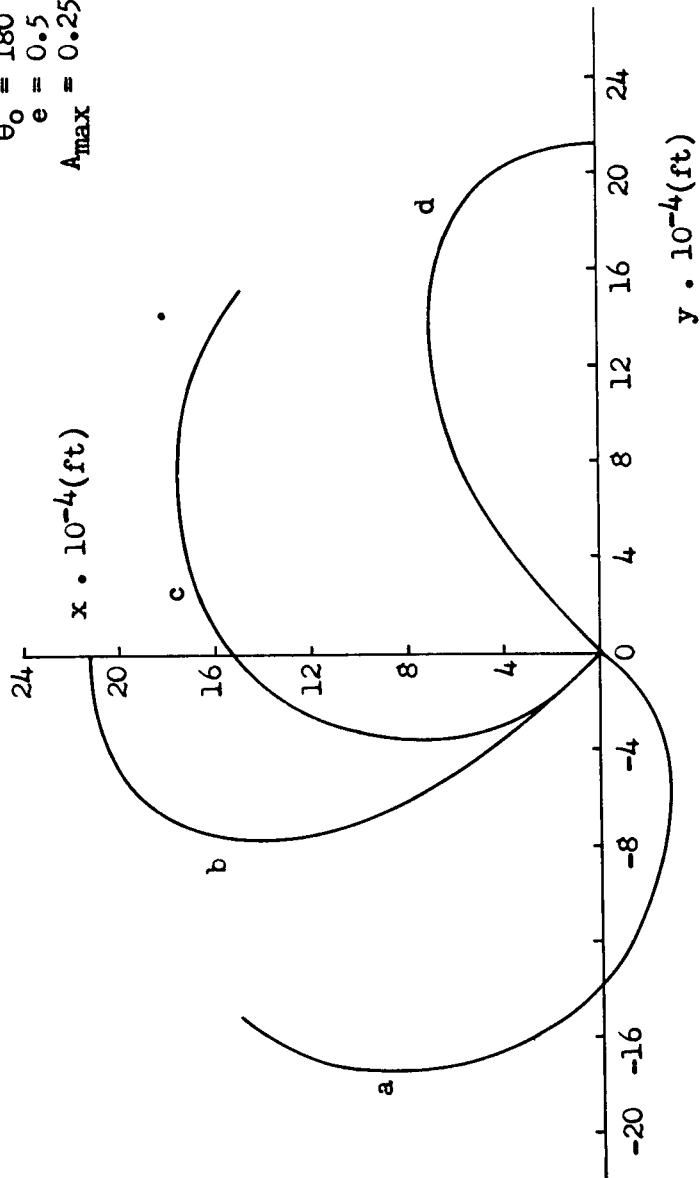


Figure 21. Optimum rendezvous trajectories in x-y plane for various initial conditions with $A_{\text{max}} = 0.25 \text{ ft/sec}^2$ and $\theta_0 = 180 \text{ degrees}$

	$x(0)$ (ft)	$\dot{x}(0)$ (ft/sec)	$y(0)$ (ft)	$\dot{y}(0)$ (ft/sec)	θ_f (deg)
(a)	150,000	100	-150,000	-100	195.8
(b)	150,000 $\sqrt{2}$	100 $\sqrt{2}$	0	0	199.2
(c)	150,000	100	150,000	100	196.0
(d)	0	0	150,000 $\sqrt{2}$	100 $\sqrt{2}$	198.4

$\theta_0 = 180 \text{ deg}$
 $A_{\text{max}} = 0.5 \text{ ft/sec}^2$
 $e = 0.5$

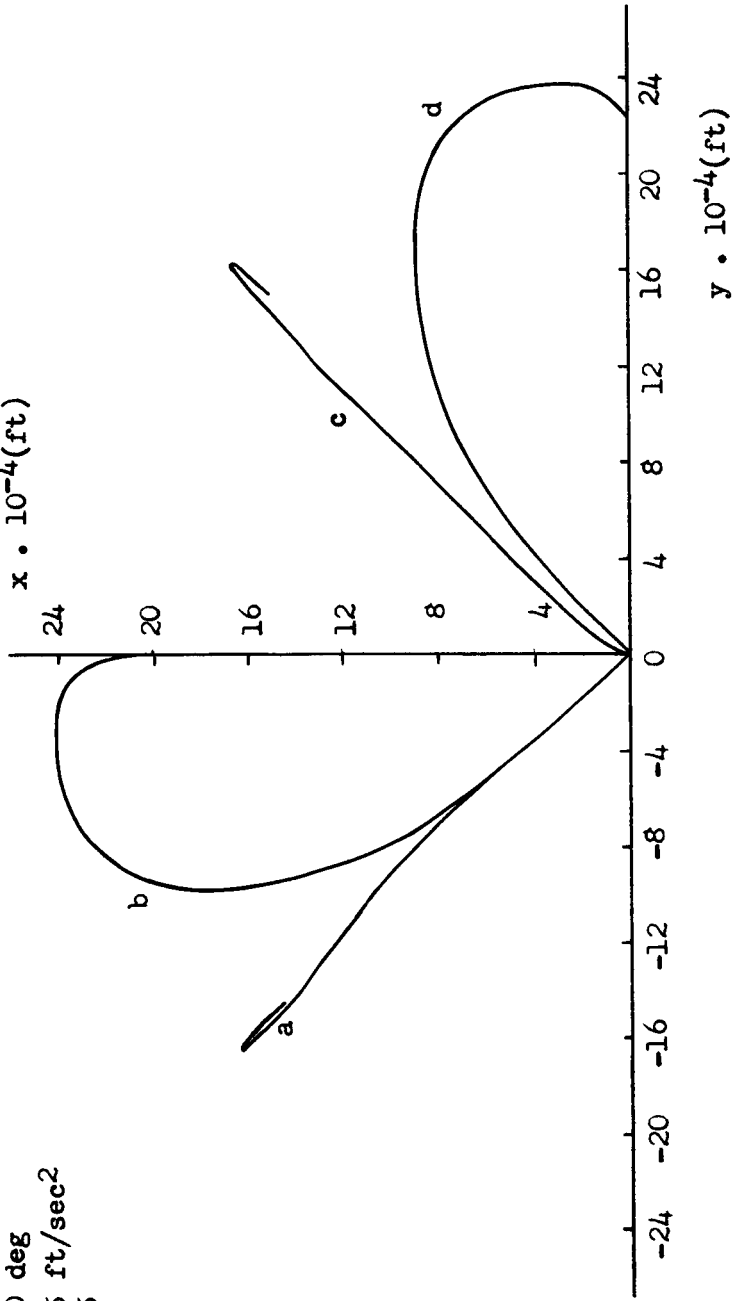


Figure 22. Optimum rendezvous trajectories in x-y plane for various initial conditions with $A_{\text{max}} = 0.5 \text{ ft/sec}^2$ and $\theta_0 = 180 \text{ degrees}$

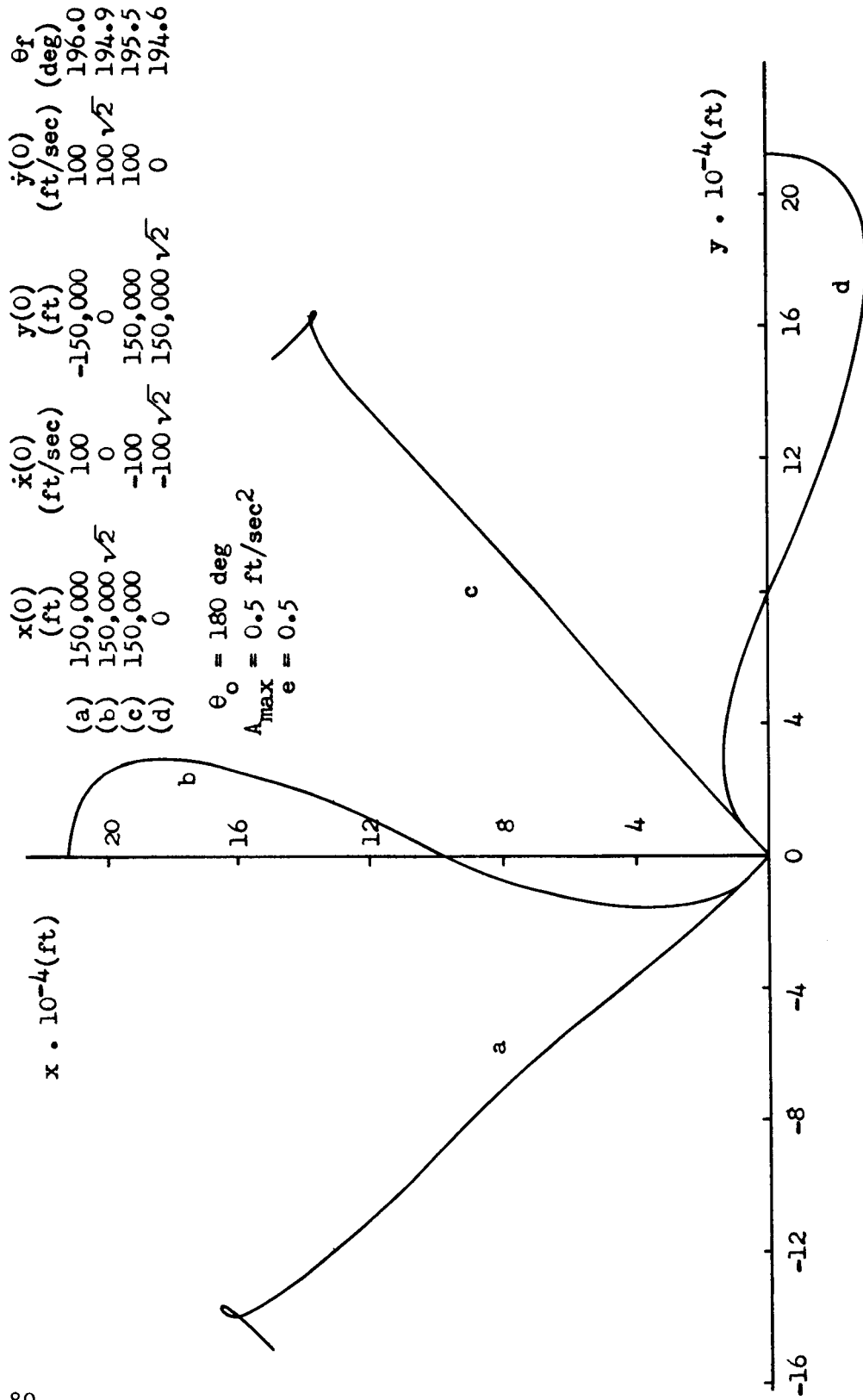


Figure 23. Optimum rendezvous trajectories in x-y plane for various initial condition with $A_{max} = 0.5$ ft/sec² and $\theta_0 = 180$ degrees

	$x(0)$ (ft)	$\dot{x}(0)$ (ft/sec)	$y(0)$ (ft)	$\dot{y}(0)$ (ft/sec)	θ_f (deg)
(a)	150,000	100	-150,000	-100	457.7
(b)	150,000 $\sqrt{2}$	100 $\sqrt{2}$	0	0	501.0
(c)	150,000	100	150,000	100	509.1
(d)	0	0	150,000 $\sqrt{2}$	100 $\sqrt{2}$	428.5

$$\theta_0 = 270 \text{ deg}$$

$$e = 0.5$$

$$A_{\max} = 0.25 \text{ ft/sec}^2$$

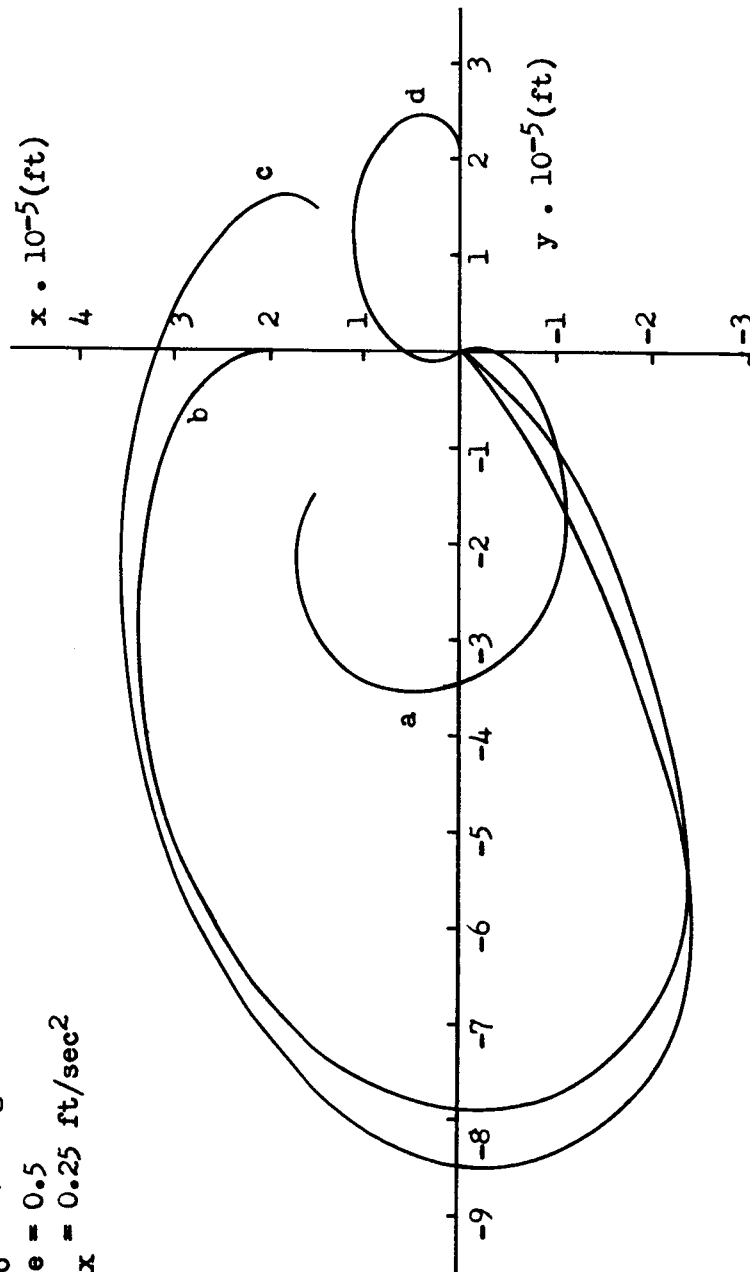


Figure 24. Optimum rendezvous trajectories in x-y plane for various initial conditions with $A_{\max} = 0.25 \text{ ft/sec}^2$ and $\theta_0 = 270 \text{ degrees}$

	$x(0)$ (ft)	$\dot{x}(0)$ (ft/sec)	$y(0)$ (ft)	$\dot{y}(0)$ (ft/sec)	θ_f (deg)
(a)	150,000	100	-150,000	100	495.5
(b)	150,000 $\sqrt{2}$	0	0	100 $\sqrt{2}$	526.4
(c)	150,000	-100	150,000	100	496.4
(d)	0	-100 $\sqrt{2}$	150,000 $\sqrt{2}$	0	432.4

$\theta_0 = 270$ deg
 $A_{max} = 0.25$ ft/sec²
 $e = 0.5$

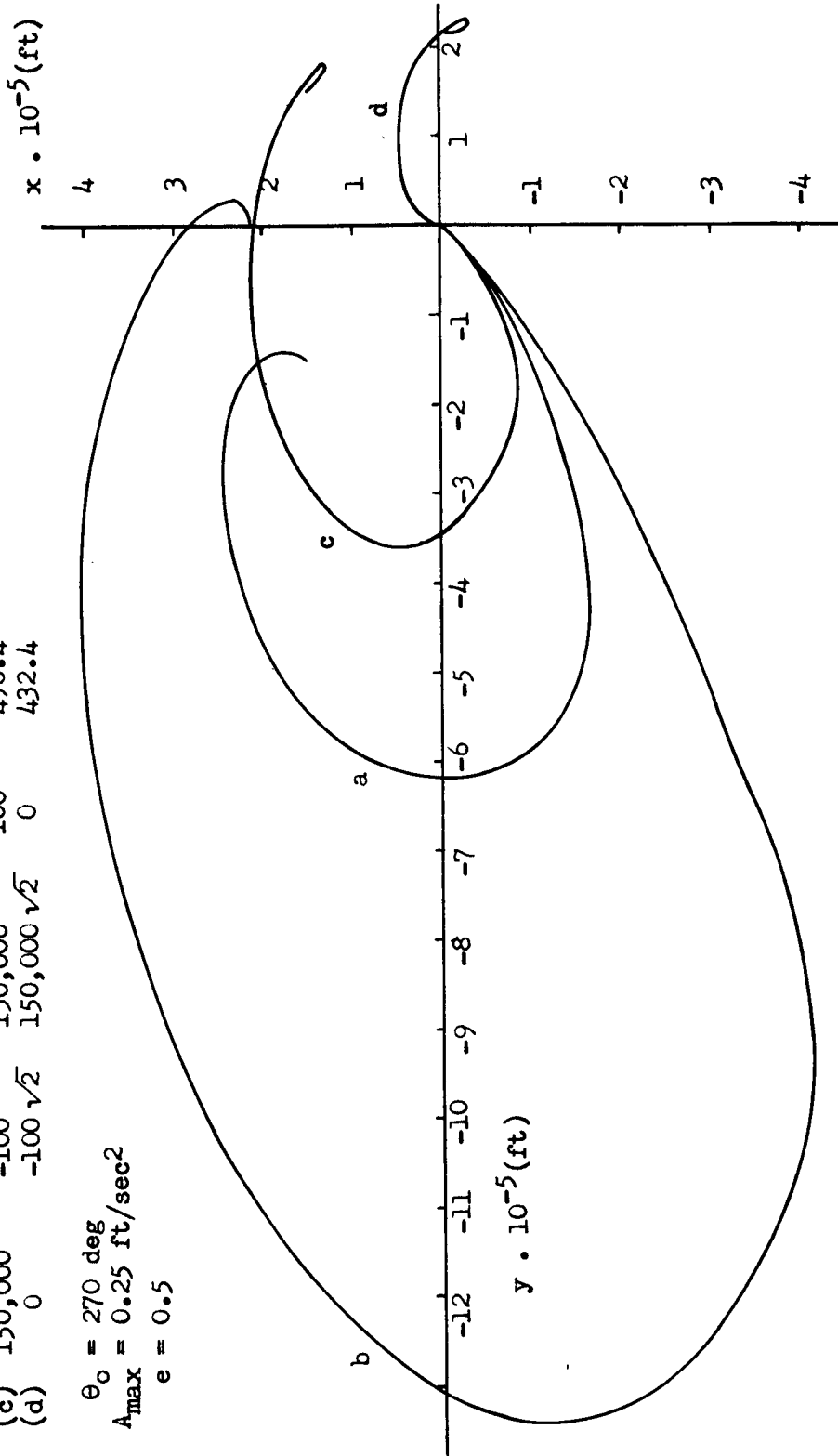


Figure 25. Optimum rendezvous trajectories in x-y plane for various initial conditions with $A_{max} = 0.25$ ft/sec² and $\theta_0 = 270$ degrees

	$x(0)$ (ft)	$\dot{x}(0)$ (ft/sec)	$y(0)$ (ft)	$\dot{y}(0)$ (ft/sec)	θ_f (deg)
(a)	150,000	-100	-150,000	-100	398.9
(b)	150,000 $\sqrt{2}$	0	0	-100 $\sqrt{2}$	443.9
(c)	150,000	100	150,000	-100	449.2
(d)	0	100 $\sqrt{2}$	150,000 $\sqrt{2}$	0	385.5

$\theta_0 = 270$ deg
 $e = 0.5$
 $A_{max} = 0.25$ ft/sec²

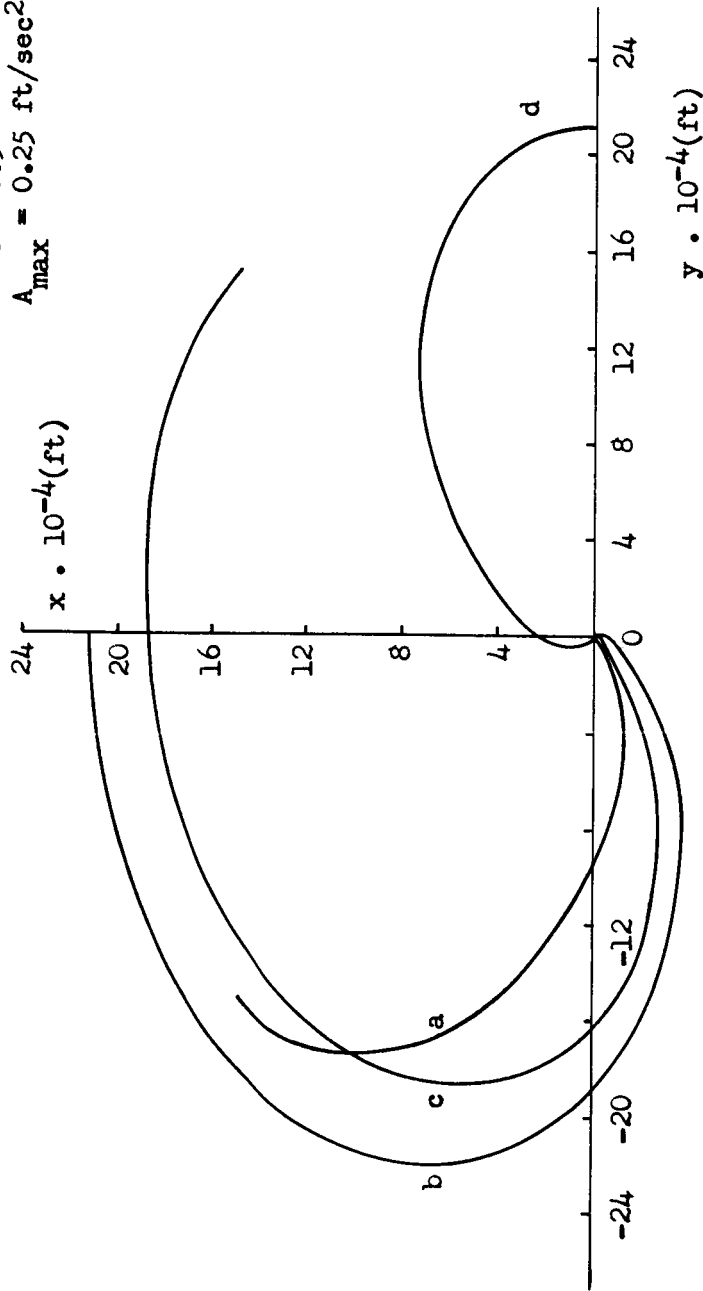


Figure 26. Optimum rendezvous trajectories in x-y plane for various initial conditions with $A_{max} = 0.25$ ft/sec² and $\theta_0 = 270$ degrees

$x(0) = 150,000 \text{ ft}$
 $\dot{x}(0) = 100 \text{ ft/sec}$
 $y(0) = -150,000 \text{ ft}$
 $\dot{y}(0) = -100 \text{ ft/sec}$
 $\theta_0 = 0 \text{ deg}$
 $e = 0.5$

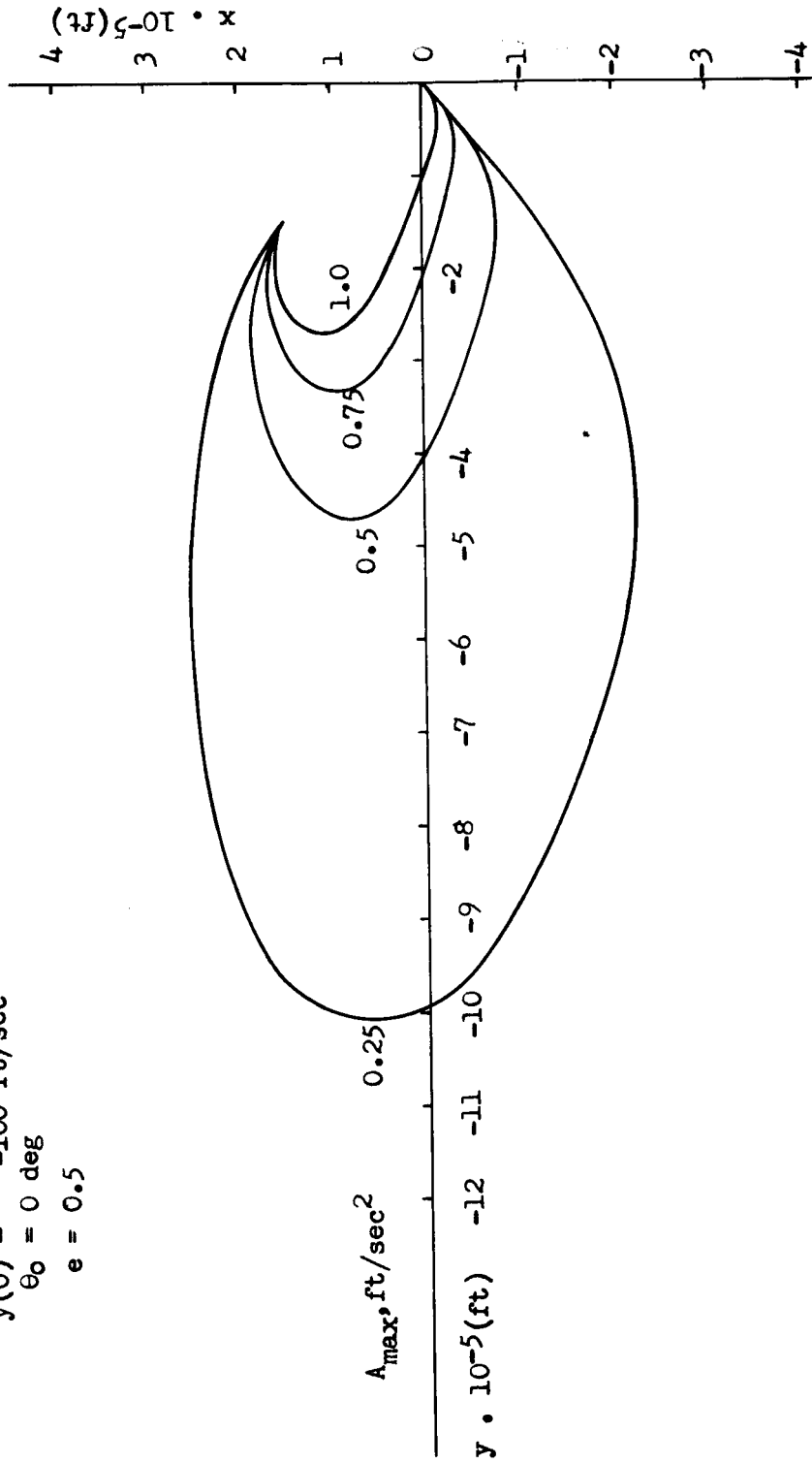
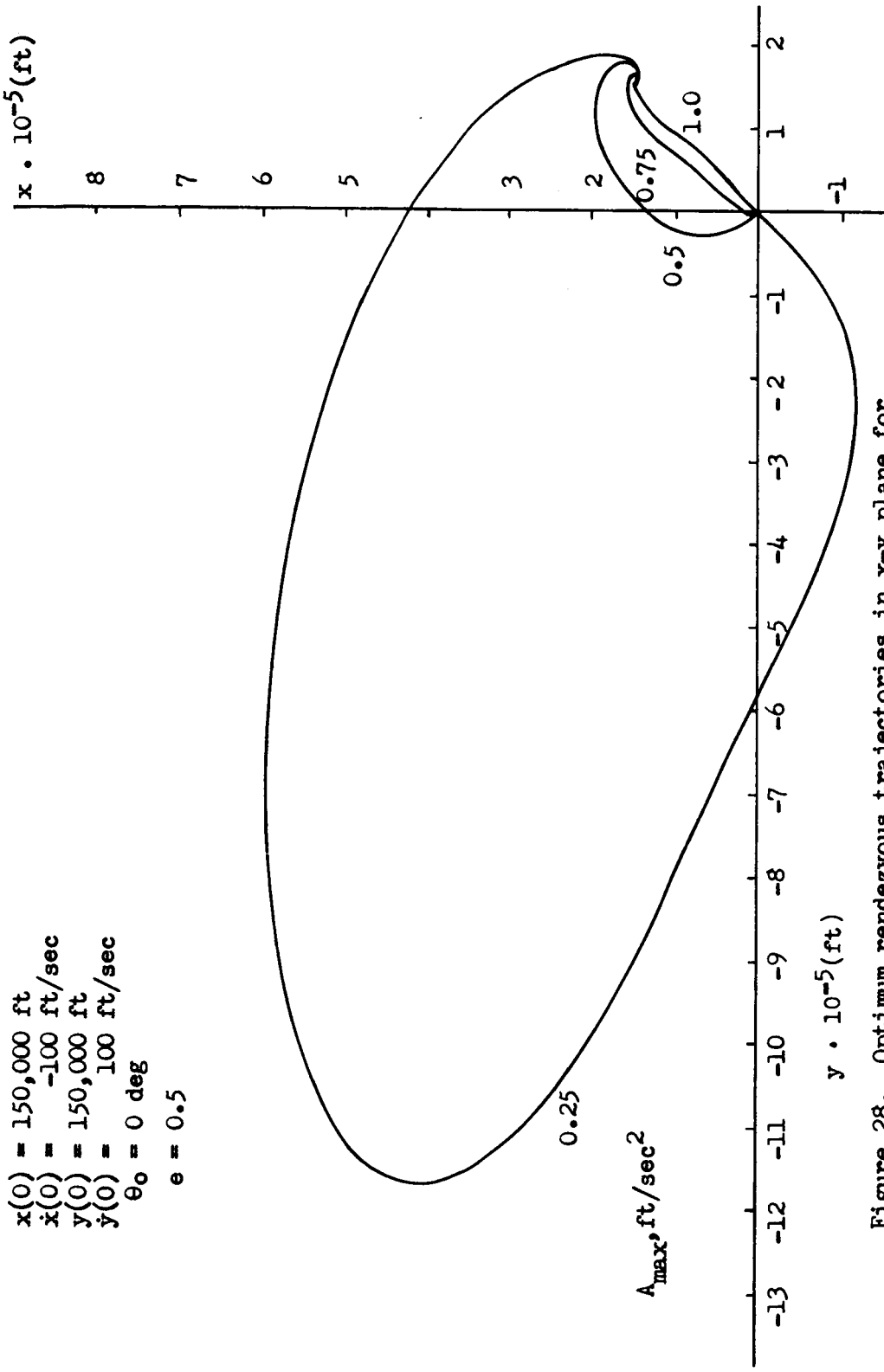


Figure 27. Optimum rendezvous trajectories in x-y plane for different maximum allowable accelerations



$x(0) = 150,000$ ft
 $\dot{x}(0) = -100$ ft/sec
 $y(0) = 150,000$ ft
 $\dot{y}(0) = 100$ ft/sec
 $\theta_0 = 0$ deg
 $e = 0.5$

Figure 28. Optimum rendezvous trajectories in x-y plane for different maximum allowable accelerations

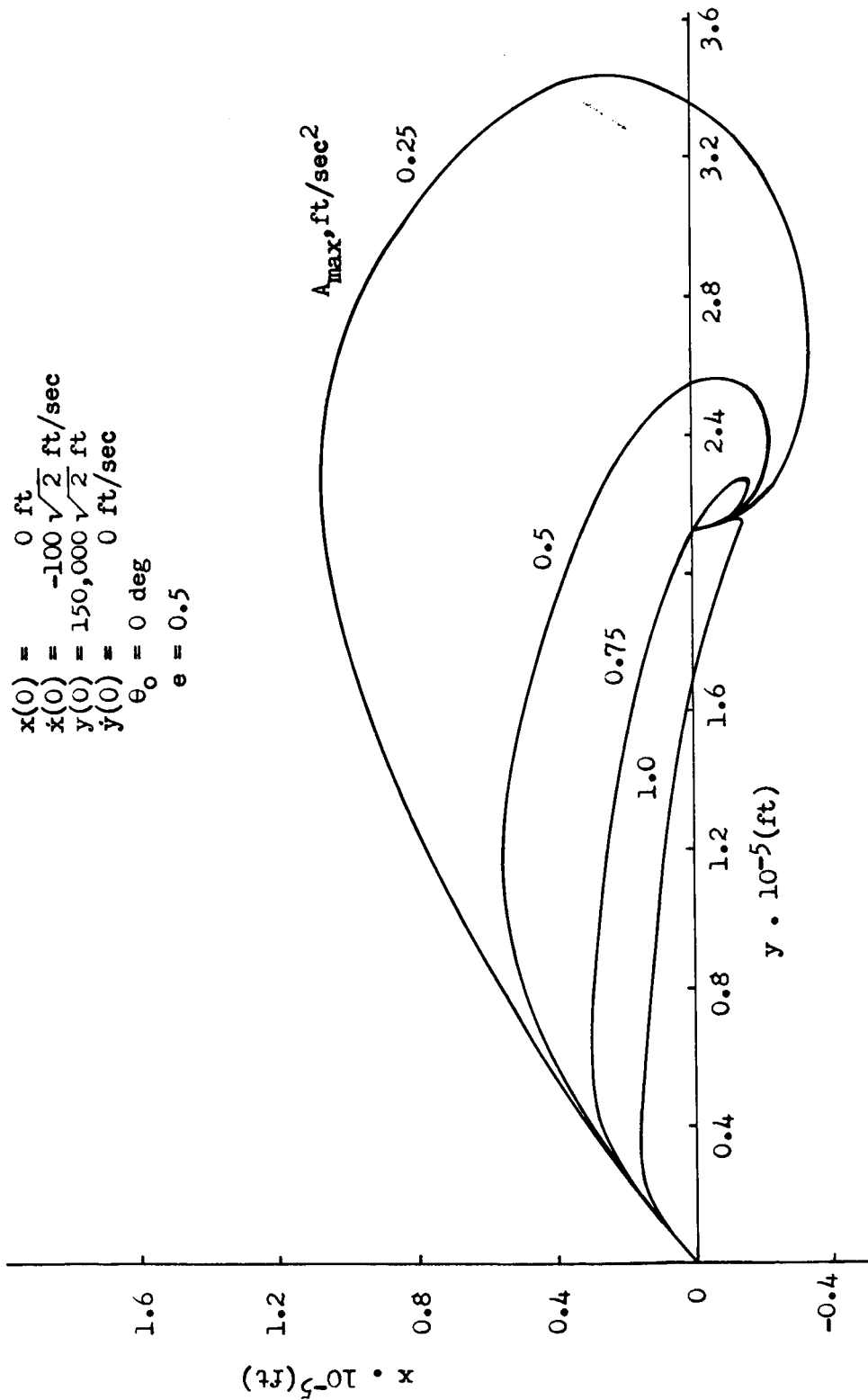


Figure 29. Optimum rendezvous trajectories in x-y plane for different maximum allowable accelerations

$$\begin{aligned}
 x(0) &= 150,000 \sqrt{2} \text{ ft} \\
 \dot{x}(0) &= 100 \sqrt{2} \text{ ft/sec} \\
 y(0) &= 0 \text{ ft} \\
 \dot{y}(0) &= 0 \text{ ft/sec} \\
 \theta_0 &= 0 \text{ deg} \\
 e &= 0.5
 \end{aligned}$$

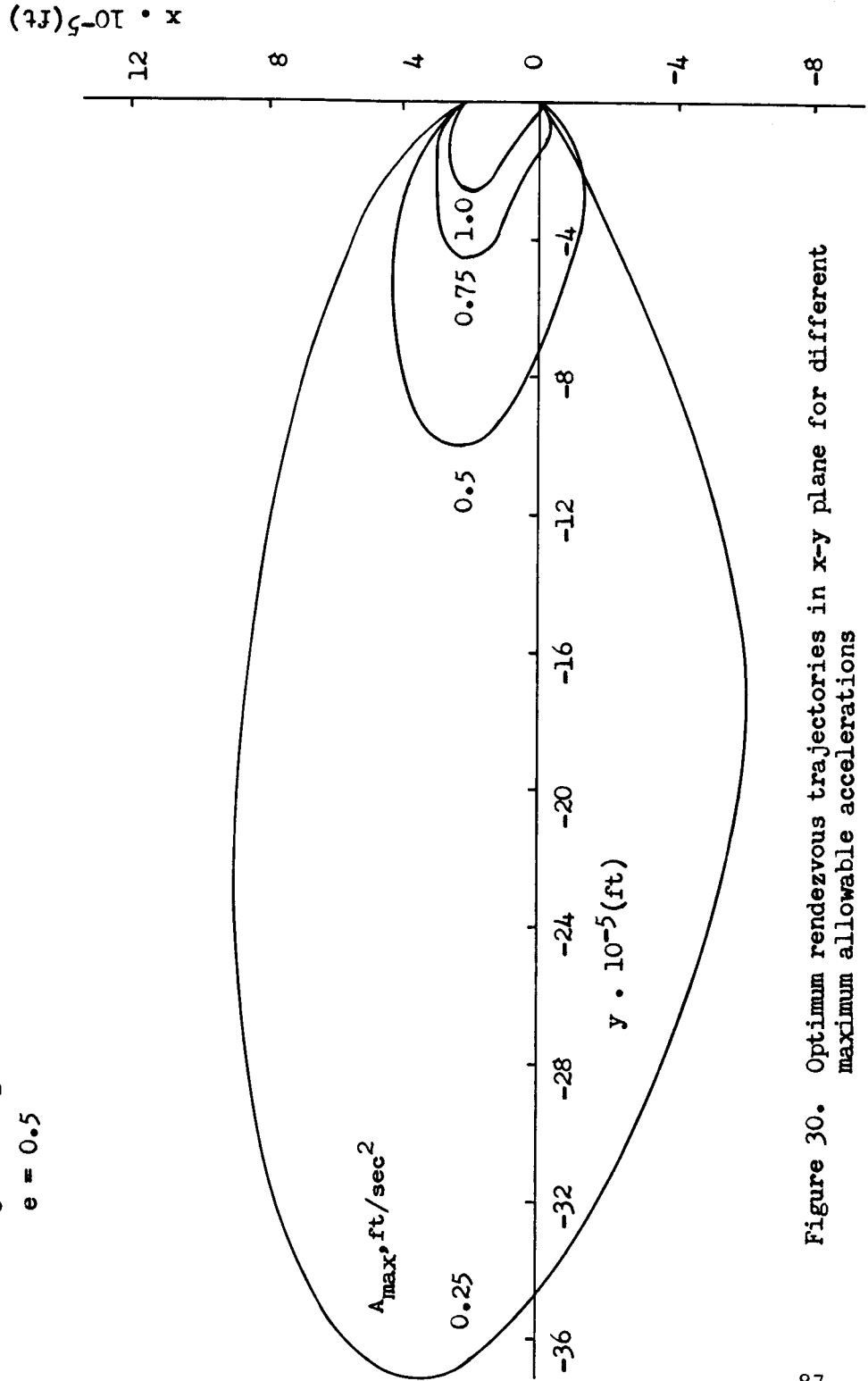


Figure 30. Optimum rendezvous trajectories in x-y plane for different maximum allowable accelerations

$$\begin{aligned}
 x(0) &= 150,000 \text{ ft} \\
 \dot{x}(0) &= 100 \text{ ft/sec} \\
 y(0) &= -150,000 \text{ ft} \\
 \dot{y}(0) &= -100 \text{ ft/sec} \\
 \theta_0 &= 0 \text{ degrees} \\
 e &= 0.5
 \end{aligned}$$

$$\begin{aligned}
 x(0) &= 150,000 \text{ ft} \\
 \dot{x}(0) &= -100 \text{ ft/sec} \\
 y(0) &= 150,000 \text{ ft} \\
 \dot{y}(0) &= 100 \text{ ft/sec} \\
 \theta_0 &= 0 \text{ degrees} \\
 e &= 0.5
 \end{aligned}$$

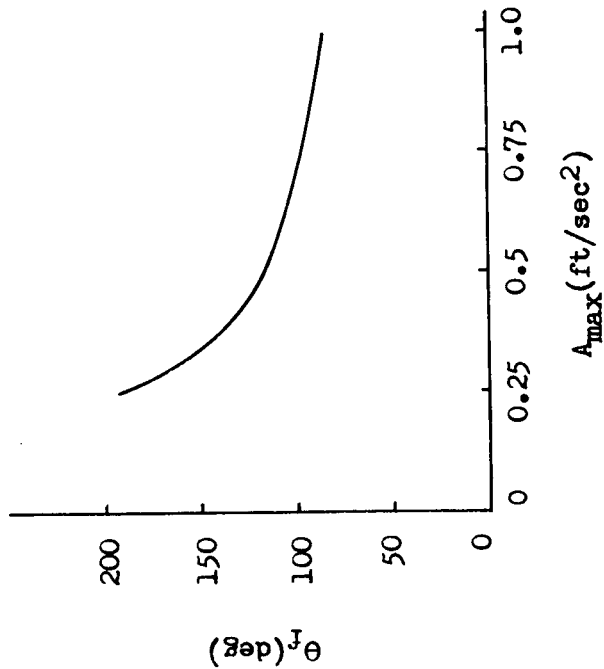
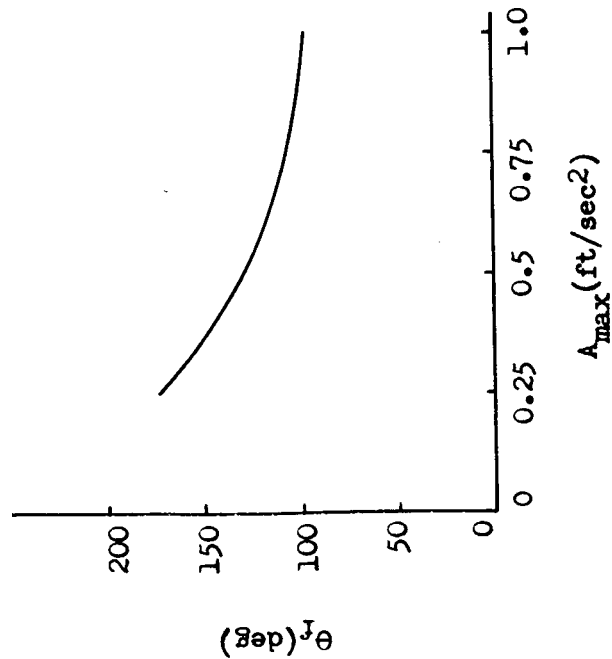


Figure 31. Optimum time vs. maximum allowable acceleration

$x(0) = 150,000 \text{ ft}$
 $\dot{x}(0) = 100 \text{ ft/sec}$
 $y(0) = -150,000 \text{ ft}$
 $\dot{y}(0) = -100 \text{ ft/sec}$
 $e = 0.5$
 $A_{\max} = 0.25 \text{ ft/sec}^2$

θ_0 , true anomaly,
 degrees

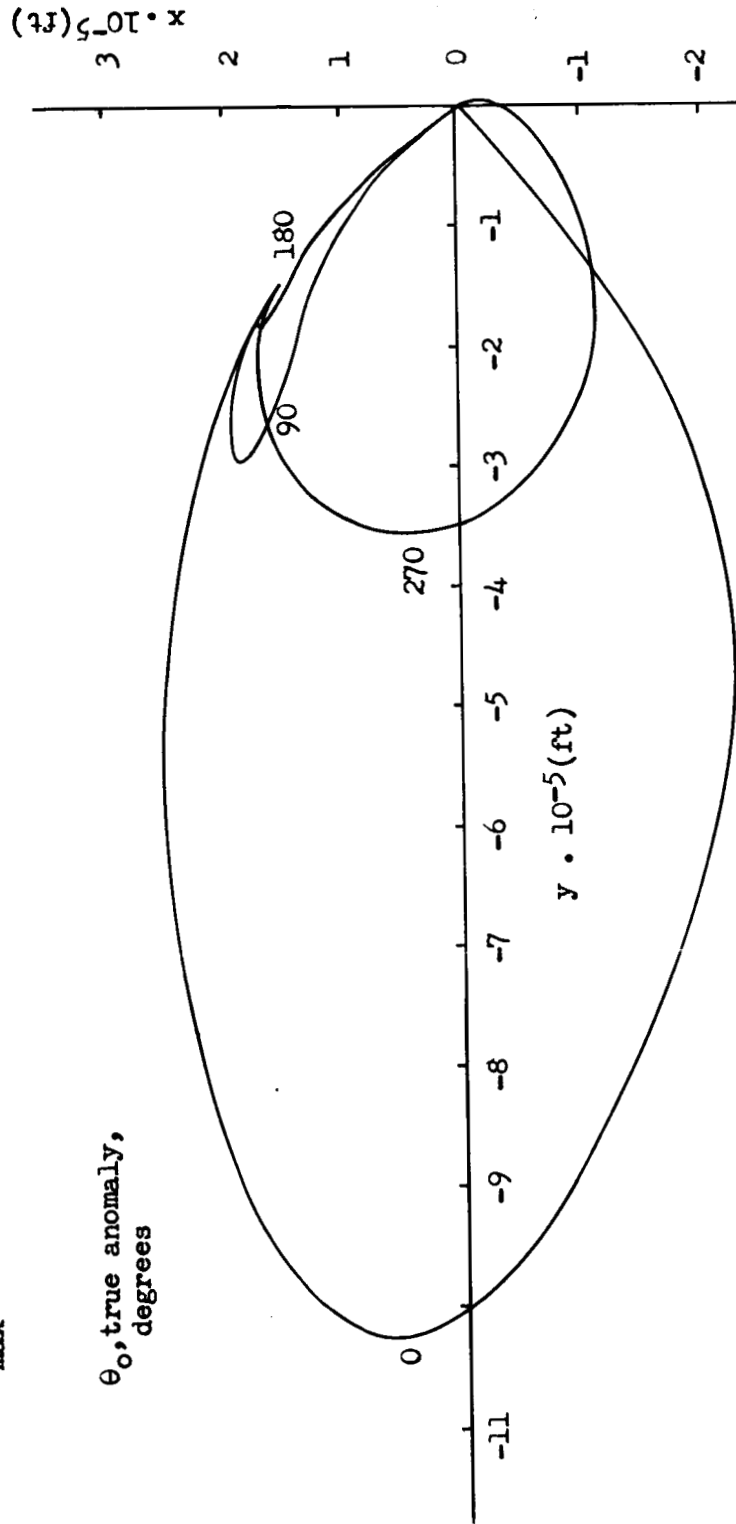


Figure 32. Optimum rendezvous trajectories in x-y plane for various initial values of the true anomaly with $A_{\max} = 0.25 \text{ ft/sec}^2$

$x(0) = 0$ ft
 $\dot{x}(0) = -100\sqrt{2}$ ft/sec
 $y(0) = 150,000\sqrt{2}$ ft
 $\dot{y}(0) = 0$ ft/sec
 $e = 0.5$
 $A_{\max} = 0.25$ ft/sec²

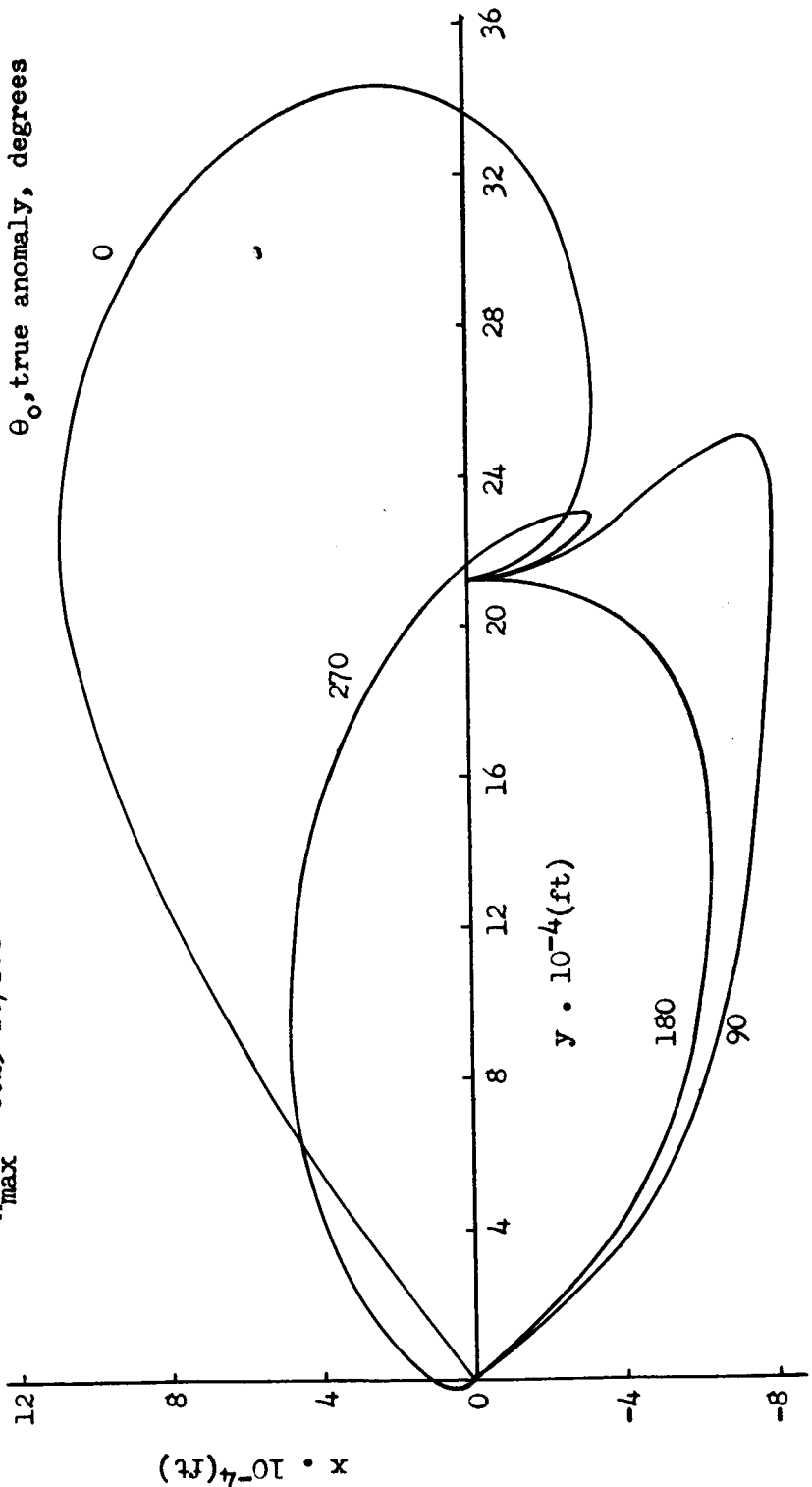


Figure 33. Optimum rendezvous trajectories in x-y plane for various initial values of the true anomaly with $A_{\max} = 0.25$ ft/sec²

$x(0) = 150,000 \text{ ft}$
 $\dot{x}(0) = 100 \text{ ft/sec}$
 $y(0) = 150,000 \text{ ft}$
 $\dot{y}(0) = -100 \text{ ft/sec}$
 $e = 0.5$
 $A_{\text{max}} = 0.25 \text{ ft/sec}^2$

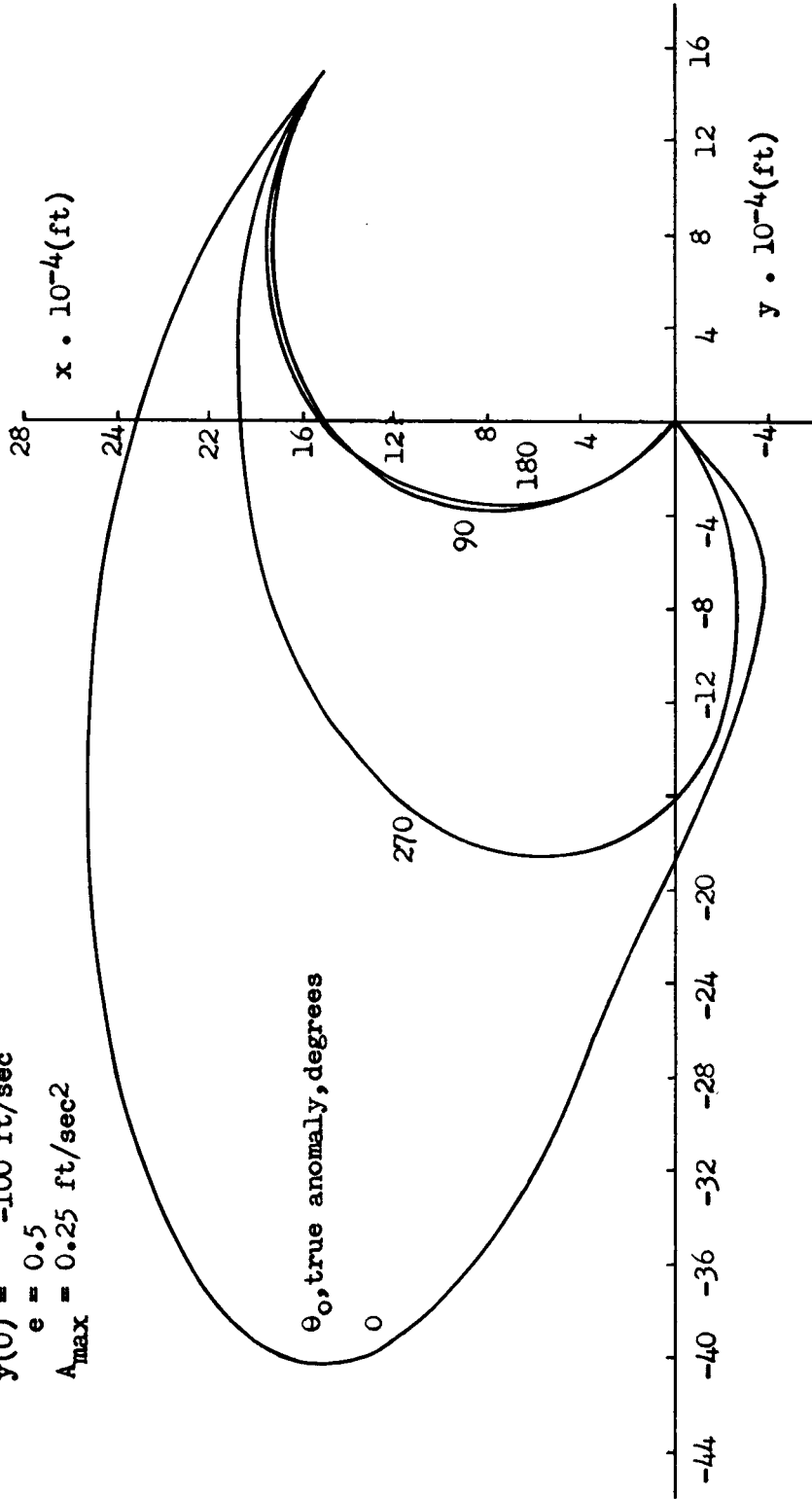


Figure 34. Optimum rendezvous trajectories in x-y plane for various initial values of the true anomaly with $A_{\text{max}} = 0.25 \text{ ft/sec}^2$

$x(0) = 200,000 \text{ ft}$
 $\dot{x}(0) = 150 \text{ ft/sec}$
 $y(0) = 0 \text{ ft}$
 $\dot{y}(0) = 0 \text{ ft/sec}$
 $A_{\text{max}} = 0.5 \text{ ft/sec}^2$
 $\theta_0 = 0 \text{ degrees}$

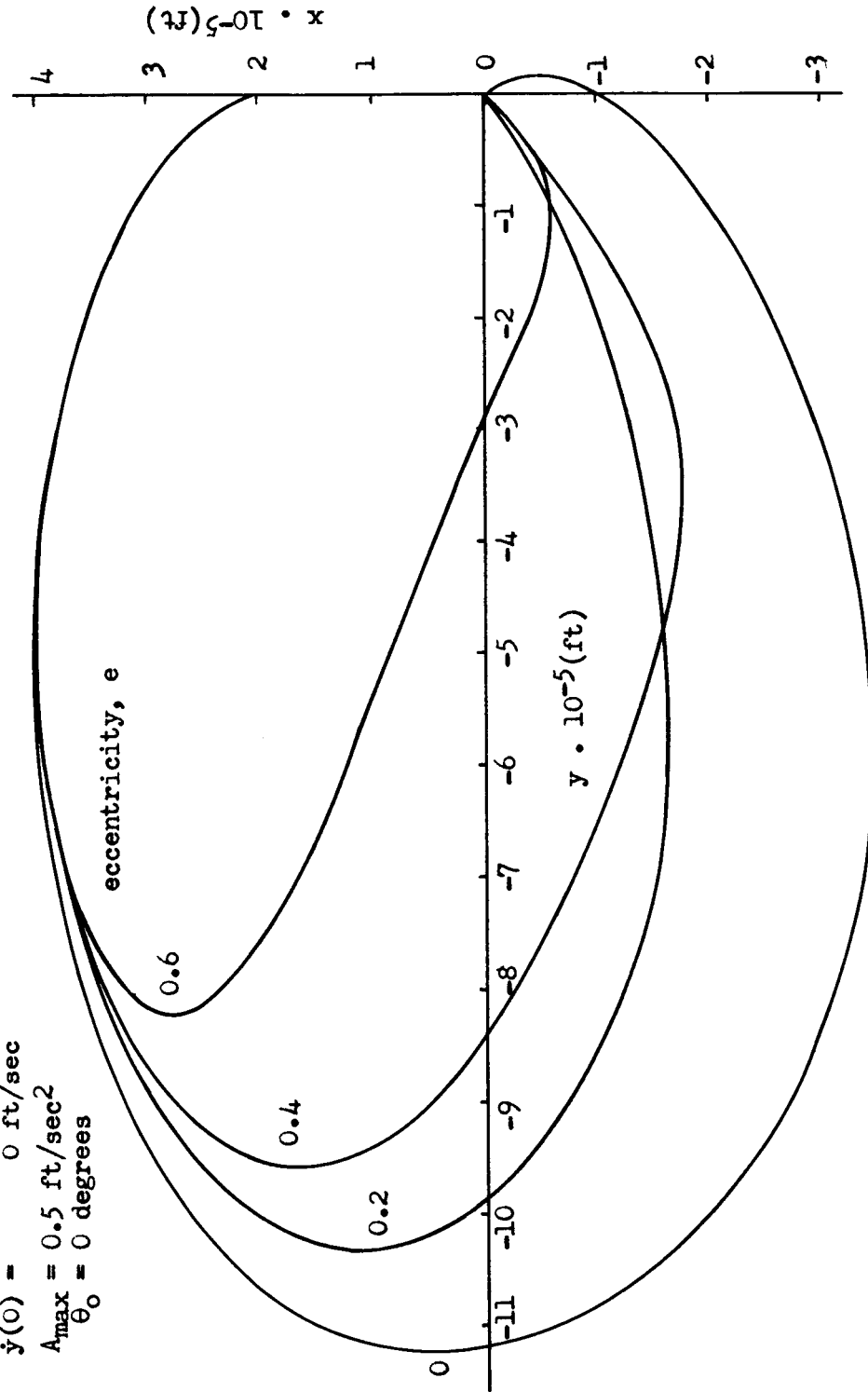


Figure 35. Optimum rendezvous trajectories in x-y plane for various values of the eccentricity with $A_{\text{max}} = 0.5 \text{ ft/sec}^2$

$x(0) = 0$ ft
 $\dot{x}(0) = 0$ ft/sec
 $y(0) = 200,000$ ft
 $\dot{y}(0) = 150$ ft/sec
 $A_{\max} = 0.5$ ft/sec²
 $\theta_0 = 0$ degrees

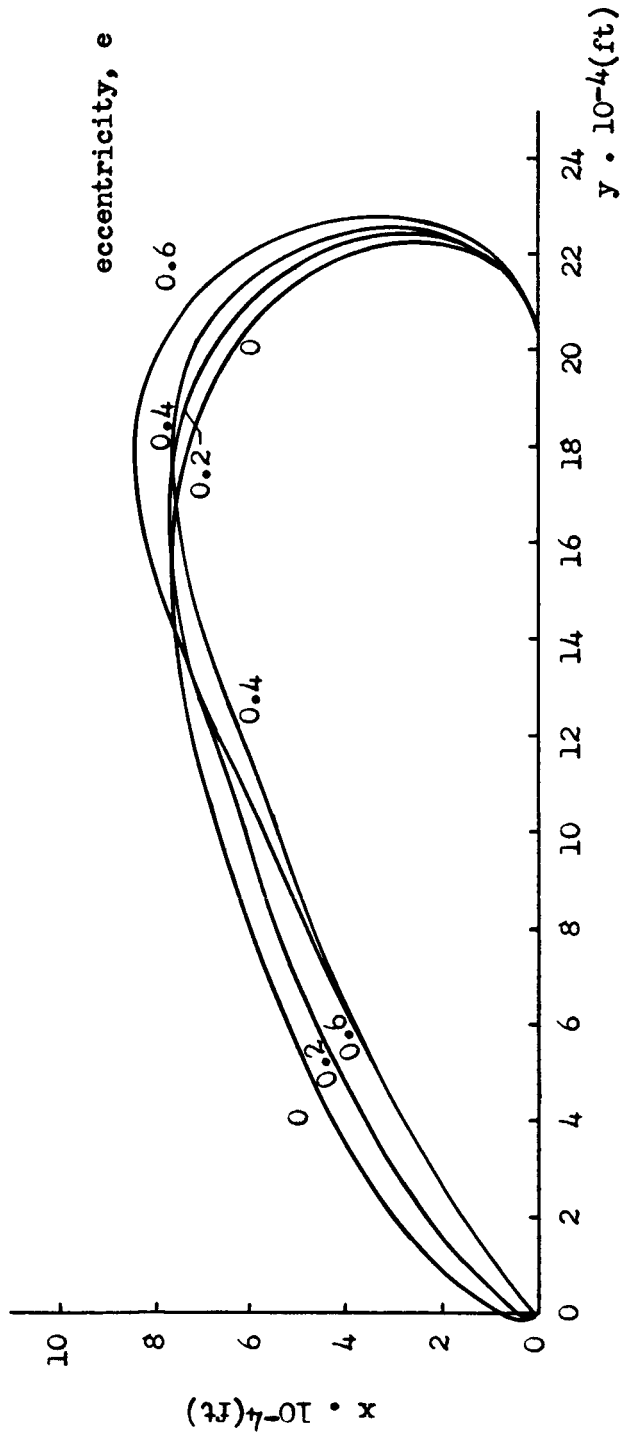


Figure 36. Optimum rendezvous trajectories for various values of the eccentricity with $A_{\max} = 0.5$ ft/sec²

$$\alpha = \tan^{-1} \frac{u_y}{u_x} = \text{direction of thrust vector}$$

$x(0) = 150,000 \sqrt{2}$ ft
 $\dot{x}(0) = 100 \sqrt{2}$ ft/sec
 $y(0) = 0$ ft
 $\dot{y}(0) = 0$ ft/sec
 $A_{\max} = 0.5$ ft/sec²
 $\theta_0 = 0$ degrees
 $R_p = 4100$ miles
 $e = 0.5$

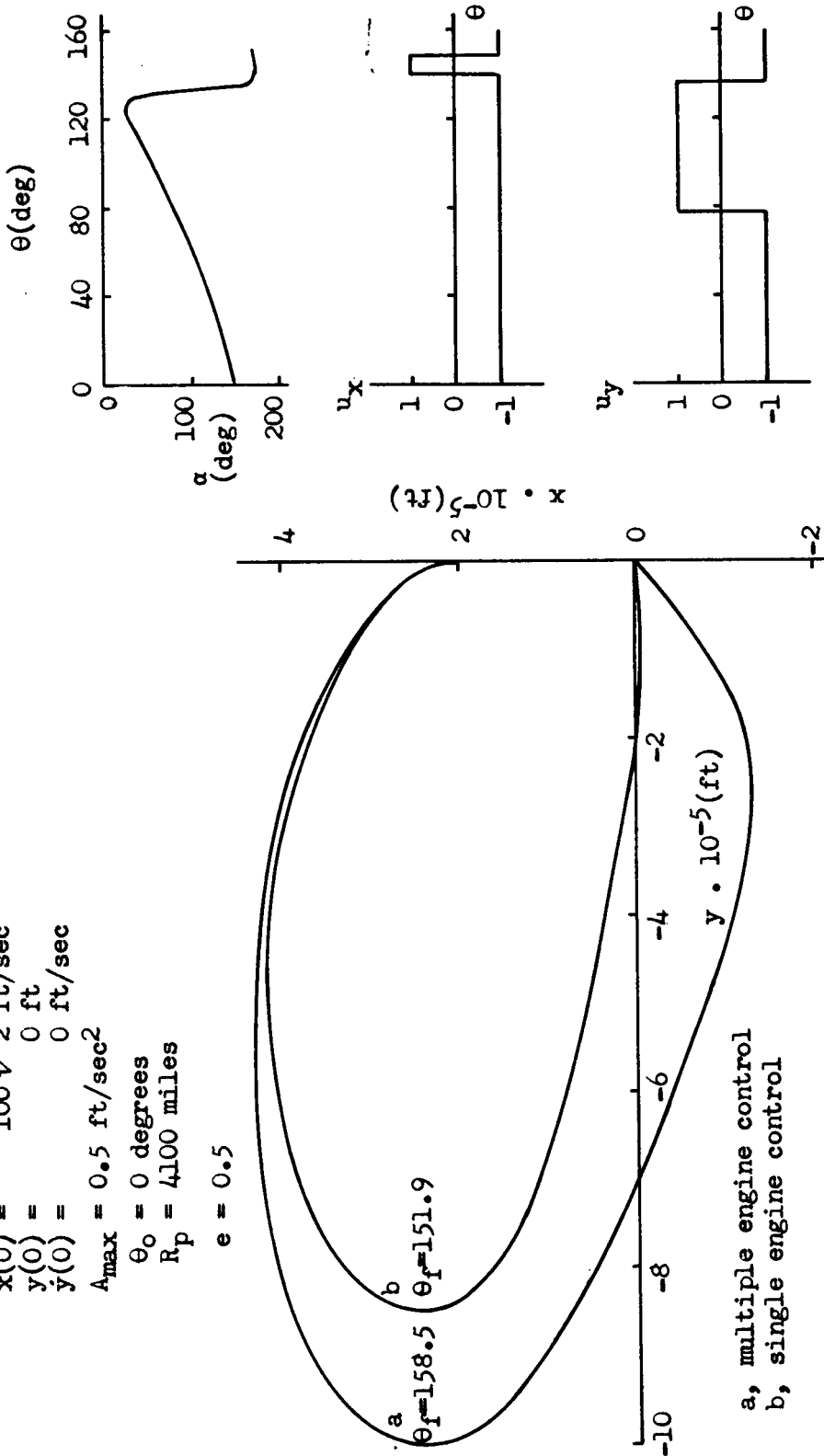
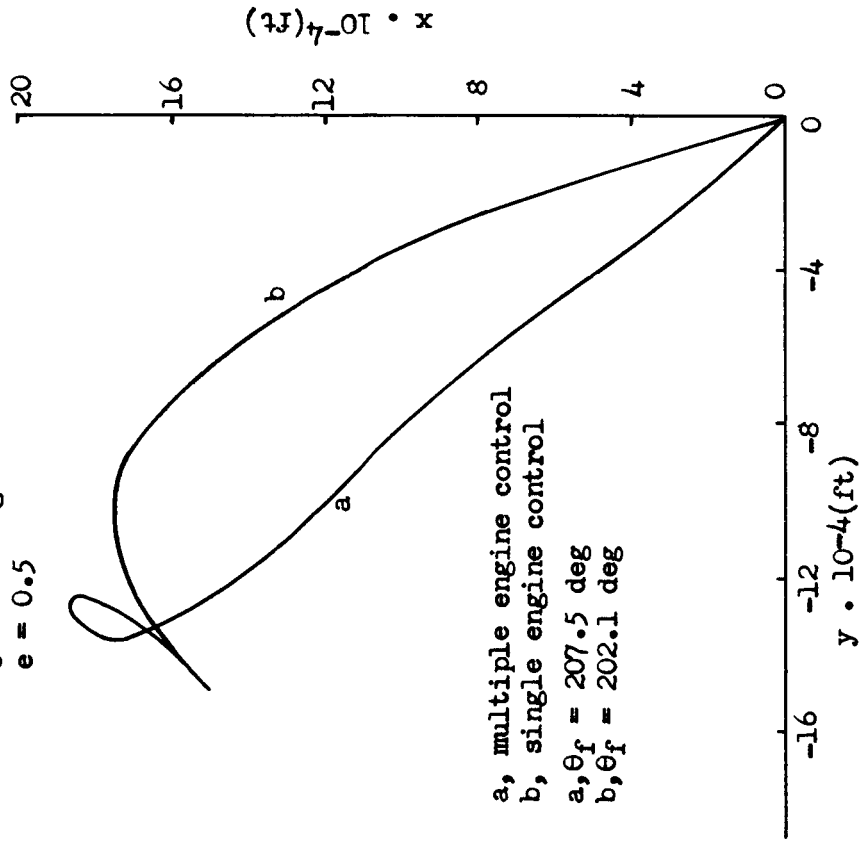


Figure 37. Comparison of single engine control and multiple engine control

$x(0) = 150,000$ ft
 $\dot{x}(0) = 100$ ft/sec
 $y(0) = -150,000$ ft/sec
 $\dot{y}(0) = 100$ ft/sec
 $A_{max} = 0.25$ ft/sec²
 $\theta_0 = 180$ degrees
 $e = 0.5$



a, multiple engine control
 b, single engine control
 $a, \theta_f = 207.5$ deg
 $b, \theta_f = 202.1$ deg

$\alpha = \tan^{-1} \frac{u_y}{u_x}$ = direction of thrust vector

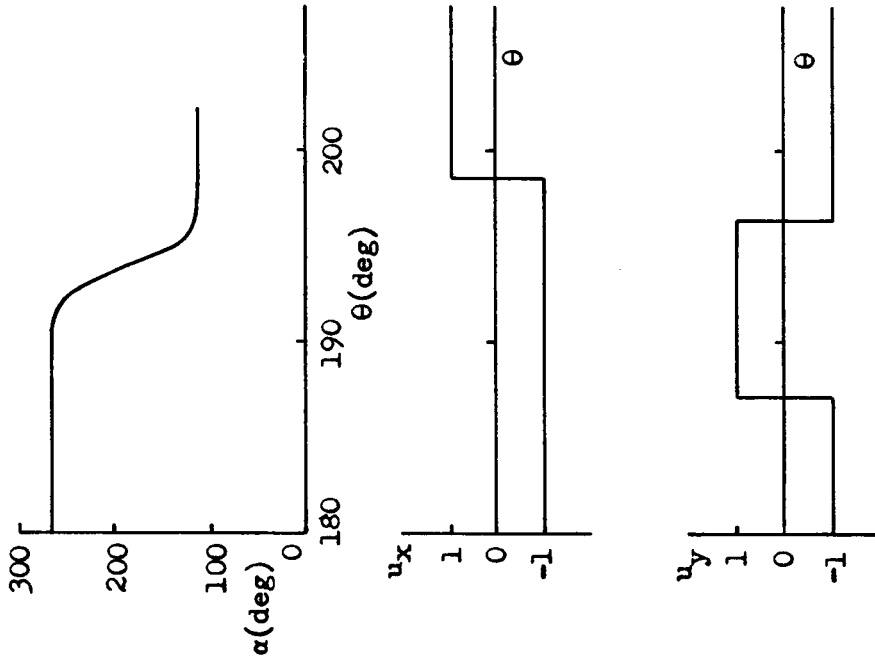


Figure 38. Comparison of single engine control and multiple engine control

	$x(0)$ (ft)	$\dot{x}(0)$ (ft/sec)	$y(0)$ (ft)	$\dot{y}(0)$ (ft/sec)	θ_f (deg)
(a)	150,000	100	-150,000	-100	139.7
(b)	150,000 $\sqrt{2}$	100 $\sqrt{2}$	0	0	205.9
(c)	150,000	100	150,000	100	146.3
(d)	0	0	150,000 $\sqrt{2}$	100 $\sqrt{2}$	88.5

$A_{max} = 0.75 \text{ ft/sec}^2$

$\theta_0 = 0 \text{ deg}$

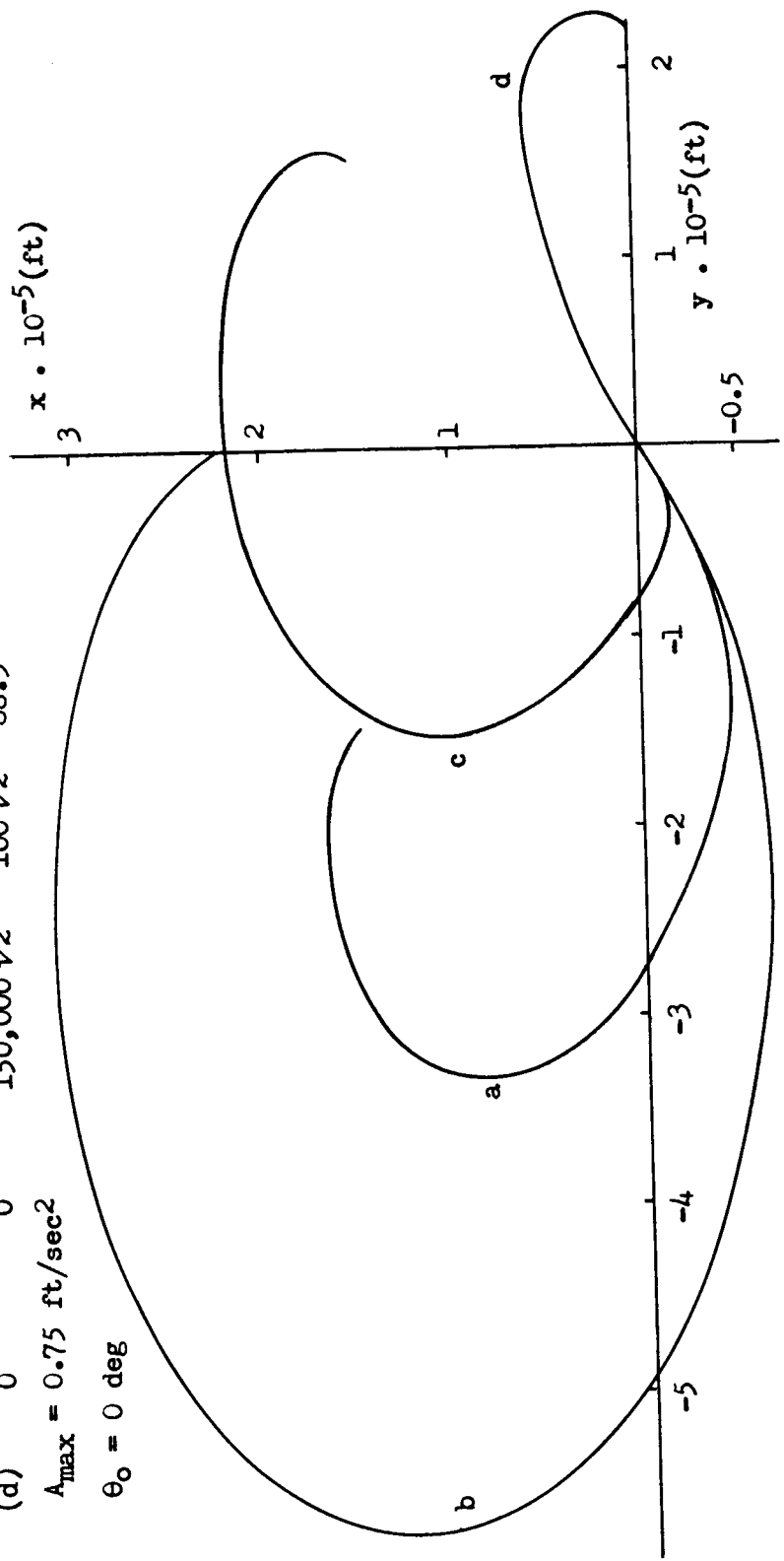


Figure 39. Optimum rendezvous trajectories for various initial conditions with a circular target vehicle orbit

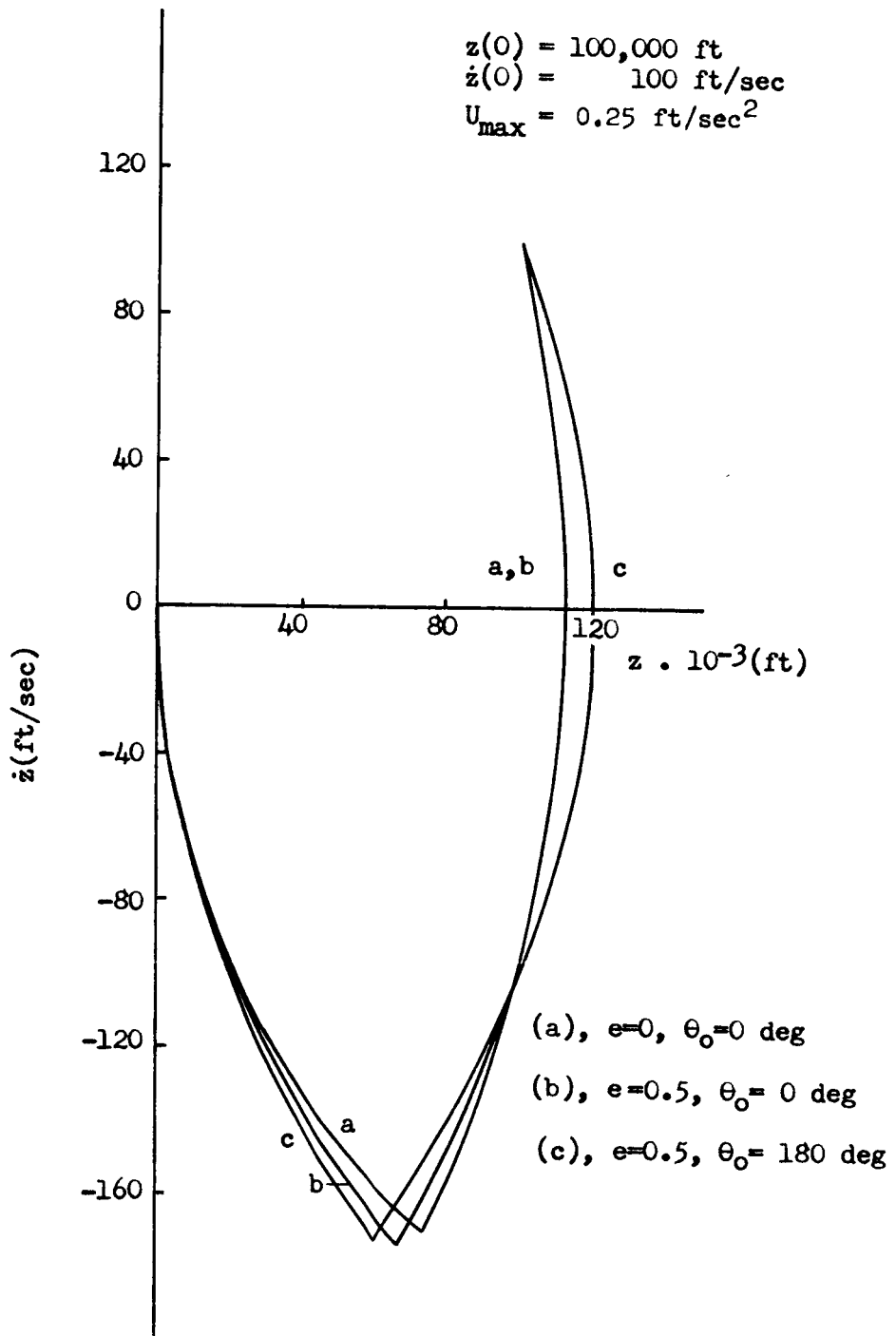


Figure 40. z - \dot{z} plots with $U_{\max} = 0.25 \text{ ft/sec}^2$

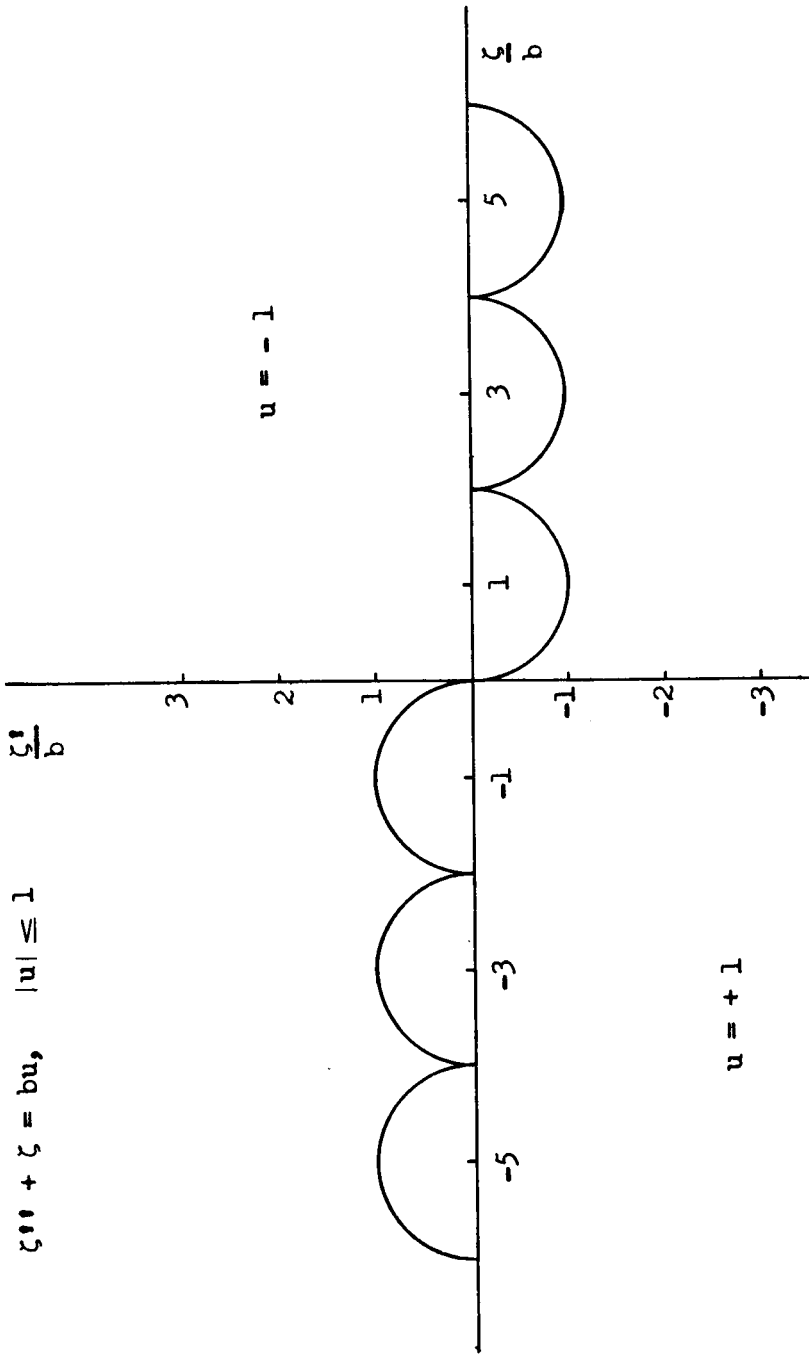


Figure 41. Switching surface for Bushaw's problem

APPENDIX A

REVIEW OF LINEAR SYSTEM THEORY

In this appendix a review of the theory of linear differential equations is given.

Consider the set of n first order linear differential equations

$$\dot{\underline{x}}(t) = A(t) \underline{x}(t) + B(t) \underline{u}(t), \quad \underline{x}(t_0) = \underline{x}_0 \quad (A1)$$

where $A(t)$ is an $n \times n$ matrix, $B(t)$ is an $n \times r$ matrix, and $\underline{u}(t)$ is an r dimensional vector.

Theorem: Let $X(t, t_0)$ be the $n \times n$ matrix which is the solution of the differential equation

$$\frac{d}{dt} X(t, t_0) = A(t) X(t, t_0), \quad X(t_0, t_0) = I, \quad (A2)$$

and if the elements of $A(t)$ are continuous functions of time, then the solution of (A1) is

$$\underline{x}(t) = X(t, t_0) \left[\underline{x}_0 + \int_{t_0}^t X^{-1}(\tau, t_0) B(\tau) \underline{u}(\tau) d\tau \right] \quad (A3)$$

The matrix $X(t, t_0)$ is called the state transition matrix.¹

¹

Any nonsingular matrix which satisfies the differential equation (A2) is called a fundamental matrix. If it also satisfies the initial condition $X(t, t_0) = I$ it is called the state transition matrix.

Proof: Substitute (A3) into (A1).

The state transition matrix $X(t, t_0)$ possesses the following properties:

$$1) \quad X(t_3, t_1) = X(t_3, t_2) X(t_2, t_1) \quad (A4)$$

$$2) \quad X^{-1}(t_2, t_1) = X(t_1, t_2) \quad (A5)$$

$$3) \quad \det X(t_2, t_1) = \exp \left[\int_{t_1}^{t_2} [\text{trace } A(\tau)] d\tau \right] \quad (A6)$$

$$4) \quad \text{If, for all } t \int_{t_1}^t A(\tau) d\tau \text{ and } A(t)$$

commute then

$$X(t_2, t_1) = \exp \left[\int_{t_1}^{t_2} A(\tau) d\tau \right]. \quad (A7)$$

It follows that if A is a constant matrix

$$X(t_2, t_1) = \exp [(t_2 - t_1)A] \quad (A8)$$

where

$$\exp [(t_2 - t_1)A] = \sum_{k=0}^{\infty} \frac{1}{k!} A^k (t_2 - t_1)^k. \quad (A9)$$

Now consider the free motion of the system (A1) where A is periodic of period T , i.e., $A(t + T) = A(t)$. Observe that $X(t + T, t_0)$ is a fundamental matrix of (A1). This is easily verified.

$$\dot{X}(t + T, t_0) = A(t + T) X(t + T, t_0)$$

But $A(t + T) = A(t)$, then

$$\dot{X}(t + T, t_0) = A(t) X(t + T, t_0) .$$

Thus, $X(t + T, t_0)$ is a fundamental matrix of (A1).

Theorem: The state transition matrix of (A1) where $A(t + T) = A(t)$ can be written as

$$X(t, t_0) = Q(t, t_0) \exp [(t - t_0)D] , \quad Q(t_0, t_0) = I \quad (A10)$$

where $Q(t, t_0)$ is a nonsingular periodic matrix of period T , and D is a constant matrix.

Proof: The columns of $X(t + T, t_0)$ are n linearly independent solutions of the homogeneous portion of (A1), therefore each of these columns is given by $\phi_k = X(t, t_0) c_k$ where c_k is an $n \times 1$ column matrix of constants. Let C be the $n \times n$ matrix whose columns are the c_k . Then

$$X(t + T, t_0) = X(t, t_0) C . \quad (A11)$$

Define D by

$$\exp (TD) \equiv C , \quad (A12)$$

then

$$X(t + T, t_0) = X(t, t_0) \exp (TD) . \quad (A13)$$

Define

$$Q(t, t_0) \equiv X(t, t_0) \exp [-(t - t_0)D] . \quad (A14)$$

$Q(t, t_0)$ is nonsingular since $X(t, t_0)$ and $\exp [-(t - t_0)D]$ are nonsingular. Also, $Q(t, t_0)$ is periodic of period T since

$$Q(t + T, t_0) = X(t + T, t_0) \exp [-(t + T - t_0)D]$$

$$Q(t + T, t_0) = X(t, t_0) \exp (TD) \exp (-TD) \exp [-(t - t_0)D]$$

$$Q(t + T, t_0) = X(t, t_0) \exp [-(t - t_0)D] = Q(t, t_0) .$$

Now let

$$Y(t, t_0) = Q^{-1}(t, t_0) X(t, t_0) = \exp[(t - t_0)D] . \quad (A15)$$

Hence, $Y(t, t_0)$ is the state transition matrix of the system

$$\underline{y}(t) = D\underline{y} \quad (A16)$$

which is a differential equation with constant coefficients. Observe that the vector \underline{y} is related to the vector \underline{x} by

$$\underline{x}(t) = Q(t, t_0) \underline{y}(t) . \quad (A17)$$

Hence, the investigation of the motion of a system with periodic coefficients can be reduced to the study of the motion of a system with constant coefficients. Any system with time varying coefficients which can be transformed into a system with constant coefficients is said to be reducible. The matrix Q is called a Lyapunov transformation.

Substitution of (A17) into the homogeneous part of (A1) gives

$$\begin{aligned} \dot{Q} \underline{y} + Q \dot{\underline{y}} &= A Q \underline{y} \\ \dot{Q} \underline{y} + Q D \underline{y} &= A Q \underline{y} \\ D &= Q^{-1} (AQ - \dot{Q}) \end{aligned} \quad (A18)$$

Comment: Although it has been proved that a system with periodic coefficients can be transformed into a system with constant coefficients there is no general method for determining the matrix Q.

By another transformation

$$\underline{y} = R \underline{z} \quad (A19)$$

the system (A16) can be transformed into its Jordan canonical form

$$\underline{z} = \Lambda \underline{z} \quad (A20)$$

where

$$\Lambda = R^{-1}DR \quad (A21)$$

The state transition matrix of the system (A1) is then given by

$$X(t, t_0) = P(t) \exp \left[(t - t_0)\Lambda \right] P^{-1}(t_0) \quad (A22)$$

where

$$\underline{x}(t) = P(t) \underline{z}(t) \quad (A23)$$

However,

$$\exp \left[(t - t_0)\Lambda \right] = R^{-1} \exp \left[(t - t_0)D \right] R \quad (A24)$$

Substitution of (A24) into (A22) gives

$$X(t, t_0) = P(t) R^{-1} \exp \left[(t - t_0)D \right] R P^{-1}(t_0) \quad (A25)$$

Comparison of (A25) and (A10) gives

$$R = P(t_0) \quad (A26)$$

and

$$Q(t, t_0) = P(t) R^{-1}$$

$$Q(t, t_0) = P(t) P^{-1}(t_0) \quad (A27)$$

Equation (A22) is the form of the state transition matrix used.

APPENDIX B

EXISTENCE AND UNIQUENESS CONDITIONS

In this appendix the existence and uniqueness conditions for a solution of the time optimal control problem as set forth by La Salle (1960) are given.

The equation of motion of the system is

$$\dot{\underline{x}}(t) = A(t) \underline{x}(t) + B(t) \underline{u}(t) . \quad (B1)$$

The optimal control found by applying Pontryagin's maximum principle is

$$\underline{u}^*(t) = \text{sgn} \left[\underline{p}^T(t_0) X^{-1}(t, t_0) B(t) \right] . \quad (B2)$$

Let

$$Y(t) = X^{-1}(t, t_0) B(t) , \quad (B3)$$

then (B2) becomes

$$\underline{u}^*(t) = \text{sgn} \left[\underline{p}^T(t_0) Y(t) \right] . \quad (B4)$$

Definitions:

Controllable System

A system is said to be controllable if for each initial state \underline{x}_0 there is an admissible control that will bring the system to the equilibrium state in finite time.

Completely Controllable System

A system is said to be completely controllable if for each initial state \underline{x}_0 and if there is no restriction on the control function it is always possible to bring the system from its initial state to any other state \underline{x}_0 at any given time t .

Proper Control System

A control system is said to be proper if $\underline{p}^T(t_0) Y(t) = \underline{0}$ on an interval of positive length implies $\underline{p}(t_0) = \underline{0}$.

Asymptotically Proper Control System

A control system is said to be asymptotically proper if

$$\int_0^{\infty} \left\| \underline{p}^T(t_0) Y(t) \right\| dt = \infty \quad (B5)$$

Normal Control System

A control system is said to be normal if no component of $\underline{p}^T(t_0) Y(t)$, $\underline{p}(t_0) \neq 0$, is identically zero on an interval of positive length. Note that all normal control systems are proper but not every proper system is normal.

Theorem 1. Proper control systems of the form (B1) are completely controllable.

Theorem 2. Asymptotically proper control systems of the form (B1) are controllable.

Therefore, if a control system is asymptotically proper there is a

control function which will transfer the system from any initial state \underline{x}_0 to the origin in finite time.

Theorem 3. The optimal control function, if it exists, of a normal control system is uniquely determined by (B2).

For the non-normal control systems the most that can be said is that if a solution exists then there is an optimal control function of the form (B2), but there may be an infinite number of optimal control functions.

APPENDIX C

FLETCHER-POWELL METHOD

In this appendix a brief description of the Fletcher-Powell method will be given. For a complete description of the method the original papers by Davidon (1959) and Fletcher and Powell (1963) should be consulted.

The problem under consideration is that of finding a local maximum¹ (or minimum) of a function $f(x_1, x_2, \dots, x_n)$ of several variables x_1, x_2, \dots, x_n . In the neighborhood of a maximum (or minimum) the second-order terms dominate. Therefore, for an iterative procedure to converge quickly for a general function it must have guaranteed rapid convergence for a general quadratic. Such a method is the Fletcher-Powell method, a modification of Davidon's variable metric method. It is an iterative gradient technique which will find the maximum (or minimum) of a quadratic of n variables in n iterations. Use of the method requires that the function and its gradient be known at any point.

¹ The presentation here will be that of finding a maximum. It will differ slightly from the presentation found in Davidon's and Fletcher and Powell's papers since they were written for the minimization of a function.

Consider the Taylor series expansion of a function $f(\underline{x})$ about some point \underline{x}_0 .

$$f(\underline{x}) = f(\underline{x}_0) + \sum_{i=1}^n \frac{\partial f(\underline{x}_0)}{\partial x_i} (x_i - x_{0_i}) + \frac{1}{2} \sum_{i=1}^n \sum_{j=1}^n \frac{\partial^2 f(\underline{x}_0)}{\partial x_i \partial x_j} (x_i - x_{0_i})(x_j - x_{0_j}) + \text{higher order terms} \quad (C1)$$

where x_i and x_{0_i} , $i = 1, 2, \dots, n$, are the components of the vectors \underline{x} and \underline{x}_0 . Let $\underline{g}(\underline{x})$ be the gradient of $f(\underline{x})$, and let $G(\underline{x})$ be the $n \times n$ matrix whose components are given by

$$G_{ij}(\underline{x}) = \frac{\partial^2 f(\underline{x})}{\partial x_i \partial x_j} \quad (C2)$$

The matrix G is called the Hessian. In matrix notation, equation (C1) becomes

$$f(\underline{x}) = f(\underline{x}_0) + \underline{g}^T(\underline{x}_0)(\underline{x} - \underline{x}_0) + \frac{1}{2} (\underline{x} - \underline{x}_0)^T G(\underline{x}_0) (\underline{x} - \underline{x}_0) + \dots \quad (C3)$$

Also,

$$\underline{g}(\underline{x}) = \underline{g}(\underline{x}_0) + G(\underline{x}_0) (\underline{x} - \underline{x}_0) + \dots \quad (C4)$$

Now let \underline{x}_0 be the maximum point and consider the maximization of a quadratic. Equations (C3) and (C4) become

$$f(\underline{x}_0) - f(\underline{x}) = -\frac{1}{2} (\underline{x} - \underline{x}_0)^T G(\underline{x}_0) (\underline{x} - \underline{x}_0), \quad (C5)$$

and

$$\underline{x}_0 - \underline{x} = - G^{-1}(\underline{x}_0) \underline{g}(\underline{x}) = H\underline{g}(\underline{x}) \quad . \quad (C6)$$

Note that G is a symmetric, negative definite matrix.

From equation (C6) we see that the direction toward the maximum is not necessarily in the direction of the gradient. The two vectors $(\underline{x}_0 - \underline{x})$ and \underline{g} will be in the same direction only if $(\underline{x}_0 - \underline{x})$ is an eigenvector of the Hessian matrix G . If the ratios between the corresponding eigenvalues are large there will probably be considerable difference in the directions of the two vectors.

If the Hessian matrix is constant and known it is obvious that the maximum can be found in one step. However, in general, G is not constant and may be unknown. The Fletcher-Powell modification of Davidon's method is an iterative procedure which searches for the point where $\underline{g} = 0$ and the Hessian matrix is negative definite. An initial guess is made for H ($H = -G$), and H is modified each set on the basis of the changes in \underline{x} and $\underline{g}(\underline{x})$. The initial value of H is usually chosen to be the unit matrix, i.e., the initial step is in the direction of steepest ascent.

The procedure at the i -th step is as follows where the subscript indicates the stage of the iterative procedure.

1. Set

$$\underline{s}_i = H_i \underline{g}_i \quad . \quad (C7)$$

Find the optimum step¹ in the direction \underline{s}_i . That is,

¹ The method for finding the optimum step is given in Appendix D.

find α_i , $\alpha_i > 0$, such that $f(\underline{x}_i + \alpha_i \underline{s}_i)$ is a maximum with respect to λ along $\underline{x}_i + \lambda \underline{s}_i$.

2. Set

$$\underline{\sigma}_i = \alpha_i \underline{s}_i \quad (C8)$$

3. With

$$\underline{x}_{i+1} = \underline{x}_i + \underline{\sigma}_i \quad (C9)$$

evaluate $f(\underline{x}_{i+1})$ and $\underline{g}(\underline{x}_{i+1})$. Note that \underline{g}_{i+1} is orthogonal to $\underline{\sigma}_i$, i.e.,

$$\underline{g}_{i+1}^T \underline{\sigma}_i = 0.$$

4. Set

$$\underline{y}_i = \underline{g}_i - \underline{g}_{i+1} \quad (C10)$$

5. Modify H by

$$H_{i+1} = H_i + A_i + B_i \quad (C11)$$

where

$$A_i = \frac{\underline{\sigma}_i \underline{\sigma}_i^T}{\underline{\sigma}_i^T \underline{y}_i} \quad (C12)$$

$$B_i = - \frac{(\underline{H}_i \underline{y}_i)(\underline{H}_i \underline{y}_i)^T}{\underline{y}_i^T \underline{H}_i \underline{y}_i} \quad (C13)$$

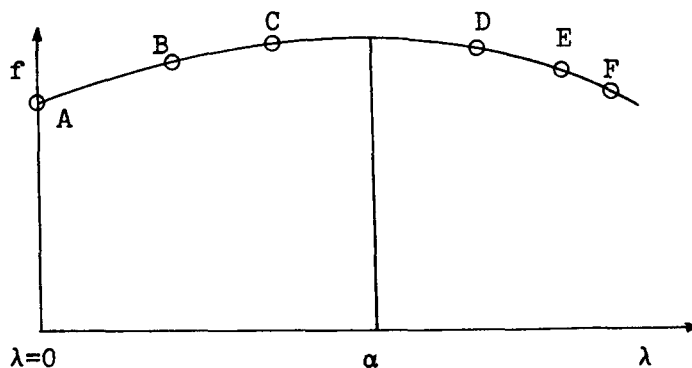
6. Set $i = i + 1$ and repeat.

APPENDIX D

METHOD FOR DETERMINING AN OPTIMUM STEP

In this appendix the method for obtaining the maximum along a line is given. Davidon (1959) suggested a cubic interpolation which Fletcher and Powell (1963) found satisfactory, but this procedure was not satisfactory in this problem.

The problem is to find the maximum of a function $f(\underline{x})$ of n variables in a given direction $\underline{x} + \lambda \underline{s}$, $\lambda > 0$. A plot of this function in a specified direction is given in the figure below. When the function $f(\underline{x})$ and its gradient $\underline{g}(\underline{x})$ are not known analytically but have to be computed digitally the maximum point cannot be found exactly. An iterative procedure is used to find this point, hence several iterations are required for each optimum step.



The slope of the function at the initial point (point A) is denoted by g_{xs} where

$$g_{xs} = \underline{g}^T \underline{s} = \underline{g}^T H \underline{g} \quad (D1)$$

This slope is positive since H is positive definite. The function $f(\underline{x})$ and its gradient $\underline{g}(\underline{x})$ are then calculated at a point \underline{z} on the line $\underline{x} + \lambda \underline{s}, \lambda > 0$. The slope at this point is denoted by g_{zs} where

$$g_{zs} = \underline{g}^T(\underline{z}) \underline{s} \quad (D2)$$

The value of λ used is $\lambda = \alpha_{i-1}$ except for the first step when $\lambda = 1$ is used. At the point \underline{z} if g_{zs} is positive (point B) the maximum point has not yet been reached. An estimate for the location of the maximum is then made by linearly extrapolating the slopes g_{xs} and g_{zs} . The length of this step is then increased by 1.25 so that the next point will be on the other side of the maximum, i.e., the slope will be negative. If the slope is not negative this procedure is continued using the previous two points to estimate the next point until a point is found for which the slope is negative (points D, E, or F). When a point is found where the slope is negative the next guess is made using a linear interpolation of the slopes of two points, the one with a positive slope closest to the maximum and the one with a negative slope nearest the maximum (points C and D). This process is continued until the optimum step is found, or until the maximum allowable number of iterations per step is exceeded.

When the maximum allowable number of iterations per step is exceeded the last step is used as the optimum step. Twelve was usually used in this problem as the maximum number of iterations per step. The criteria for a point \underline{z} to be the maximum point is

$$\left| \frac{\epsilon_{zs}}{\epsilon_{xs}} \right| < \beta .$$

A value of 0.01 for β was usually used in this study.